2001

Isomalathion and related compounds as active site probes of acetylcholinesterase

Todd T. Talley
The University of Montana

INFORMATION TO USERS

This manuscript has been reproduced from the microfilm master. UMI films the text directly from the original or copy submitted. Thus, some thesis and dissertation copies are in typewriter face, while others may be from any type of computer printer.

The quality of this reproduction is dependent upon the quality of the copy submitted. Broken or indistinct print, colored or poor quality illustrations and photographs, print bleedthrough, substandard margins, and improper alignment can adversely affect reproduction.

In the unlikely event that the author did not send UMI a complete manuscript and there are missing pages, these will be noted. Also, if unauthorized copyright material had to be removed, a note will indicate the deletion.

Oversize materials (e.g., maps, drawings, charts) are reproduced by sectioning the original, beginning at the upper left-hand corner and continuing from left to right in equal sections with small overlaps.

Photographs included in the original manuscript have been reproduced xerographically in this copy. Higher quality 6" x 9" black and white photographic prints are available for any photographs or illustrations appearing in this copy for an additional charge. Contact UMI directly to order.

ProQuest Information and Learning
300 North Zeeb Road, Ann Arbor, MI 48106-1346 USA
800-521-0600

UMI®

ISOMALATHION AND RELATED COMPOUNDS AS ACTIVE SITE PROBES OF ACETYLCHOLINESTERASE

by

Todd T. Talley

B.S. University of Utah, 1995

A thesis submitted in partial fulfillment of the requirements for the degree of

Doctor of Philosophy

The University of Montana

August 2001

Approved by:

Chairperson

Dean, Graduate School

8-30-01

Date

Talley, Todd T. Ph.D., August 2001 Chemistry

Isomalathion and Related Compounds as Active Site Probes of Acetylcholinesterase

Director: Charles M. Thompson

To examine the interactions of asymmetric organophosphorus compounds within the steric confines of the acetylcholinesterase (AChE) active site, the synthesis of the stereoisomers of isomalathion [*S*-(1,2-dicarboethoxyethyl) *O*,*S*-dimethyl phosphorodithiolate] was conducted. The methodology used was also adapted for the first synthesis of the stereoisomers of the novel isoparathion thiosuccinate phosphorothiolate (ITP) compound [*S*-(1,2-dicarboethoxyethyl) *O*-methyl *O*-(4-nitro-phenyl) phosphorothiolate]. The kinetic parameters k_i, K_D, and k_p for the inhibition of electric eel AChE (EEAChE) and soluble recombinant mouse AChE (rMAChE) by the isomalathion and ITP stereoisomers were determined. EEAChE demonstrated a 4-fold difference in anti-AChE potency between the strongest, S_PR_C, and weakest, S_PS_C, isomalathion isomers and an 8-fold difference in anti-AChE potency between the strongest ITP stereoisomer, R_PR_C, and the weakest, S_PS_C. rMAChE demonstrated a 40-fold difference in anti-AChE potency between the weakest isomalathion isomer, S_PS_C, and the most potent, R_PR_C, and a 24-fold difference in anti-AChE potency between the strongest ITP stereoisomer, R_PR_C, and the weakest, S_PS_C, thus demonstrating both stereochemical and species differences in the inhibitory profiles of the two compounds. The rate constants for reactivation, k_3, both spontaneous and in the presence of the oximes 2-PAM and TMB-4, were determined for both enzyme sources inhibited by the stereoisomers of both compounds. Both sources of AChE inhibited by isomalathion stereoisomers that were *R* at phosphorus demonstrated both spontaneous and oxime mediated reactivation while inhibition by the isomers that were *S* at phosphorus resulted in phosphorylated adducts resistant to reactivation even in the presence of an oxime suggesting distinct postinhibitory pathways dependent upon the stereochemical orientation at phosphorus. This is in contrast with the results obtained following inhibition with the ITP stereoisomers where the postinhibitory mechanisms appeared to be dependent upon the stereochemical orientation of the asymmetric carbon present in the diethylmalonate portion of the molecule. These observations suggest that despite the similarities of the two compounds their steric and electrostatic differences cause them to interact with the AChE active center by distinct mechanisms.

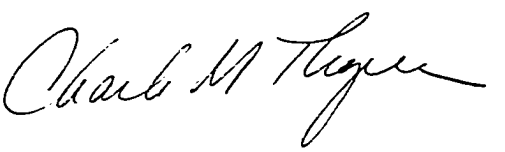

ACKNOWLEDGMENTS

I would like to gratefully acknowledge the help and support received from the students, staff, and faculty of both the Department of Chemistry and the Department of Pharmaceutical Science at the University of Montana. Their collective warmth and generosity has made my stay at this institution tremendously enjoyable and exceptionally instructive. The active pursuit of academic excellence at the University of Montana, integrated with the humility and compassion that is so often forgotten by our society, provides a stunning example of how things should be, and will supply me with a metaphor to model my life after for years to come.

In particular, I am filled with overwhelming gratitude for the assistance of my advisor, Dr. Charles Thompson. Dr Thompson's munificence, wit, and guile are without equal, and when these attributes are combined with his personal integrity and unbridled curiosity the truly renaissance nature of his persona becomes evident. I have been exceedingly fortunate to have had the opportunity work with him, learn from him, and to also know him as a friend. This combined with the opportunities afforded by my experience with Dr. Thompson leave me forever indebted to him.

Another undeniably key component of my success at the University of Montana has been the individual members of the Thompson Group. Their camaraderie, collective wisdom, and continued assistance have contributed to my accomplishments in countless ways, and each of them rightfully deserves volumes of praise for their individual contributions. Further, I am very grateful for the opportunity of working with Dr. Joseph DeGraw. As an astute chemist, shrewd observer, and consummate interpreter of the human

condition, Dr. DeGraw provides an example of professionalism rarely encountered. A special note of appreciation is in order for the countless edits, sage advice, and continued friendship of Dr. Katie George. Acknowledgements are also due to Dr. Palmer Taylor at the University of California in San Diego for providing our group with his recombinant mouse acetylcholinesterase that was of pivotal importance to our studies.

Finally, I must express my infinite gratitude to my wife Karen and my children Kristian, Isaac, and Sadria. Throughout my education, they have faithfully endured both my triumphs and failures with unquestioning love and support. Their limitless devotion to my endeavors is humbling beyond description.

TABLE OF CONTENTS

LIST OF FIGURES

LIST OF SCHEMES

LIST OF TABLES

LIST OF ABBREVIATIONS

Abs.	absorbance
AcCoA	acetyl coenzyme A
ACh	acetylcholine
AChE	acetylcholinesterase
AD	Alzheimer's disease
BChE	butyrylcholinesterase
c	concentration (g/100 mL)
d	doublet
dd	doublet of doublets
DMF	dimethylformamide
dq	doublet of quartets
dt	doublet of triplets
DTNB	5,5'-dithiobis(2-nitrobenzoic acid)
EEAChE	electric eel acetylcholinesterase

Et	ethyl
eq	equivalents
Eqn.	equation
g	gram
GD	Grateful Dead
h	hour
Hz	hertz
ITP	isoparathion thiosuccinate phosphorothiolate
J	NMR coupling constant (in Hz)
L	liter
m	multiplet
m	meta
M	molar (molarity)
*m*CPBA	*m*-chloroperoxybenzoic acid
MeOH	methanol

MHz	megahertz
MMPP	monoperoxyphthalic acid, magnesium salt
min	minute
mL	milliliter
μL	microliter
mmol	millimole
mol	mole
mp	melting point
NMR	nuclear magnetic resonance
p	para
2-PAM	2-pyridinium aldoxime methiodide
Ph	phenyl
ppm	parts per million
RBAChE	rat brain acetylcholinesterase
rMAChE	recombinant mouse acetylcholinesterase

s	singlet
t	triplet
TEA	triethylamine
THF	tetrahydrofuran
TLC	thin layer chromatography
UGIG	you go I go

Chapter 1

INTRODUCTION

In the early 19th century, the chemistry of organophosphorus (OP) compounds was launched by Lassaigne's investigation of the reaction of alcohol with phosphoric acid. Since then, more than 50,000 OP compounds have been synthesized, many of which have demonstrated therapeutic and insecticide utility. Tetraethyl pyrophosphate (TEPP) **1** (Figure 1.1), a highly potent OP compound, was first synthesized by Clermont in 1854 and likely influenced Lange and Krueger's 1932 paper on the synthesis of dimethyl- and diethyl-phosphorofluoridates and later spawned the modern investigation of toxic OP compounds (Eto 1974).

Many OP compounds possess the potential for insidious use as chemical warfare agents (Taylor 1994). Prior to and during World War II, the efforts of the Schrader's (Germany) and Saunders' (England) research groups were directed toward the development of chemical warfare agents. The synthesis of the compounds *O*-isopropyl methylphosphonofluoridate (sarin) **2**, 1,2,2-trimethylpropyl-methylphosphonofluoridate (soman) **3**, and *O*-ethyl-*N*, *N*-dimethyl-cyanophosphate (tabun) **4** were kept secret by the German government while the researchers from Allied countries focused their research on compounds related to diisopropylphosphorofluoridate (DFP) **5** (Gallo 1991).

Figure 1.1. Neurotoxic Organophosphorus Compounds.

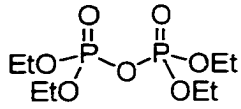

1: TEPP

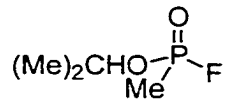

2: sarin

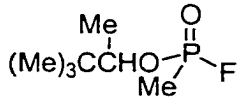

3: soman

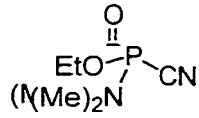

4: tabun

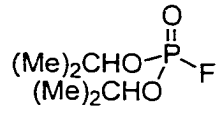

5: DFP

Many of these compounds have been stockpiled for military use as neurotoxic agents or nerve gas (Caglioti 1983). Despite an international ban on the use and production of these compounds, there is evidence that sarin **2** was used by Iraq during its conflict with Iran and during the Gulf War (Black 1993). This has led to the suggestion that exposure to sarin may be a contributing factor to the so-called Gulf War Syndrome (Ember 1996). Sarin **2** was also used by terrorists in an attack on a Tokyo subway in 1995 which resulted in twelve deaths and more than 5,000 injuries (Noort 1998; Satoh 2000)

A far more benign use of OP compounds has been their development as insecticides. Schrader and coworkers demonstrated that several OP compounds exhibited contact insecticidal activity. Their work led to the development and subsequent marketing of the first practical insecticide, Bladen, in 1944 (Eto 1974). Since then, thousands of new OP pesticides have been developed. As OP insecticides are generally short-lived in the environment, they have replaced the environmentally persistent chlorinated hydrocarbon

pesticides such as DDT. The use of DDT was banned during the 1970's in the U.S. due to the compound's retention in body tissue and biomagnification (Matolczy 1988).

Pesticide use has significantly increased crop yields by diminishing the populations of threatening organisms, thus impacting numerous economic considerations. In addition, some insecticides have been instrumental in the reduction of insect-borne diseases such as malaria and encephalitis (Caglioti 1983). The United States Environmental Protection Agency (EPA) estimates that approximately 60 million pounds of organophosphate pesticides are applied to agricultural crops annually and that nonagricultural uses account for another 17 million pounds per year in the U.S (EPA 2000). The structures of some common OP insecticides are shown in Figure 1.2.

Figure 1.2. Common OP Insecticides

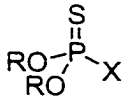

6: malathion R = CH_3, X = 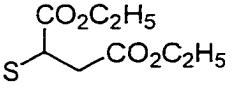

7: parathion methyl R = CH_3, X = 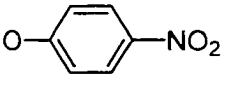

8: parathion R = CH_3CH_2 X = 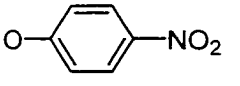

9: chlorpyrifos R = CH_3CH_2 X = 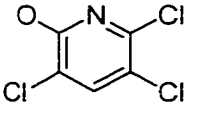

Toxicity and insecticidal activity of OP compounds is mainly attributed to their ability to inhibit the enzyme acetylcholinesterase (AChE, choline hydrolase, EC 3.1.1.7) (Fukuto 1990). Inhibition of AChE is caused by the formation of a covalent bond between the OP compound and a reactive serine residue present within the active site of the enzyme

that results in a phosphorylated enzyme intermediate (Aldridge 1952; Wilson 1960; Cohen 1963). The phosphonyl moiety may then react with water or other suitable nucleophiles, such as an oxime-reactivating agent, to regenerate an active enzyme. Alternatively, it may undergo post-inhibitory reactions resulting in an enzyme that is intractable to reactivation, a process referred to as aging (Millard 1999b). In addition to the acute toxicity caused by the inhibition of AChE, there is a mounting body of evidence that suggests chronic low-level exposure to OP compounds may play a role in a number of pathologies (Ragnarsdottir 2000).

An understanding of the pathologies caused by OP poisoning (both acute and chronic) necessitates knowledge of the chemical mechanism of inhibition. It was previously thought that all OP's caused toxicity by an similar mechanism (covalent modification of AChE active site). However, kinetic and crystallographic studies combined with site-specific mutagenesis have demonstrated that the structure, chemical reactivity, and stereochemical orientation of OP compounds can dramatically influence their rate and ability to inhibit AChE, and the ability of AChE to reactivate following inhibition (Debord 1986; Fukuto 1990; Harel 1993; Ashani 1995; Hosea 1995, 1996; Bourne 1999a; Jianmongkol 1999; Dembele 2000; Doorn 2000; Kraut 2000; Lesser 2000; Radic 2000). In addition, many commercially available insecticides have been shown to contain contaminants that are potentially more toxic than the parent compounds from which they are derived (Metcalf 1953; Chukwudebe 1989; Thompson 1989; Monje Argiles 1990). Commercial OP pesticides, such as malathion **6** (Figure 1.2), are racemic mixtures and have been shown to contain OP contaminants that also have centers of asymmetry

(Berkman 1993b). In order to fully understand the effectiveness and dangers of these compounds it is necessary to delineate the stereo-dependent nature of these interactions.

In order to discus these phenomena in a cohesive fashion, the first portion of this thesis is divided into three main sections. In Section 2.1, the enzyme AChE will be introduced in greater detail. This will be followed by a discussion of some salient features of OP chemistry in Section 2.2. Finally, this portion of the thesis will conclude with a discussion of how OP compounds interact with AChE in Section 2.3.

Chapter 2

BACKGROUND

2.1.1-Acetylcholinesterase (AChE) and the Cholinergic System

Long before the concept of enzymes had evolved, AChE was an important pharmacological target. An alkaloid obtained from the Calabar, or ordeal bean, from the perennial plant *Physostigma venenosum* Balfour found in tropical West Africa contains the compound physostigmine. The Calabar bean, also called Esere nut, chop nut, or bean of Etu Esere, was once used by native tribes of West Africa as an "ordeal poison" in trials for witchcraft. It was brought to England in 1840 and investigations of its pharmacological properties were conducted. Jobst and Hesse isolated the pure alkaloid in 1864. Observations during the early exploration of the cholinergic nervous system led to the suggestion that physostigmine inhibited the enzyme (AChE) that catalyzed the hydrolysis of choline esters and eventually established the role of acetylcholine (ACh) as a labile neurotransmitter. The first therapeutic use of the drug was in 1877 by Laqueur, in the treatment of glaucoma, one of its clinical uses today (Holmstedt 1972).

In cholinergic presynaptic neurons, ACh is synthesized by the acetylation of choline by acetyl coenzyme A (AcCoA). The reaction is catalyzed by choline acetyltransferase in the cytoplasm (Parsons 1993) and is followed by the majority of ACh being sequestered within synaptic vesicles. During signal ⊐ubocurarine, a self-propagating action potential transverses the neuron and triggers the synchronous release of the contents

of more than 100 vesicles into the synaptic cleft. Single synaptic vesicles are estimated to contain from 1000 to over 50,000 ACh molecules each, and it has been calculated that a single motor-nerve terminal contains 300,000 or more vesicles (Katz 1965).

After being released into the synaptic cleft, ACh activates cholinergic receptors positioned on extracellular membranes of the presynaptic and postsynaptic neurons and on proximal glia (Aschner 2000). There are two major types of cholinergic receptors that have been classified as either nicotinic or muscarinic depending on their differential response to the plant alkaloids from *Nicotiana tabacum* (nicotine) and *Amanita muscaria* (muscarine), respectively. Evidence that tubocurarine inhibited nicotinic and atropine inhibited muscarinic effects of ACh provided further support for the proposal of two distinct types of cholinergic receptors. Nicotinic receptors are ligand-gated ion channels. Their activation causes a rapid (millisecond) increase in cellular permeability to Na^{+} and Ca^{2+}, depolarization, and excitation. Muscarinic receptors belong to the G protein-coupled class of receptors and act by facilitating the binding of GTP to specific G proteins. GTP binding activates the G protein, which then regulates the activity of specific effectors. These second messengers include enzymes such as adenylyl cyclase and phospholipases A_2, C, and D; channels that are specific for Ca^{2+}, K^{+}, or Na^{+}; and certain transport proteins. Muscarinic receptors contrast with nicotinic receptors in that responses to muscarinic agonists are slower and may be either excitatory or inhibitory. Also, these responses are not necessarily linked to changes in ion permeability.

Figure 2.1. The Cholinergic System.

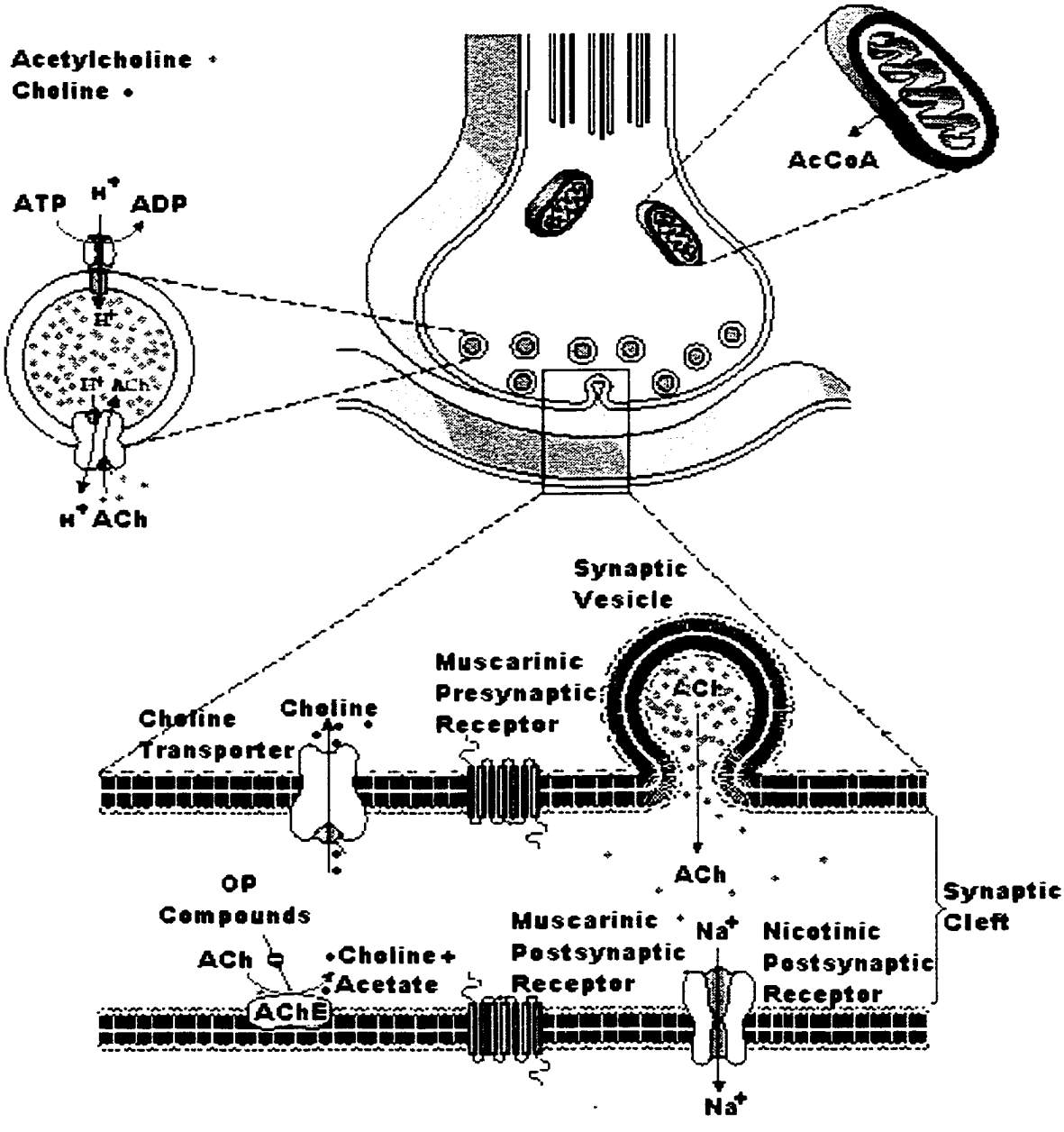

Adapted from *Fundamentals of Neuropharmacology*

2.1.2-AChE Hydrolysis of Acetylcholine

The primary biological role of AChE is the rapid termination of the neuronal impulse that occurs when ACh is released into the synaptic cleft. Following the production of an end-plate potential at the motor end plates of skeletal muscle or the polarization of the postsynaptic neurons, AChE removes ACh from the synaptic cleft by catalyzing its hydrolysis to acetate and choline (Ch) (Figure 2.2). In order to avoid hyperpolarization, which results in desensitization and/or cell death, ACh must be removed from the synaptic cleft almost immediately. Removal is accomplished by strategic localization of AChE in presynaptic and postsynaptic membranes and in the basal lamina in the neuromuscular junction. AChE has one of the highest rate constants known (k_{cat} = 1.6 x 10^4 s^{-1}) and k_{cat}/K_M = 2 x 10^8 (Rosenberry 1975; Quinn 1987), implying a rate close to the limit of diffusion controlled reactions.

Figure 2.2. Acetylcholine Hydrolysis.

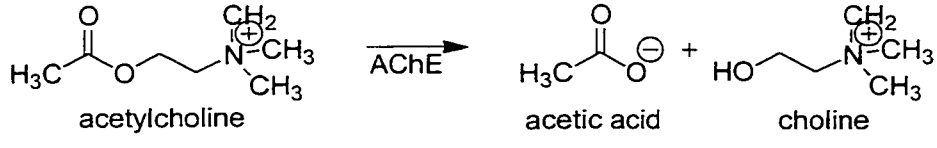

A number of studies have demonstrated that the probable mechanism for AChE catalyzed hydrolysis of ACh is as represented in Scheme 2.1. A peripheral anionic site near the surface of the enzyme facilitates initial association and alignment of ACh (Szegletes 1999). ACh is propelled toward the active site of the enzyme by electrostatic interactions between the negative charge of an anionic site, or choline binding subsite (Trp86), and the positive charge on the ACh nitrogen (E + S) resulting in an enzyme-

substrate complex (ES). There is also evidence that AChE posses a permanent dipole moment that assists with this orientation and docking of positively charged substrates (Porschke 1996). Acetylation of the serine hydroxyl (-OH, Ser203) within the esteratic site is catalyzed by the basic imidazole moiety B (His447) and the acidic moiety AH (tyrosine hydroxyl), which leads to the acetylated enzyme EA. Free enzyme E is then regenerated by a deacetylation step that occurs within milliseconds.

AChE hydrolysis of ACh demonstrates the hallmark elements of an acid-base catalyzed reaction, including both the acetylation and deacetylation reactions. While the reaction steps outlined in Scheme 2.1 provide a simplistic representation of the AChE active site and demonstrate a reasonable mechanism for the hydrolysis of ACh, it must be emphasized that the enzyme is a highly complex and dynamic protein. Consequently, in addition to the regions described above, there are a number of peripheral sites and hydrophobic/hydrophilic regions that may be involved in allosteric modulation of the enzyme's activity and in protein-protein interactions (Shafferman 1992).

Scheme 2.1. The Mechanism of Acetylcholine Hydrolysis by Acetylcholinesterase.

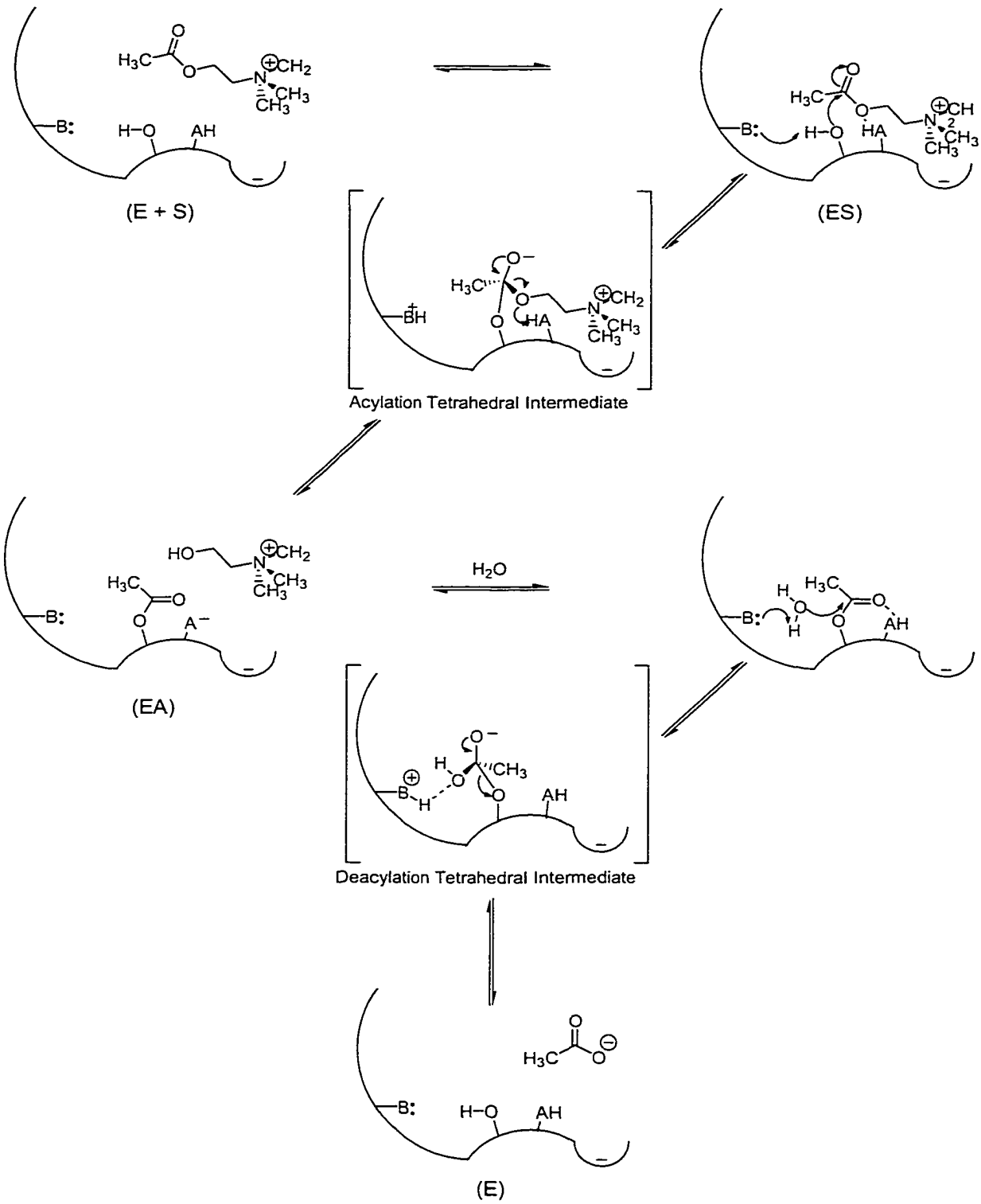

2.1.3-Inhibition of AChE

Many substances, including a number OP compounds, have demonstrated varying degrees of anti-AChE potential. When inhibited, the enzyme is unable to hydrolyze ACh resulting in the rapid accumulation of the neurotransmitter in neuromuscular junctions and nerve synapses. The build-up of ACh leads to hyperpolarization of the postsynaptic neuron, which may eventually result in cell death. The *in vivo* manifestations range from mild confusion to convulsions, coma, and death (Sultatos 1994). The chemically altered enzymes may also possess the ability to elicit an autoimmune response with potentially deleterious consequences (Rosenberg 1999). The inhibition of AChE by OP compounds defines a central concept of this thesis and will be discussed in greater detail in the following sections.

2.1.4-Structural Features of AChE

The three-dimensional structure of acetylcholinesterase demonstrates three functional regions of the enzyme (Sussman 1991; Bourne 1995; Bourne 1999b). The catalytic triad is nearly centrosymmetric to each subunit and resides at the base of a narrow gorge. The gorge is approximately 20 Å in depth and is lined with 14 highly conserved aromatic residues (Koellner 2000), which may contribute up to 60% of its surface (Axelsen 1994). The residues of the catalytic triad, Ser203, His447, and Glu334, are at the base of the gorge. The catalytic mechanism resembles that of other hydrolases, where the serine hydroxyl group is rendered highly nucleophilic through a charge-relay system involving the glutamate carboxyl group, the imidazole on the histidine, and the hydroxyl of the serine. Adjacent to this region is an oxyanion hole formed by the main chain N-H functions of

Gly121, Gly122, and Ala204. Residues Gly122, Trp233, Phe295, Phe297 and Phe338 form the acyl pocket responsible for AChE's acetyl ester specificity (Harel 1995; 1996). The peripheral anionic site, located near the gorge opening and defined by Trp286, Tyr72, and Tyr124, has been demonstrated to be involved in catching and guiding substrate molecules into the active site, and likely gives rise to allosteric modulation of the enzymes activity (Zhou 1998; Botti 1999; Golicnik 2001). A point of constriction, formed mainly by the side chains of Tyr121 and Phe330, separates the upper and lower parts of the gorge (Koellner 2000). As the cross-section of ACh is much larger than the narrowest part of the gorge, large-amplitude fluctuations of at least part of the gorge wall are necessary to allow substrate to enter. Such fluctuations are actually seen in molecular dynamics simulations of tacrine-*torpedo californica* AChE (*Tc*AChE) complex (Wlodek 1997; 2000).

Figure 2.3. Crystal Structure of AChE.

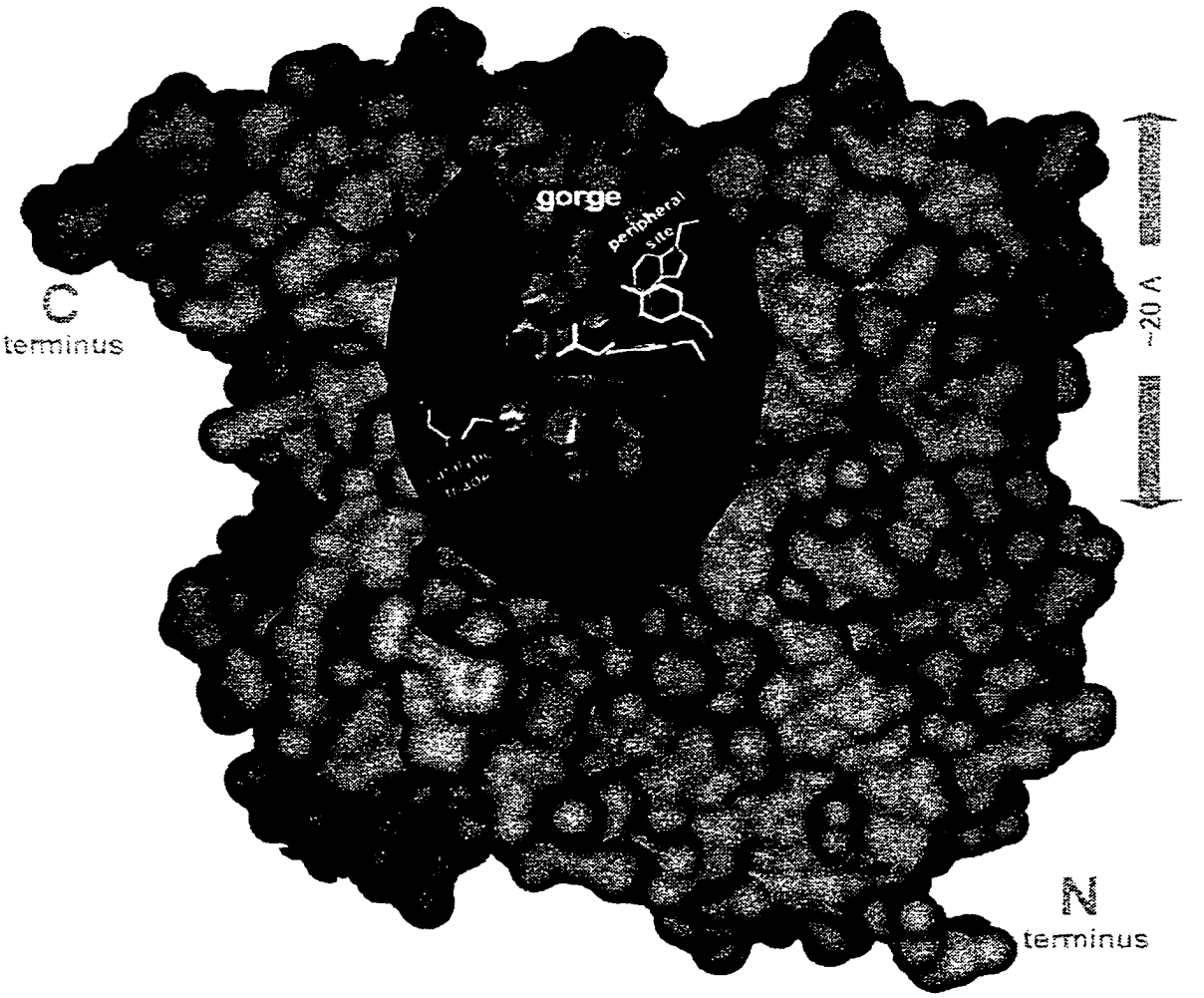

Zoran Radic http://phrtayl0.ucsd.edu/zoran/

AChE has been isolated from a wide variety of animals (Fukuto 1990; Sultatos 1994) including insects, fish, reptiles, birds, and mammals and belongs to a large family of proteins that demonstrate a common folding motif, termed the α/β hydrolase fold (Ollis 1992). This gene family of serine hydrolases contains such exquisite diversity that members such as thyroglobulin (Swillens 1986a; 1986b) and the tactins, glutactin, electrotactin, and neurotactin (de la Escalera 1990; Olson 1990; Botti 1998), are typified by their non-hydrolase functions while maintaining the common structural matrix (Taylor

1994). Members of this family from mammalian sources include butyrylcholinesterase (Lockridge 1987), cholesterol esterase (Kyger 1989), lysophospholipase (Han 1987), and the microsomal carboxyl esterases (Korza 1988; Long 1988).

Analysis of the three-dimensional structure and residues necessary for catalytic activity divide the serine hydrolases into subgroups. Members of the subgroup that includes AChE, contain a catalytic triad similar to the one described prior for AChE. This arrangement is essentially the mirror image of that found in serine proteases, such as trypsin and chymotrypsin (Sussman 1991). As with serine proteases, esterases of the α/β-hydrolase fold, including AChE, are susceptible to inhibition by OP compounds. The His440 is conserved by all members of the family and serves as a reference position (Taylor 1994). Several members of the family, including all of the cholinesterases, contain three conserved disulfide loops.

Amino acid sequencing and molecular cloning have demonstrated that a single gene encodes acetylcholinesterase. Alternate processing of the mRNA leads to the formation of multiple products (Schumacher 1986; Gibney 1988). AChE exists in two general classes of molecular forms, heteromeric associations of catalytic subunits with structural subunits and simple homomeric oligomers of catalytic subunits (*i.e.*, monomers, dimers, and tetramers). One heterologous form is a tetramer of catalytic subunits disulfide-linked to a lipid-linked subunit and is found on the outer surface of the membrane. The other consists of tetramers of catalytic subunits, disulfide linked to each of three strands of a collagen-like structural subunit. The homomeric forms are found as soluble species in the cell, presumably for export, or associated with the outer membrane of the cell through either an intrinsic

hydrophobic amino acid sequence or an attached glycophospholipid (Massoulie 1993; Taylor 1994; Bourne 1999b).

2.1.5-Non-catalytic Properties of AChE

Certain brain regions contain large amounts of AChE, but lack acetylcholine and the biosynthetic capacity to generate it. This disparity in localization combined with the significant amount of AChE that is secreted into the extracellular space implies that AChE may have signaling functions that are independent of its function in ACh catalysis (Small 1996; Bourne 1999b). AChE has been shown to play an important role during both pre- and postnatal development in animal studies (Dembele 2000; Eriksson 2000; Lesser 2000; Xie 2000; Fordham 2001). It has been demonstrated that the level of ACh regulates expression of both nicotinic and muscarinic receptors (Schwartz 1983; Aronstam 1987; Buccafusco 1987; Buccafusco 1991) thus AChE plays a modulatory role in learning, memory, and behavior (Greenfield 1984; Terry 1993; Prendergast 1997, 1998; Cummings 2000). Further, AChE and ACh have been described as being involved in the modulation of cell movement and proliferation during development (Lauder 1999). AChE is transiently expressed during discrete periods of neural development of the thalamocortical pathways. Transient AChE activity is correlated with the specific growth of thalamic axons into the cortex and synaptogenesis with cortical neurons (Robertson 1993). Recently, it has been shown that there are significant sequence similarities between AChE and cell adhesion proteins that function during morphogenic events. AChE has been shown to play a specific morphogenic role during neurite outgrowth (Dupree 1994; 1995;

Bigbee 1999; 2000; Sharma 2001) and this neuritogenic ability of AChE has been shown to be independent of its traditional catalytic role (Layer 1995a; 1995b; Sternfeld 1998).

These non-catalytic properties of AChE may play a role in some neuropathologies. Alzheimer's disease (AD) is a complex and multifaceted neurodegenerative disease affecting aged populations. The pathogenesis and the etiology are not well defined, although a "cholinergic deficit hypothesis" has been suggested (Perry 1986). One of the most specific and consistent features is an early and severe degeneration of the forebrain cholinergic system, as demonstrated by the correlation observed between the cholinergic pathology and dementia (Geula 1994). There is a colocalization of AChE with amyloid β-peptide in the brain of AD patients that indicates a presence, if not an active role, in amyloid plaque formation (Bertoni-Freddari 1990; Ulrich 1990a; 1990b; Carson 1991; Moran 1993; Geula 1994). It has also been demonstrated that AChE accelerates the assembly of amyloid β-peptides into Alzheimer's fibrils (Alvarez 1997; Reyes 1997; Alvarez 1998; Inestrosa 1998).

Structure and sequence comparisons between recombinant mouse AChE (rMAChE) and amyloid β-peptide reveal a conserved helix-loop-helix motif (Sticht 1995; Bourne 1999b). This region of monomeric rMAChE interacts with the peripheral anionic site of other rMAChE monomers to assist in the aggregation of the enzyme's tetrameric form (Bourne 1999b). This information, combined with the colocalization of AChE with amyloid β-peptide deposits has led to the hypothesis that the helix-loop-helix domain of the amyloid β-peptide may interact in a similar fashion with the peripheral anionic site of AChE, that could then serve as a nucleation site to promote aggregation (Bourne 1999b).

Furthermore, in the amyloid β-peptides and prion proteins, an α-helix to β-sheet conversion has been proposed to accompany aggregation (Soto 1995). Sequence analysis has demonstrated that Gln15-Gly37 region of the amyloid protein is very similar to the Met120-Gly142 portion of the prion protein (Sticht 1995). This region has been suggested to undergo α-helix to β-sheet transition during pathogenic states (Beyreuther 1994; Kocisko 1994; Nguyen 1995). That these regions share structural and sequence similarities with the helix-loop-helix domain of AChE is quite intriguing.

The enhancement of cholinergic transmission in AD is a major goal for potential therapeutic agents such as Tacrine (COGNEX). AChE has long been an attractive target for the rational design of mechanism-based inhibitors because of the pivotal role it plays in the central nervous system (Trabace 2000a; 2000b). Current AD therapies focus upon central inhibition of AChE, which enhances the function of central cholinergic neurons by permitting ACh to remain in the synaptic cleft longer. The resulting increase in extracellular ACh concentrations may reverse central cholinergic hypofunction and improve cognitive functions in AD (Kelly 1999). Most drugs currently used therapeutically have been shown to improve AD symptomatically, but it is controversial whether there is an effect on the disease progression (Giacobini 1998b; 2000a). The clinical usefulness of AChE inhibitors in the treatment of AD has been limited by either an extremely short or an excessively long half-life, hepatic toxicity, and severe peripheral cholinergic side effects (Kelly 1999; Giacobini 2000).

2.2.1-Organophosphorus Compounds

In order to discuss OP insecticides in detail, a brief review of nomenclature, structure, and chemical reactivity is necessary. Systematic analysis of the relationships between the structure of OP compounds and their ability to inhibit AChE have demonstrated chemical reactivity to be the single most important property in dictating anti-AChE potency, i.e., the phosphorus ester must be reactive enough to phosphorylate the hydroxyl moiety of the active center serine (Fukuto 1990). The rate and extent of the AChE inhibition depends upon the nature of the OP structure, which influences phosphorylation through the electronic environment around the phosphorus. OP insecticides are esters of pentavalent phosphorus acids and typically belong to the phosphorothionate (P=S) class of compounds. General structures of several OP insecticide compound types are shown in Figure 2.4. It is a requirement for anti-AChE activity that one of the ligands attached to the phosphorus atom be a good leaving group. This aspect of OP reactivity and its relationship to biologically activity is of pivotal importance and will be discussed in greater detail in the following sections.

Figure 2.4. General Structure of OP Compounds

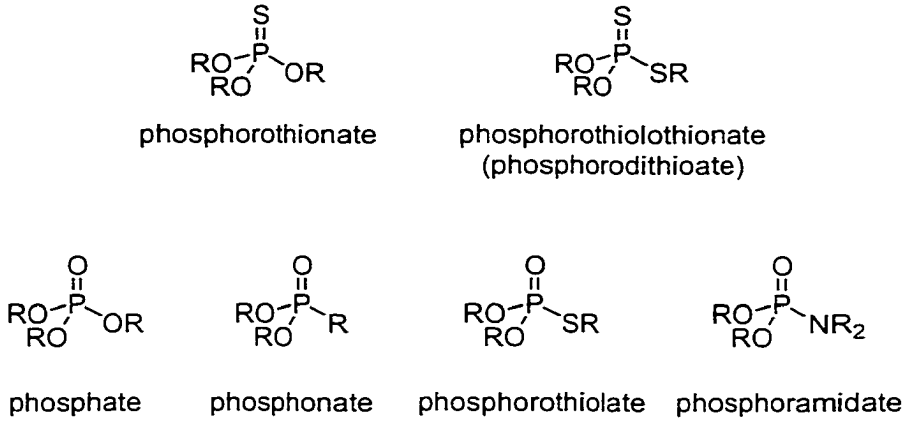

Rates of alkaline hydrolysis for a series of compounds that included diethyl *p*-nitrophenyl phosphate (paraoxon, **10**) and some of its substituted phenyl analogs were found to parallel their bimolecular rate constants for inhibition (k_i) of erythrocyte AChE via pseudo first order kinetics (Aldridge 1952). A subsequent study using a larger series of diethyl phenylphosphates demonstrated that the rate of inhibition of fly-head AChE by paraoxon analogs was dependent upon the effect of phenyl substituents (Fukuto 1956). The authors demonstrated a linear relationship for the anti-AChE potency of the compounds vs their Hammett's sigma constants, hydrolysis rates, and P-O-phenyl infrared stretching frequencies. The data indicated that activity was directly related to the electron-withdrawing properties of the respective substituents. Compounds with strongly electron-withdrawing substituents demonstrated enhanced reactivity toward AChE, and compounds with weakly electron-withdrawing or electron-donating substituents were poor inhibitors or were devoid of activity. For example, the concentration of paraoxon **10** needed to affect 50% inhibition of AChE was 10,000-fold less than dimethyl-*p*-methylphenylphosphate.

These trends are due to the ability of strongly electron-withdrawing substituents to attract electrons away from the phosphorus atom. The resulting electron-deficient center is more susceptible to nucleophilic attack by the serine hydroxyl moiety of the enzyme.

Figure 2.5. Parathion, Paraoxon, and Isoparathion

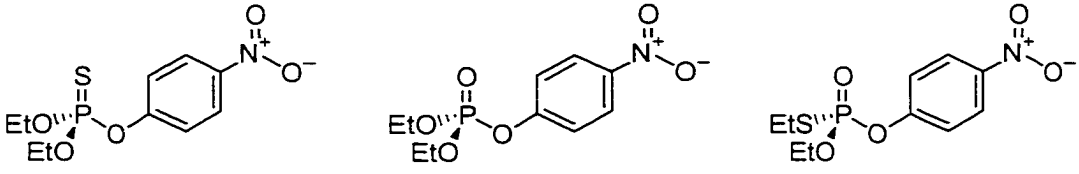

8: parathion **10**: paraoxon **11**: isoparathion

The chemical reactivity of an OP compound also depends on the π-atom linkage and the σ-ligand connectivity. When comparing phosphorothiolate esters (P-S-R) with their phosphate analogues, it is apparent that phosphorothiolates are more chemically reactive. Paraoxon **10**, with a P-O-R linkage, undergoes hydrolysis nearly 500 times slower than its phosphorothiolate analog, isoparathion **11**, which contains a P-S-R linkage (Heath 1961). The greater polarizability imparted by the sulfur atom and the decreased pπ-dπ contribution to the P-S bond due to less efficient orbital overlap is at least partially responsible for the difference in reactivity (Eto 1974). In the π-bond case, oxygen is more electronegative than sulfur and, consequently, P=O bonds are more polarized than P=S bonds. Greater polarization imparts greater electrophilicity to the phosphorus atom thus increasing its susceptibility to hydrolysis and nucleophilic attack (Van Wazer 1958; Fest 1973; Matolczy 1988). An example of this feature is demonstrated by comparing the

hydrolytic $t_{1/2}$ values for parathion **8** (203,000 h) and paraoxon **10** (22,200 h), a difference of approximately 10-fold (O'Brien 1967).

2.2.2-Thiono-Thiolo Rearrangement

Dialkyl phosphorothionate compounds are prone to undergo thiono-thiolo rearrangements. Isomerization can be induced by thermal, chemical, and to a lesser extent, photochemical means (Chukwudebe 1989).

Figure 2.6. Thiono-Thiolo Rearrangement

phosphorothionate phosphorothiolate

The rearrangement can be promoted by reaction of a phosphorothionate with an alkyl iodide to form the S-alkyl isomer by first alkylating the thionate followed by dealkylation. Bimolecular or self- isomerization occurs at elevated temperatures (80-180 °C) when one phosphorothionate is dealkylated to form an ambient ion pair that realkylates at the more nucleophilic sulfur atom (Fest 1973; Eto 1974). Isomerization may also occur at room temperature over long periods of time when phosphorothionates are stored in polar atrophic solvents and is fastest when the alkyl group transferred is a methyl (Eto 1974; Matolczy 1988). These reactions are summarized in Figure 2.7.

Figure 2.7. Alkyl Iodide Catalyzed- and Self-Isomerization of the Thiono-Thiolo Rearrangement.

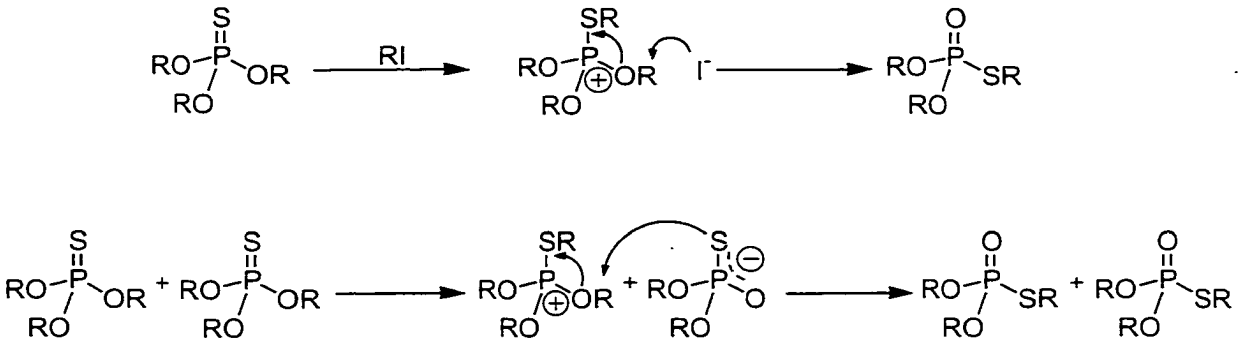

This type of transformation can have very deleterious results when it occurs during the manufacture and storage of phosphorothionate insecticides. The resulting phosphorothionate compounds are considerably more toxic than the original phosphorothionate compounds due, in part, to the increased chemical reactivity of the P=O moiety relative to that of P=S. In formulations of the commercially available pesticide malathion **6**, as much as 10% of the resultant isomalathion contamination has been found. It has been shown that approximately 90% of malathion **6** is isomerized to isomalathion **12** at 150 °C (Figure 2.8). In the same study, parathion **8** and parathion methyl **7** were isomerized to the S-ethyl or S-methyl thiolate in 80% and 90% yield, respectively, under the same conditions (Metcalf 1953).

Figure 2.8. Isomerization of Malathion to Isomalathion.

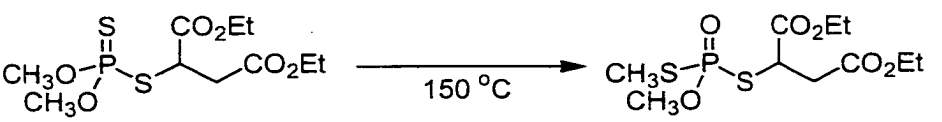

6: malathion **12**: isomalathion

2.2.3-OP Structure–Reactivity Relationships

Other factors affecting the anti-AChE potential of OP esters are the steric properties of the individual compounds. The importance of steric influences becomes apparent when comparing a series of ethyl *p*-nitrophenyl alkylphosphonates where the alkyl group substituent was correlated with their alkaline hydrolysis rates and anti-AChE potency (Fukuto 1958). In general, the rates of hydrolysis decreased with increasing chain length and/or chain branching. While this trend was typically mirrored by a decrease in the compounds reactivity toward AChE, a close examination of the data revealed that as chain length increased from three to six carbons the inhibitory ability of the compounds decreased dramatically. Hansch and Deutsch (1966) later verified these observations by demonstrating the anti-AChE activities of the compounds correlated with the Taft's steric substitution constant E_s. It has also been shown that the rate of inhibition decreases with increasing bulkiness of the ligands that remain attached following inhibition of AChE, i.e., compounds that contain methoxy groups react with AChE fastest, followed by compounds containing ethoxy, n-propoxy, and isopropoxy ligands (Gallo 1991).

2.2.4-Stereochemical Aspects of OP Compounds

Many OP compounds are pentavalent at phosphorus and are asymmetric if the ligands attached to the sp^3-tetracoordinated phosphorus atom are non-equivalent. The ligands attached to the phosphorus may also possess centers of asymmetry, thus dictating the possibility of three basic types of stereogenic OP compounds: those that contain phosphorus stereogenicity, those with carbon stereogenicity, and those with both carbon and phosphorus stereogenicity. Examples of these three types of asymmetric OP

compounds are given in Figure 2.9. This steric subtlety has been demonstrated to have direct consequences on the interactions of AChE with a number of OP compounds and will be discussed in greater detail in subsequent sections.

Figure 2.9. Three Basic Types of OP Stereogenicity.

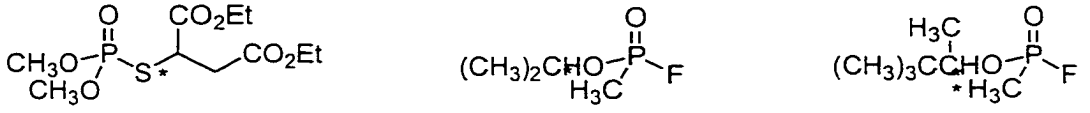

13: malaoxon
C-asymmetry

2: sarin
P-asymmetry

3: soman
P- and C-asymmetry

2.2.5-Metabolic Activation of OP Insecticides

Many common insecticides contain a P=S moiety despite the fact that phosphorothionate esters typically exhibit very poor anti-AChE activity. The comparative lack of inhibitory potency demonstrated by P=S esters is explained primarily in terms of their reduced chemical reactivity due to the decreased polarization of a P=S bond compared to a P=O bond. Compounds that contain P=S esters still maintain insecticidal efficacy despite their apparent lack of anti-AChE activity, and this implies some form of metabolic activation for the compounds.

It has been demonstrated that the toxicity of phosphorothionate insecticides is due primarily to metabolic oxidation of the P=S moiety to its corresponding P=O form. This metabolic activation of phosphorothionate insecticides is mediated, in part at least, by the mixed function oxidases (MFO), including several members of the cytochrome P-450 family of enzymes (Hajjar 1982; Hodgson 1982; Levi 1985, 1988). These proteins represent a ubiquitous system of enzymes that are responsible for the oxidation of foreign

compounds in animals. A classical example of this oxidation of a phosphorothionate to its corresponding oxon is found in the conversion of parathion **8**, which is essentially devoid of anti-AChE activity, to paraoxon **10**, an OP compound that demonstrates comparatively high inhibitory potency (Fukuto 1990).

2.2.6-Metabolic Degradation of OP Insecticides

OP insecticides are tertiary esters and as such they are susceptible to hydrolytic degradation. Enzymatic or chemical hydrolysis of any ester bond attached to the phosphorus generally leads to a non-toxic product (Eto 1974). Enzymatic hydrolysis is mediated by a number of different esterases that are typically referred to as hydrolases or phosphotriester hydrolases (Fukuto 1990). Metabolic degradation may also take place at a site on the molecule that is distant from the phosphorus center. An example of this is the carboxylesterase-catalyzed hydrolysis of malathion **6** to its nontoxic carboxylic acid derivatives, malathion α- and β-monoacid (**14** and **15**) and malathion diacid **16**. Alternatively, the S-C bond of malathion may be cleaved to form *O*, *O*-dimethyldithiophosphate (DMDTP) **17** which can then undergo further oxidation to form *O*, *O*-dimethylthiophosphate (DMTP) **18**. DMTP is also the primary hydrolytic metabolite of malaoxon **13** the toxic product of metabolic oxidation of malathion. In turn, DMTP can be oxidized to form *O*, *O*-dimethylphosphate (DMP) **17**. These reactions are summarized in Figure 2.10.

Figure 2.10. Metabolic Activation and Degradation of Malathion.

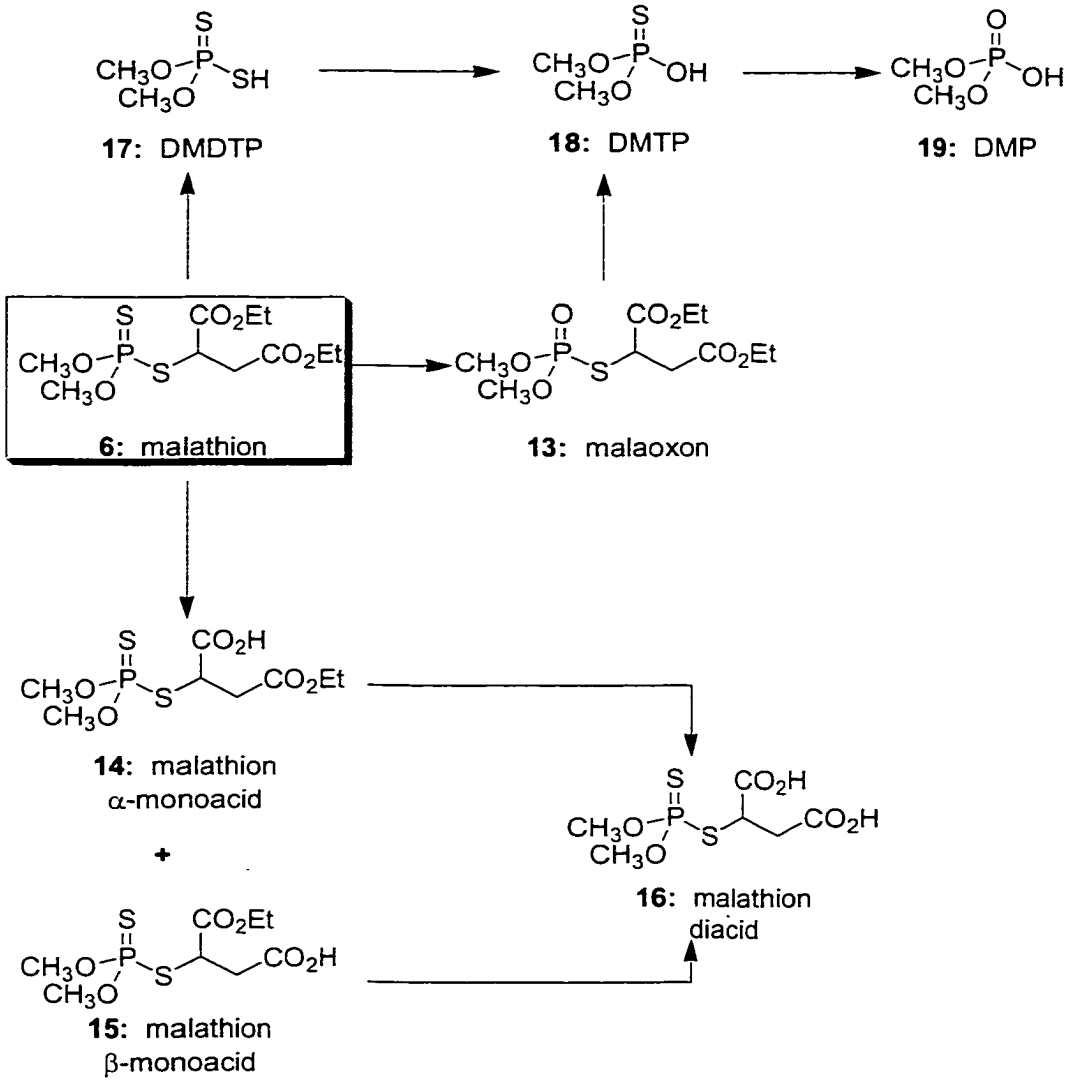

2.2.7-Malathion and Isomalathion

Malathion **6**, when pure, is relatively nontoxic to mammals (see Table 2.1). Because the rate of metabolic degradation of malathion to the nontoxic compounds (Figure 2.10) is faster than the rate of metabolic oxidation of the P=S in malathion **6** to the P=O of malaoxon **13**. Insects, however, possess comparatively lower concentrations of the

enzymes responsible for detoxication. Consequently, insects are much more susceptible to the toxic effects of malathion **6**.

Table 2.1. Relative Toxicity of Biologically Active Compounds.

Compound	LD_{50} mg/kg (oral, rats)
Glucose	35,000
Ethanol	10,000
Aspirin	3,750
NaCl	3,500
Malathion	3,000
Valium	710
Diazinon	400
Caffeine	300
Nicotine	230
DDT	120
Malaoxon	90
Cocaine	17
Strychnine	5
Paraoxon	2

Malathion **6** has been employed to manage the medfly problem in California (Barinaga 1991) and in Florida (1996-1997). Malathion **6** also has been established in veterinary medicine (Osweiler 1984), and in public health practices as an anti-infective agent (Wester, 1989) to control insect vector-borne diseases such as malaria (*anopheles mosquito*), dengue (*aedes aegypti*), yellow fever (*aedes*) (Caglioti 1983), and West Nile virus in New York. However, as one of the class of phosphorothionate insecticides it is prone to thermal and photochemical induced isomerization (Section 2.2.2) to form toxic impurities including trimethyl phosphorothioates and isomalathion **12** which have been shown to potentiate or enhance the toxicity of malathion formulations (Aldridge 1979;

Mallipudi 1980; Toia 1980; Lin 1984). Therefore, the safety of malathion usage is linked to its purity and storage.

Isomalathion **12** is the *S*-methyl isomeride of malathion **6** found in commercial formulations of the insecticide and is formed as a result of a thiono-thiolo rearrangement. Like most S-alkyl isomerides of phosphorothionate insecticides, isomalathion shows dramatically enhanced anti-AChE potency relative to malathion due to the enhanced chemical reactivity of the P=O bond, and the decreased $p\pi$-$d\pi$ contribution of the S-alkyl ligands (Fest 1973; Thompson 1989). Consequently, racemic isomalathion is a 3000-fold more potent anti-AChE agent than malathion (Thompson 1989).

Isomalathion **12** has been shown to be not only an inhibitor of AChE but also an inhibitor of the mammalian detoxifying enzyme, carboxylesterase (Talcott 1979; Toia 1980; Lin 1984; Ryan 1985). When carboxylesterase is inactivated, the normal side chain ester hydrolysis detoxification pathway is removed (2.2.6), and metabolic activation from malathion **6** to malaoxon **13** dominates the metabolism causing the latent toxicity (anti-AChE potency) to be observed in mammals (Cohen 1984; De Matteis 1989).

Of all the impurities found in malathion formulations, isomalathion **12** is the strongest potentiator of toxicity. A 0.5% isomalathion contamination of malathion formulations reduced the LD_{50} from 12,500 to 4400 mg/kg (Umetsu 1977; Toia 1980). The isomalathion content in malathion formulations, therefore, has been a matter of considerable concern, especially since the 1976 epidemic malathion poisoning in Pakistan. 2800 Pakistani pesticide applicators were acutely poisoned while 5 died during a malaria control program (Baker 1978; Iyer 1984). The poisonings were attributed to the unusually high isomalathion content of the formulation employed (Aldridge 1979; Iyer 1984).

A structurally significant feature of malathion **6** is the presence of a center of asymmetry at the succinate carbon. While the chiral integrity at the carbon is maintained in the formation of the S-methyl isomer, a new chiral center is generated at the phosphorous providing four total stereoisomers of isomalathion (Figure 2.11). It has been shown in several cases that differing sources of AChE may be stereoselectively inhibited by chiral OP isomers (Ooms 1965; Wustner 1973; Eya 1985; Armstrong 1987). A most striking case was reported by Jarv in which there was a 4200-fold difference in the inhibition rate of AChE between the enantiomers of isopropyl- methylphosphonofluoridate (Jarv 1984). In the case of isomalathion the relationship between AChE inhibition and asymmetry at both carbon and phosphorous was investigated (Berkman 1993a; 1993b; 1994).

Figure 2.11. Stereoisomers of Isomalathion.

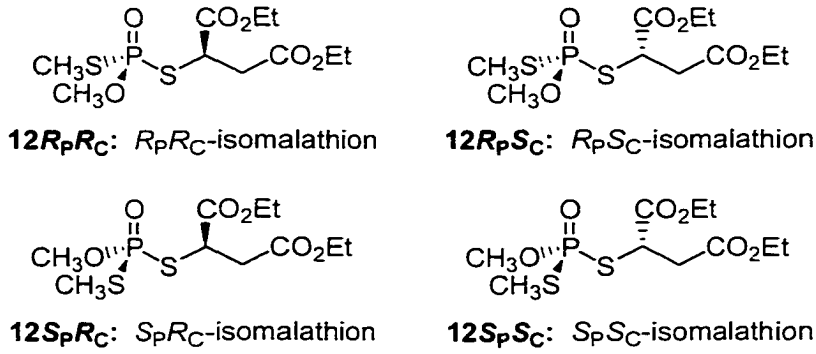

12R_PR_C: R_PR_C-isomalathion **12R_PS_C**: R_PS_C-isomalathion

12S_PR_C: S_PR_C-isomalathion **12S_PS_C**: S_PS_C-isomalathion

2.2.8-Pesticide Utility

There are estimates that pests destroy nearly half of all agricultural produce during production and storage (Perutz 1991). Prior to harvest, grain losses in developing countries of the Near East are reported to be approximately 23% with the largest losses in the

production of cereal crops, especially rice (Hayes 1991). It is believed that nearly one third of all potential crop, livestock, and timber yields are lost to insects or other pests (Caglioti 1983).

Approximately 3 billion pounds of pesticides are produced in the U.S. annually, one-third of which are insecticides. U.S. consumers purchased roughly 25% of all insecticides resulting in annual sales of nearly $900 million (Welling 1988). National and international agricultural organizations estimate that as much as 45 percent of the world's crops continue to be lost to insects and other pests. In the United States alone, about $20 billion worth of crops (one-tenth of production) are lost each year. It has been estimated that without the use of pesticides, the price for fruits and vegetables would increase 50 to 100% in first world countries (Schuhmann 1976). Some have suggested that the increase in cost would result in drastic changes of both diet and personal disposable income that may result in thousands of premature fatalities (Gray 2000). In addition, some insecticides have been instrumental in the reduction of insect-borne diseases such as malaria and encephalitis (Caglioti 1983). Such factors have contributed to the continued use of pesticides despite their potential dangers as neurotoxic agents.

2.2.9-Risks Associated with OP Insecticides

The World Health Organization estimates that approximately 3 million acute pesticide poisonings occur annually leading to approximately 250,000 fatalities, of which 99% occur in developing countries. In Sri Lanka nearly 13,000 people are admitted annually to hospitals for pesticide poisonings that result in approximately 1000 fatalities. Provincial hospitals in Thailand reported that OP poisoning alone was the eighth most

common illness requiring hospitalization in 1995 (Satoh 2000). This is in stark contrast with the United States. Of the more than 2 million human poisonings reported in 1996 only 4% were associated with pesticide exposure and only 20 cases, 4 of which were suicide, resulted in death (Lockridge 2000).

The risk of pesticide overexposure is greatest for those who are directly involved in their application including mixing concentrates and loading aircraft for aerial pesticide application (Barnes 1976). EPA guidelines for protecting U.S. agricultural workers from pesticide exposure include the use of protective clothing. In 1974 protective clothing was documented as "at least a hat or other suitable head covering, a long sleeve shirt and long legged trousers or a coverall type garment, shoes and socks". Revision of these recommendations by the EPA and USDA include a liquid-proof raincoat or apron, trousers outside of boots, unlined neoprene gloves, wide brimmed waterproof hats, unlined neoprene boots, and goggles or face shields (Stone 1988). Unfortunately, recent studies have demonstrated protective clothing may actually serve as a toxin delivery device by sequestering the toxic compounds in close proximity to the skin (Wester 2000) and that dermal exposure is a major route of intoxication (Krieger 2000). Other steps have also been taken to prevent the occurrence of acute poisoning such as medical monitoring of agricultural workers (Ames 1989). However, the efficacy of these measures has recently been questioned (Barnes 1999; Ohayo-Mitoko 2000).

While these protective measures may have reduced the number of acute pesticide intoxications among U.S. agricultural workers, considerable risk remains for those in developing countries. An estimated 40,000 farm workers of third world countries die each year from pesticide poisoning. Many of these poisonings result from "lack of knowledge,

unsafe attitudes, and dangerous practices" (Forget 1991). Often workers are poisoned because either they are unable to read, understand, or implement safety instructions, or the instructions themselves are inadequate (Perutz 1991). Inferior technology available to small farmers such as "faulty sprayers, lack of protective equipment adapted for tropical conditions, and non-existent first aid provisions" combined with an overall lack of information are perhaps the most important factors contributing to pesticide poisonings in developing countries (Forget 1991).

2.3.1-Inhibition of AChE by OP Compounds

The acyl pocket of the active center, the choline subsite of the active center, and the peripheral anionic site of AChE constitute three distinct binding domains for inhibitory ligands and form the basis for specificity differences between AChE and BChE (Taylor 1994). Reversible inhibitors, such as propidium and the peptide toxin fasciculin, bind to the peripheral anionic site on AChE (Bourne 1995; Radic 1999). Edrophonium and tacrine bind to the choline subsite in the vicinity of Trp86 and Glu202 (Harel 1993). AChE inhibitors that have a carbamoyl ester linkage, such as physostigmine and neostigmine, are hydrolyzed by AChE, but much more slowly than ACh. At physiological pH both the quaternary amine, neostigmine, and the tertiary amine, physostigmine, exist as cations. By serving as alternate substrates with a binding orientation similar to acetylcholine, attack by the active center serine yields the carbamoylated enzyme. In contrast to the acetyl enzyme, methylcarbamoyl AChE or dimethylcarbamoyl AChE is very stable with $t_{1/2}$ for hydrolysis of the dimethylcarbamoyl enzyme of 15 to 30 minutes. Sequestration of the enzyme in its carbamoylated form inhibits the enzyme-catalyzed hydrolysis of ACh for extended periods of time, 3 to 4 hours *in vivo* (Taylor 1996).

OP esters inhibit AChE by a process analogous to that of the carbamates. Specifically, inhibition is caused by a chemical reaction between the phosphorous containing moiety of the OP compound and the hydroxyl functionality of the serine residue within the active site of AChE, resulting in a phosphorylated enzyme. Unlike the intermediates formed by carbamoylation of the enzyme's active site, phosphorylated enzymes are highly stable and resistant to hydrolysis. The authors of one study demonstrated that it took several weeks for brain AChE activity to return to normal after

exposure to the neurotoxic OP compound diisopropyl phosphorofluoridate (DFP) (Sung 1987).

OP's inactivate AChE by phosphorylation of the active site serine hydroxyl where one ligand (X) about phosphorus is displaced (Scheme 2.2). The resulting covalently modified enzyme is essentially without catalytic activity. The first step in the inactivation of AChE involves the reversible formation of an enzyme-inhibitor complex and is represented by the dissociation constant, K_D (Main 1964). K_D is generally considered a measure of the OP-inhibitor's affinity for the enzyme's active site (Fukuto 1990). The second step of inhibition results in the irreversible phosphorylation of AChE by an OP inhibitor. Covalent modification of the serine hydroxyl of the enzyme is responsible for the ultimate loss in the enzyme's activity (i.e. the inability to hydrolyze ACh). The phosphorylation rate constant, k_p, is considered a quantification of the reactivity of the OP inhibitor or the enzyme-inhibitor complex (Main 1964; Fukuto 1990).

Scheme 2.2. Inhibition of Acetylcholinesterase by an OP Compound.

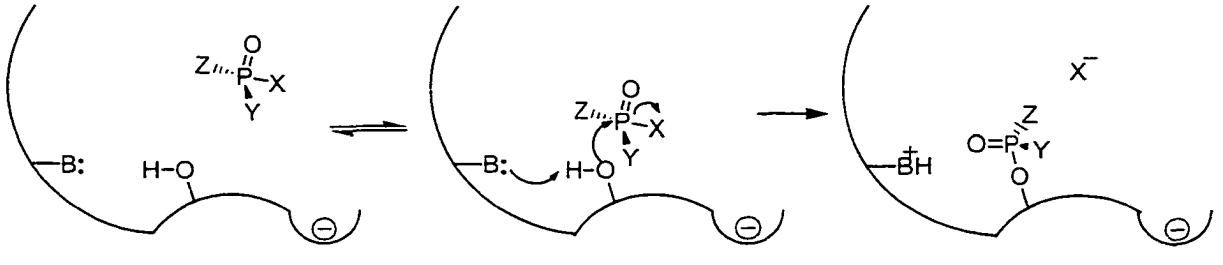

$$ENZ + OP\text{-}X \underset{}{\overset{K_D}{\rightleftharpoons}} [ENZ{\cdot}OP\text{-}X] \xrightarrow{k_p} ENZ\text{-}OP + X^- \quad (1)$$

$$k_i$$

A more useful parameter that describes the overall rate of inhibition is the bimolecular reaction (or rate) constant, k_i. This parameter is a function of both K_D and k_p ($k_i = k_p/K_D$) and is a measure of the potency of an OP inhibitor. The bimolecular inhibition reaction constant, k_i (as well as K_D) for OP's are determined experimentally by the following equation:

$$1/[i] = (\Delta t/\Delta \ln v)k_i - 1/K_D \quad (2)$$

where $[i]$ is the concentration of the OP inhibitor, Δt is the time that the AChE is reacted with the inhibitor, v is the activity or velocity of substrate breakdown by AChE, and $k_i = k_p/K_D$. Typically $1/[i]$ is plotted vs. $\Delta t/\Delta \ln v$ or $1/\Delta \ln v$ and k_i is the slope of the resultant line (Main 1964).

Inhibitory potencies (k_i) can also be determined experimentally by the use of the following equation:

$$\Delta \ln v = [i]k_i \Delta t \quad (3)$$

where the time dependent loss of enzyme activity is monitored in the presence of a single concentration of OP inhibitor (Aldridge 1950). This equation is more convenient to work with from an experimental point of view as it has one less variable and requires only one inhibitor concentration. This equation, however, ignores the reversible step of inhibition and is consequently most valid when K_D is several-fold greater than the inhibitor

concentration (Main 1964). Furthermore, Main (1964) established that k_i values obtained using this approach vary inversely with inhibitor concentration. This implies that the comparison of inhibitory potencies may be invalid if the inhibitor concentrations used for the evaluation are significantly different.

The bimolecular rate constant of inhibition, k_i, can also be expressed in terms of an IC_{50} value. This parameter represents the molar concentration of inhibitor that will result in a 50% reduction of enzyme activity during a discrete period of incubation with the inhibitor. Consequently, when used as a measure of OP reactivity toward AChE lower IC_{50} values are indicative of greater inhibitory potency. The IC_{50} value of a compound can be determined from the bimolecular rate constant of inhibition by the following relationship (Eto 1974).

$$IC_{50} = 0.695/(\Delta t k_i) \quad (4)$$

2.3.2-Physiologic Implications of OP Intoxication

OP inactivation of AChE results in the rapid accumulation of ACh in neuromuscular junctions and neural synapses promoting continued and uncontrolled neural transmission which eventually leads to desensitization, neuronal failure, and cell death. Inactivation of AChE is manifested in stimulation of the nicotinic and muscarinic receptors of autonomic organs and skeletal muscles, as well as over stimulation of cholinergic receptors (predominantly muscarinic) of the CNS. Consequently, the numerous symptoms elicited by exposure to OP compounds can be explained by considering the locations of nicotinic and muscarinic receptors throughout the central and peripheral nervous system

and the consequences of their activation. Many of these symptoms are summarized in Table 2.2. In addition to their potentially lethal acute cholinergic effects, organophosphorus compounds have been shown to: induce apoptosis of neuroblastoma cells (Carlson 2000); disrupt regulation of antioxidant enzymes (Panemangalore 2000); and interact with cholinergic receptors (Ward 1993; 1996; Zhang 1997; Lim 2000).

Table 2.2. Symptoms of Acetylcholinesterase Inhibition.

Nervous System	Receptor Type	Target Tissue	Symptoms
Central	Muscarinic and Nicotinic	Brain	Confusion, Hypothermia, Lethargy, Tremors, Slurred Speech, Loss of Reflexes, Depression, Convulsions, Coma, Paralysis
Peripheral	Muscarinic	Heart and Blood Vessels Lungs Bladder GI Tract Exocrine Glands	Bradycardia, Hypotension Bronchial Constrictions, Excess Secretions Incontinence Nausea, Vomiting, Diarrhea Salivation, Miosis, Sweating, Blurred Vision, Lacrimation
	Nicotinic	Heart and Blood Vessels Skeletal Muscle	Tachycardia, Hypertension Fasciculations, Ataxia, Weakness, Involuntary Twitching, Convulsions, Paralysis

Following inhibition, AChE may recover its enzymatic activity if the serine-phosphate bond is cleared via hydrolysis to regenerate an active serine residue. The mechanism of this type of reactivation is analogous to the second step of the AChE-catalyzed hydrolysis of ACh, i.e., the water facilitated hydrolysis of the acetoxy moiety depicted in Scheme 2.3. Unfortunately, the rate of this spontaneous reactivation for an enzyme inhibited by an OP compound is often far less ($>10^7$ fold) than the turnover rate of

the natural substrate (Eto 1974). Sequestration of the enzyme in its phosphorylated form inhibits the enzyme-catalyzed hydrolysis of ACh for extended periods of time *in vivo*.

Scheme 2.3. Spontaneous Reactivation of AChE.

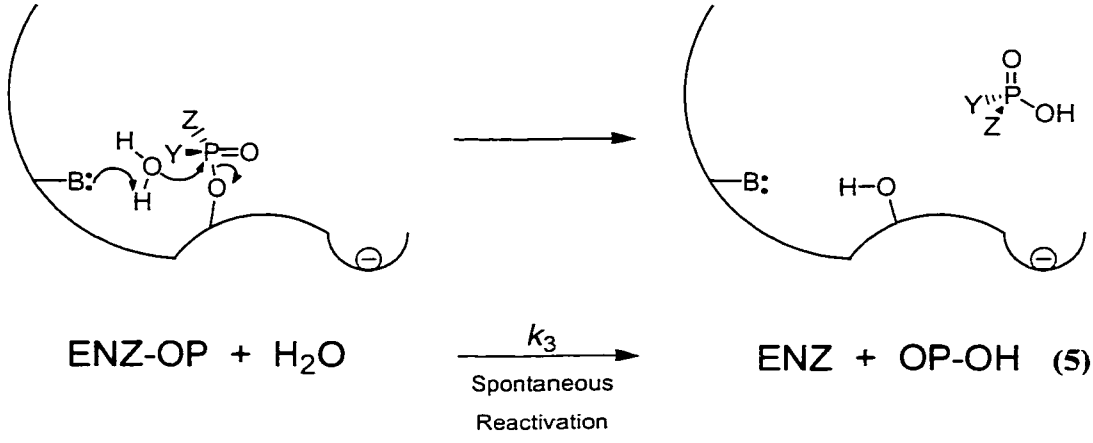

$$\text{ENZ-OP} + H_2O \xrightarrow[\text{Spontaneous Reactivation}]{k_3} \text{ENZ} + \text{OP-OH} \quad (5)$$

2.3.3-Non-Anticholinesterase Effects Associated with OP Exposure

Chronic low-level exposure to OP compounds has also been demonstrated to have deleterious effects. Since the introduction of these compounds, there have been several epidemics of OP poisonings including Ginger Jake paralysis, the Moroccan oil crisis, Spanish toxic oil syndrome, and Cuban blindness syndrome (Stine 1996; Purdey 1998). Further, OP compounds are implicated in a number of pathologies including organophosphorus compound-induced delayed neurotoxicity (OPIDN) (Randall 1997), polyneuropathy (McConnell 1994; Lotti 1999), sensory neuropathy (Stephens 1995; Moretto 1998), peripheral neuropathy (Ernest 1995; Amitai 1998; Burns 1998), Parkinson's disease (Bhatt 1999; Muller-Vahl 1999), motor neuron disease and multiple sclerosis (Purdey 1998), chronic neurological sequelae (Steenland 1994; Ames 1995),

distal axonopathies accompanied by disintegration of myelin (Stine 1996), asthma (Hodgson 1992), immune dysfunction (Thomas 1995), farmers' flu (Stephens 1995), psychiatric disorder (Stephens 1995), schizophreniform and depressive psychosis (Marrs 1995), chronic dietary poisoning (Hodgson 1992), miscarriages (Ballantyne 1992), induced hypothermia (Gordon 1998a), systemic illness (Weinbaum 1997), sleep disturbance (Bell 1996), skin disease (Weinbaum 1995), eye injury (Weinbaum 1995), Saku disease (Dementi 1994), birth defects (Sherman 1996), mental retardation (Claudio 2000; Goldman 2000; Weiss 2000), Gulf War syndrome (Ember 1996; Jamal 1998), intermediate syndrome (Mani 1992; Sudakin 2000), myalgic encephalomyelitis (ME) or chronic fatigue syndromes (Corrigan 1994), multiple chemical sensitivity (MCS) syndrome (Ashford 1998), delayed psycho-neurodegenerative syndrome (Purdey 1998), childhood leukemia (Meinert 2000; Schuz 2000), and a host of developmental abnormalities (Barr 1999; Xie 1999, 2000; Eriksson 2000; Lockridge 2000; Fordham 2001). OP compounds have also been cited as a potential cause of bovine spongiform encephalitis (BSE or mad cow disease) and the related human condition known as Creutzfeldt-Jakob disease (CJD) (Brugere-Picoux 1996; Purdey 1996a, 1996b, 1998; Axelrad 1998; Gordon 1998b).

2.3.4-Spontaneous Reactivation of AChE Inhibited by OP Compounds

The ability of AChE to spontaneously recover from inhibition by an OP compound is dependent upon a number of factors including the enzyme source, pH, ionic strength, and temperature (Lieske 1980, 1990; Lanks 1981; Fisher 2000). In addition, the rate at which AChE recovers from OP inhibition is also dependent upon the nature and reactivity of the

appended phosphoryl group (Lieske 1980, 1992; Clothier 1981; Langenberg 1988; Wallace 1988; Lotti 1991; Wilson 1992; Berkman 1993b; Ashani 1995; Wong 2000). The rate of spontaneous reactivation is greatest when OP compounds that contain less bulky ligands (Y and Z in Scheme 2.3) are used to inhibit AChE. One example of this phenomena is the observation that dimethoxy phosphorylated AChE (Y = Z = OCH_3) reactivates with rates that are 15 and 30-fold faster than the corresponding diethoxy and di-*n*-propoxy phosphorylated AChE, respectively (Gallo 1991). As a result, AChE possessing a di-isopropoxy phosphate moiety is essentially recalcitrant toward reactivation but is susceptible to other possible mechanisms (Eto 1974).

2.3.5-Oxime Mediated Reactivation of AChE Inhibited by OP Compounds

The observation that inhibited AChE could be reactivated by the nucleophilic attack of water led Wilson and colleagues to explore the possibility that reactivation may be promoted by use of stronger nucleophiles such as oximes (Wilson 1955; 1958). It has since been shown that reactivation of AChE is affected by several factors including the relative strength of the nucleophile, the orientation of the nucleophile with respect to the OP-AChE conjugate, and the prevention of the process known as 'aging' which is discussed in greater detail in the following section. These considerations have led to the development of various oximes as potential antidotes to AChE poisoning (Froede 1971; Wilson 1992) including 2-pralidoxime (2-PAM) **20**, 1-[4'-(aminocarbonyl)-1'-pyridinio]-methoxymethyl-2-(hydroxyiminomethyl)pyridinium (HI-6) **21**, and *N,N'*-trimethylenebis(pyridinium-4-aldoxime) (TMB-4) **22** (Wilson 1992). The structures of these compounds are illustrated in Figure 2.12.

Figure 2.12. Oxime Reactivating Agents.

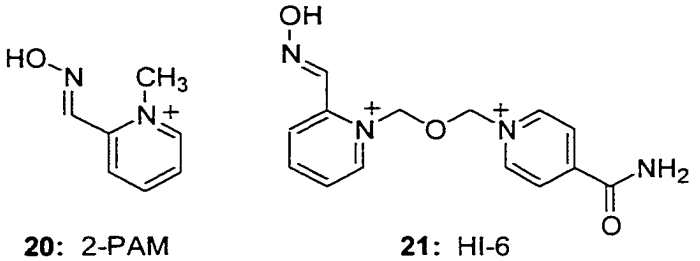

20: 2-PAM

21: HI-6

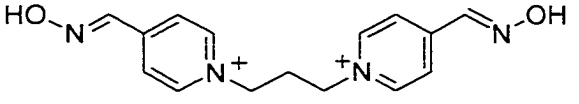

22: TMB-4

Nucleophilic reactivation of OP inhibited AChE is proposed to proceed via the mechanism outlined in Scheme 2.4 (Aldridge 1975; Luo 1999). As the process is similar to that of spontaneous reactivation it is not surprising that oxime-mediated displacement of the OP moiety is dependent upon both the source of the enzyme and the nature of the ligands attached to the phosphorus atom (Lotti 1991). As in the case of spontaneous reactivation, smaller ligands are displaced with greater efficacy than compounds with bulkier functionalities. This is demonstrated by the observation that the reactivation rate constant, k_3, for dimethyl phosphorylated AChE (Y = Z = OMe) is 60-fold greater than for the corresponding diethyl conjugate (Clothier 1981) which has been demonstrated to reactivate significantly faster than the diisopropyl OP-AChE conjugate (Taylor 1996). It is postulated that this trend is due in part to the dimensional constraints imposed by the gorge structure obstructing oxime access (Ashani 1995; Wong 2000).

Scheme 2.4. Oxime-Mediated Reactivation.

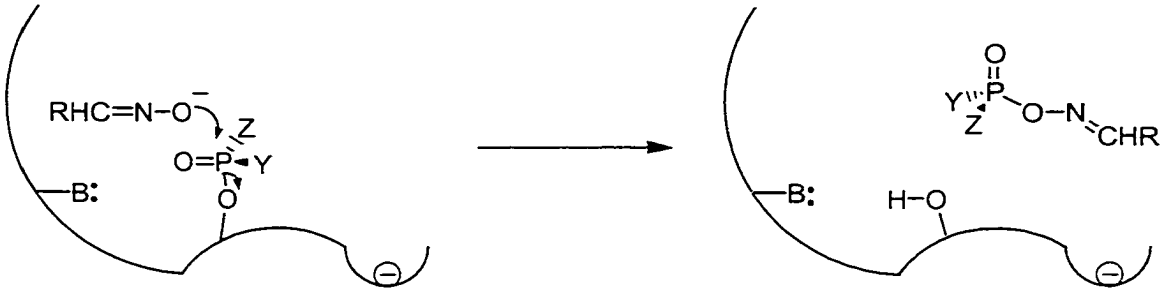

$$\text{ENZ-OP} + {}^{-}\text{ON=CHR} \xrightarrow[\text{Oxime-Mediated Reactivation}]{k_3} \text{ENZ} + \text{OP-ON=CHR} \quad (6)$$

2.3.6-Non-Reactivation and Aging of AChE Inhibited by OP Compounds

Some OP-enzyme adducts may undergo post-inhibitory reactions that include secondary dealkylation of the conjugated OP, resulting in an anionic phosphylated conjugate that is particularly resistant to all forms of reactivation, a process known as aging (Scheme 2.5). When compared to other serine hydrolases that catalyze phosphylation reactions with OP inhibitors, AChE has a remarkably enhanced rate of aging (Millard 1999b). The rate enhancement for AChE toward aging has been primarily attributed to the precise juxtaposition of the departing alkyl group with specific amino acid residues within the enzyme active site (Ashani 1995; Wong 2000).

Scheme 2.5. Aging of Phosphorylated AChE.

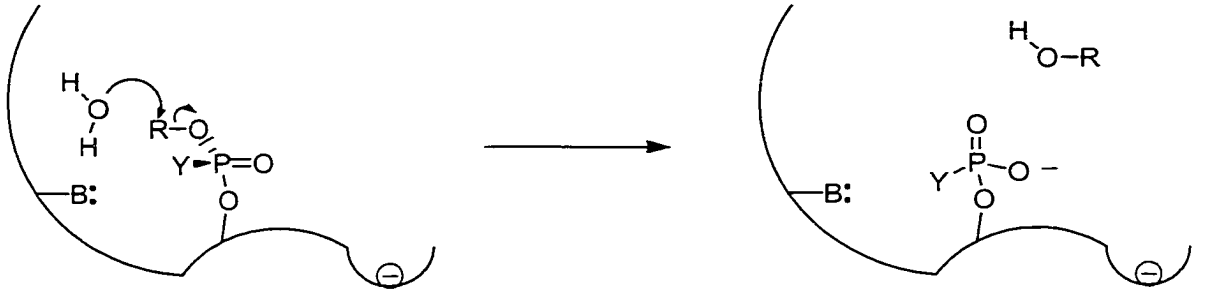

$$\text{ENZ-OP} + H_2O \xrightarrow{k_{AG}} \text{ENZ-OP}^- + \text{ROH} \quad (7)$$

The negative charge introduced by the loss of an alkyl group during the aging process imposes a significant subsequent barrier to dephosphylation due to the inherent resistance of anionic phosphoesters to nucleophilic attack (Westheimer 1987). However, electrostatic repulsion alone is an inadequate explanation of the truly irreversible character of aged AChE as the presence of a negative charge on simple phosphorus diesters retards nucleophilic attack by less than 100-fold (Kirby 1970). It has also been demonstrated that protein denaturation of aged AChE-DFP adducts permits significant base-catalyzed dephosphorylation (Segall 1993) and that reactivation of anionic OP-chymotrypsin conjugates by an intramolecular nucleophile is possible (Kaiser 1971). These observations suggest that aged OP-AChE resistance to reactivation is due, in part, to specific interactions between the OP and the structural constraints of the enzyme.

The report of the x-ray crystal structures of phosphylated *Tc*AChE combined with kinetic data for a number of AChEs modified by site specific mutagenesis has elucidated a number of structural futures that appear to facilitate the aging process (Millard 1999b). Prominent among these is the region defined by the amide backbone hydrogens of residues

Gly121, Gly122, and Ala204 (Sussman 1991). This portion of the enzyme active center, termed the oxyanion hole, is believed to stabilize the phosphonyl oxygen of an OP inhibitor through a hydrogen bond network and is thought to facilitate the reactions of inhibition and reactivation, and paradoxically, the mechanisms associated with aging (Hosea 1995; Wong 2000).

Polarization present in the P=O bond makes the phosphorus atom more susceptible to nucleophilic attack by both the serine hydroxyl during inhibition and the potentially reactivating nucleophiles, H_2O or oxime, during spontaneous or oxime-mediated reactivation, respectively (Hosea 1995; Wong 2000). That all of the resolved crystal structures from both aged and "pro-aged" AChE-OP conjugates available thus far have the phosphonyl oxygen positioned within hydrogen bonding distance of this region supports its putative role in stabilizing the bound OP adduct before, and after, aging (Millard 1999a; Millard 1999b; Ordentlich 1999). Aging may in fact enhance this interaction as electronic rearrangement could place the formal negative generated during the reaction partially, or entirely, in the dipolar oxyanion hole (Millard 1999b).

A final bit of evidence for the importance of this region is provided by site-specific mutagenesis. Replacement of Gly121 or Gly122 in human AChE (HuAChE) and equivalent residues in human BChE (HuBChE) has demonstrated markedly reduced reaction rate constants for OP inhibitors (Broomfield 1995; Millard 1995). In one study the decrease in inhibitory activity toward the Gly121Ala HuAChE mutant for the phosphates DEFP, DFP, and paraoxon and the phosphonates sarin and soman, was considerable (2000 to 6700-fold), irrespective of size of the alkoxy substituents on the phosphorus atom. This, however, contrasts with the data from the same study for the Gly122Ala

HuAChE mutant where the relative decline in reactivity toward phosphonates (460 to 500 fold) differed from that toward the phosphates (12 to 95-fold) (Ordentlich 1998).

The choline binding subsite, which is generally considered to be Trp86 (Harel 1996), has been strongly implicated as having an active role in the aging process. It has been suggested that Trp86 contributes to aging by stabilizing the evolving carbonium ion that is thought to form during postinhibitory reactions of S_P HuAChE-somanyl conjugates via a cation-π interaction. This assertion is supported by the observation that the Trp86Ala HuAChE mutation resulted in an 1850 to 3300-fold decrease in the rate of aging relative to the wild type (Shafferman 1996). However, it has subsequently been demonstrated that the rate enhancement is virtually nonexistent for the R_P soman diastereomers (Ordentlich 1999).

The acyl pocket defined by Phe295 and Phe297 is another region that has been demonstrated to play an active role in the process of aging. The planar aromatic side chains of Phe295 and Phe297 are believed to provide an environment of steric occlusion that in addition to conferring substrate specificity may hinder the access of H_2O or oxime-reactivating agents to the appropriate face of the OP-AChE conjugate thus precluding reactivation (Hosea 1995; Ordentlich 1999; Wong 2000). It has also been suggested that congestion conferred by these residues may actually prevent OP compounds with bulky ligands from undergoing the process of aging by perturbing the optimal alignment of the phosphonyl oxygen with the afore mentioned oxyanion hole (Wong 2000).

Another important structural feature suggested by the crystal structures of aged AChE is the favorable electrostatic interaction possible between the Nϵ2 of the active site

imidazolium and one of the oxygen atoms of the anionic OP moiety. Hydrogen bonding between His447 (the donor) and an oxygen of the OP moiety (the acceptor) demonstrates a geometry similar to that observed in other aged serine hydrolases (Kossiakoff 1981; Harel 1991; Wei 1995). The observations also provide support for the hypothesis that the catalytic histidine is immobilized in a protonated state in the aged enzyme, locking the phosphylated active site in a structural and electrostatic analog of the tetrahedral intermediate assumed by the natural substrate during hydrolysis (Kossiakoff 1980). The recent study of Millard *et al.* (Millard 1999a) demonstrates that the histidine of the catalytic triad assumes a radically different orientation prior to the aging reaction. The observation implies an active role for the residue during the aging process that is separate from its function of stabilizing the anionic product of the reaction.

Aging is not the only phenomenon that results in AChE that is resistant to reactivation. Non-reactivation, as defined by Thompson *et al.* (Thompson 1992), may be caused by a number of factors including; steric occlusion of the phosphorylated active site that restricts the access of reactivating nucleophiles due to the enzyme's limited ability to accommodate bulky ligands within its structure (Hosea 1995; Wong 2000), possible modification of the enzymes tertiary structure resulting in loss of normal enzyme function (Grubic 1995; Morel 1999; Sentjurc 1999), and covalent modification of a residue other than serine (Mullner 1980). That these post inhibitory processes result in a time-dependent loss of the enzyme's ability to reactivate but do not involve a secondary dealkylation of the OP-AChE adduct demonstrate that non-reactivation is clearly distinct from aging.

2.3.7-Influence of Stereochemistry on the Mechanisms of Inhibition, Reactivation, and Aging

Numerous studies using OP compounds with centers of asymmetry have demonstrated that the stereochemical orientation of the phosphorus moiety and, to a lesser extent, the attached alkyl carbons directly effects the inhibitory potency of an OP compound (Benschop 1984a; 1984b; de Jong 1984; 1987; 1989; Berman 1989; Hosea 1995; 1996; Ordentlich 1999; Wong 2000). In addition, oxime reactivation kinetics have also demonstrated structural and chiral preferences is for the attached organophosphorus (Wong 2000). The observations suggest orientational constrains for the OP compounds attack of the active site series and oxime attack of the phosphoserine that results from inhibition of AChE by an OP compound.

Studies of the inhibition and reactivation kinetics of a series of enantiomerically pure organophosphonates demonstrated that AChE was inhibited 200-fold faster with the S_P than the R_P enantiomer of cycloheptyl methylphosphonyl thiocholine (Hosea 1995; Wong 2000). The study demonstrated that enlargement of the acyl pocket size caused the R_P enantiomer to become more reactive while reaction with the S_P enantiomer was slightly reduced. In fact, the F297I mutant of rMAChE displayed inverted stereospecificity. The authors were able to use molecular docking experiments to construct a visual correlation of the kinetic data. If the phosphonyl oxygen was positioned in the oxyanion hole and the leaving group directed out of the gorge, the R_P, but not the S_P, enantiomer engendered steric hindrance between the alkoxy group and the acyl pocket. Replacing F297 with Ile accommodated the bulky alkoxy group of the R_P isomer in the acyl pocket, allowing similar orientations of the phosphonyl oxygen and the leaving group to the S_P isomer.

Later studies by the same group demonstrated that the S_P isomers of these types of compounds were in general comparatively more potent inhibitors of wild type AChE than the corresponding R_P isomers (Hosea *et al.* 1996). In contrast, phosphorylated enzymes resulting from inhibition by the S_P isomers have been demonstrated to undergo both spontaneous and oxime-mediated reactivation readily while AChE phosphorylated by the corresponding R_P isomers reactivate at greatly reduced rates (Wong 2000). The authors of these studies concluded the S_P isomers were better positioned for both the phosphorylating and dephosphorylating reactions within the confines of the enzymes active site.

These stereochemical trends in inhibitory potency have also been observed for a number of other compounds including the methyl phosponofluoridates sarin **2** and soman **3**. However, in the case of soman the reactivity of wild type HuAChE toward the S_P soman diastereomers was an amazing 4.0 to 7.5 x 10^4-fold higher than that toward the R_P diastereomers (Ordentlich 1999). Further, the recently released crystal structures of aged *Tc*AChE inhibited by sarin **2**, soman **3**, and DFP **5** suggest the orientation proposed by Hosea *et al.* (Hosea 1995; Wong 2000), with the phosphonyl oxygen positioned in the oxyanion hole and the leaving group directed out of the gorge, is essentially correct (Millard 1999b).

2.3.8-Summary

It is evident that the phosphorylation of AChE by an OP inhibitor, and the subsequent recovery of the enzymes catalytic activity, are directly associated with both the nature and stereochemical orientation of the OP compound. When compared to planar substrates, the ground-state tetrahedral geometry of OP anti-AChE compounds adds a

distinctive feature for mapping the three-dimensional organization of the enzyme. Of late, OP compounds that contain stereocenters within their structure have generated considerable interest due to their stereodependent interactions with the dissymmetric enzyme active site (Lin 1998; Yu 1998; Greenblatt 1999; Taylor 1999; Hirashima 2000; Wong 2000). The stereoselectivity displayed by AChE in reactions with OP compounds affords another aspect of structural information in the analysis of the steric and hydrophobic elements of the enzymes active center (Ordentlich 1999).

OBJECTIVES

1. Synthesize and characterize the individual stereoisomers of isomalathion to verify the synthetic route proposed by Berkman *et al.* (1993b).
2. Combine key reactions of the synthesis of isomalathion with the synthesis of isoparathion methyl (Ryu, 1991) to generate a new stereoisomeric isoparathion thiosuccinate phosphorothiolates (ITP) to be used as probes of cholinesterase.
3. Determine and compare the inhibitory and postinhibitory kinetic profiles for the individual isomalathion stereoisomers and the individual ITP stereoisomers vs. electric eel acetylcholinesterase (EEAChE) and recombinant mouse acetylcholinesterase (rMAChE).
4. Propose stereodependent phosphorylation model(s) and/or mechanisms consistent with the data obtained in Objective 3.

Chapter 4

SYNTHESIS

4.1-Isomalathion

Highly enantioenriched samples of each isomer were necessary for this study. There were two previously reported synthetic routes from which to choose (Berkman 1993b). The first method involved demethylation of (*R*)- or (*S*)-malathion **6** with (-)-strychnine to form the methylstrychninium desmethyl (*R*)- or (*S*)- malathion salts (**23R_PS_C** and **23S_PS_C** in Scheme 4.1). Repeated fractional crystallization of the resulting diastereomeric mixtures results in separation of the individual, "resolved" diastereomers. The individual phosphorothioic salts are then reacted with dimethyl sulfate (DMS), which leads to preferential sulfur alkylation (as opposed to oxygen alkylation), to afford each isomer of isomalathion. While this procedure is not technically complicated, it first involves the preparation of enantioenriched malathion followed by two different sets of conditions for dealkylating and realkylating the salts. This is of some concern as there is a moderately acidic α -proton on the stereogenic carbon of a diethyl malate derivative that may racemize. Further, under rigorous conditions, E_2-type elimination may be possible via abstraction of this proton to produce an alkene (diethyl maleate), which removes the asymmetry of the final product - disastrous to the synthesis.

Scheme 4.1. Synthesis of Isomalathion Stereoisomers via Strychnine Resolution of Malathion.

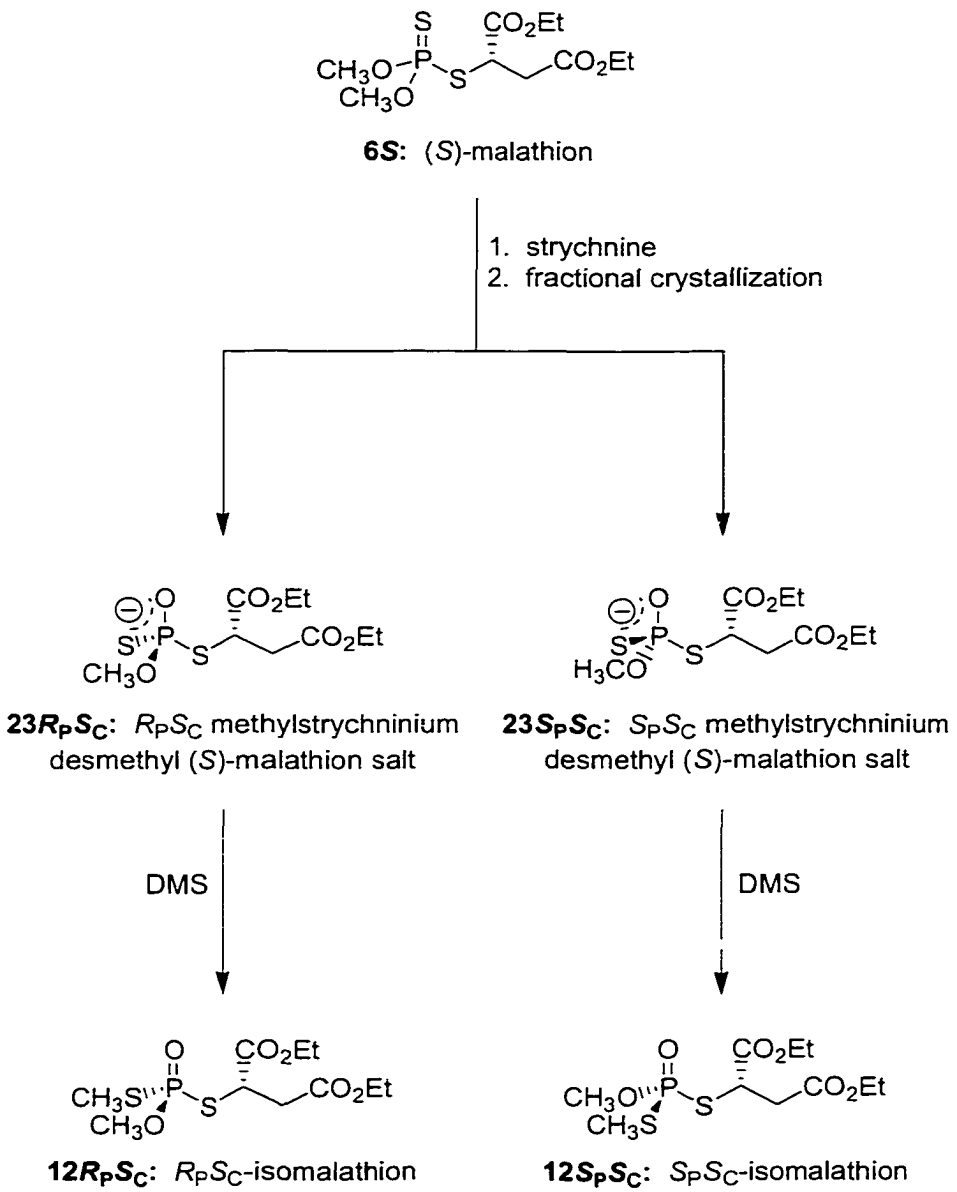

The second pathway, outlined in Scheme 4.2, begins with the demethylation of *O*,*O*,*S*-trimethylphosphorodithioate **24** by (-)-strychnine, followed by repetitive fractional recrystallization to resolve the diastereomeric methylstrychninium salts of *O*,*S*-dimethyl phosphorodithioate **25a** and **25b**. The pathway circumvents the problem of having carbon stereocenter present throughout several synthetic manipulations. The resolved salts are then reacted with the enantiomers of diethyl trifluoromethanesulfonyl malate (triflates; **26*R*** and **26*S***), which are derived from commercially available (-) and (+)-malate. As this method provided greater control over both the stereogenic carbon and phosphorus centers, it was deemed the more suitable and reliable pathway.

Scheme 4.2. Synthesis of Isomalathion Stereoisomers via Strychnine Resolution of O,O,S-Trimethylphosphorodithioate.

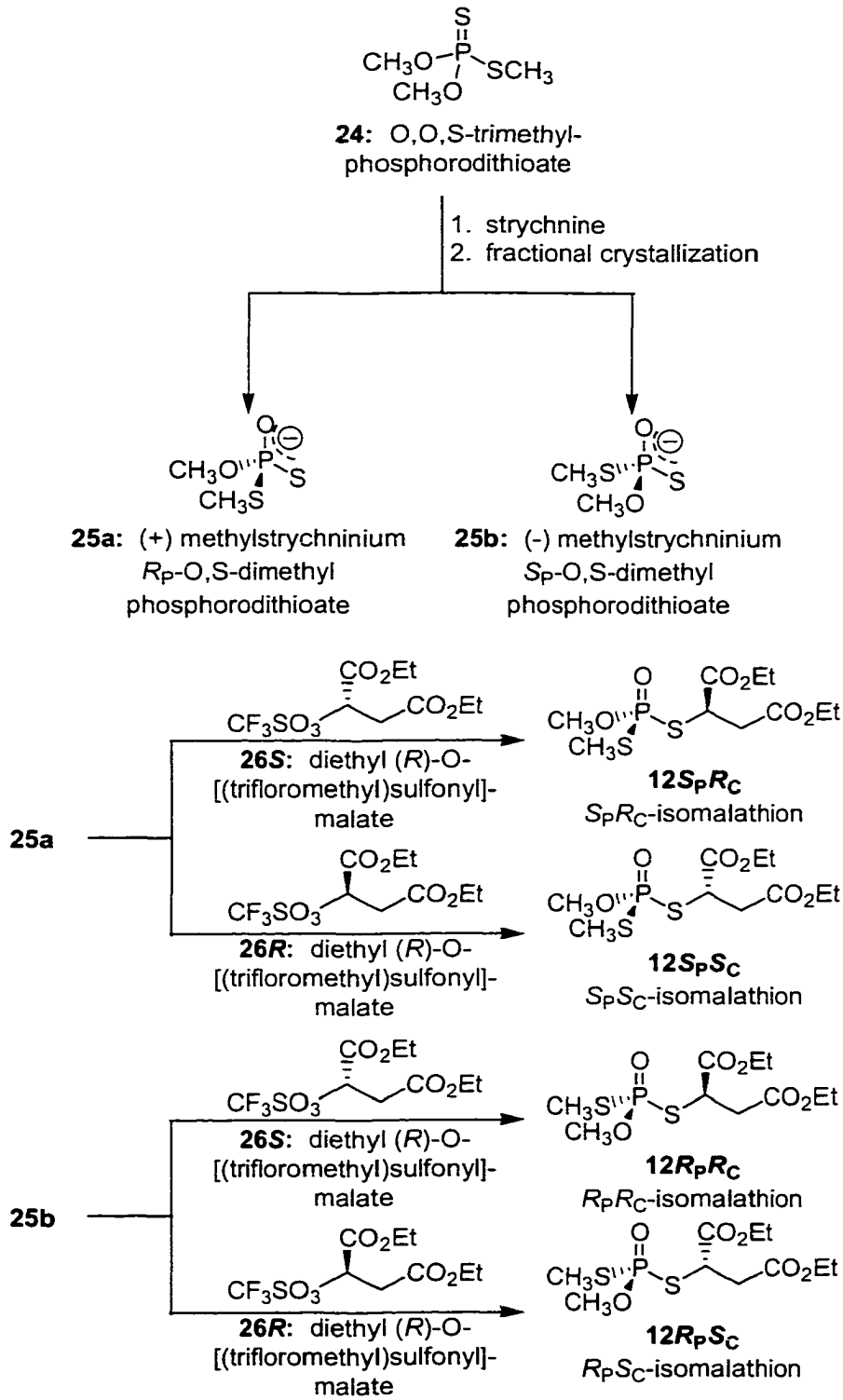

In order to attain the isomalathion stereoisomers by the path outlined in Scheme 4.2, multigram quantities of *O,O,S*-trimethylphosphorodithioate **24** were first required. *O,O,S*-Trimethyl phosphorodithioate is prepared from *O,O*-dimethyl phosphorodithioic acid **27**, which was obtained by refluxing a mixture of methanol and phosphorus pentasulfide (P_4S_{10}) in benzene for 48 h followed by filtration and evaporation of excess solvent and starting materials. The resultant reaction mixture affords a greenish, smelly oil (Scheme 4.3). This was then reacted with excess sodium bicarbonate in methanol to produce the sodium *O,O*-dimethyl phosphorodithioate salt (**28**, Scheme 4.3). Compound **28** was then alkylated by refluxing with dimethyl sulfate (DMS) in methanol for approximately three hours to generate crude *O,O,S*-trimethyl phosphorodithioate **24**. This crude solution was then filtered and dried down to a pale yellow oil which was further purified by Kugelrohr distillation (Scheme 4.3). Purified *O,O,S*-trimethyl phosphorodithioate was then refluxed in a solution of (-)-strychnine and methanol for approximately 24 hours which results in chemoselective removal of a methyl group from an oxygen ester (O-Me cleavage). Diastereomeric crystals of the methylstrychninium-*O,O,S*-dimethyl phosphorodithioate salts (**25a** and **25b**) were both deposited on cooling of the reaction mixture and upon selective fractional crystallization. The diastereomeric crystals were then dissolved in a minimum of hot methanol and allowed to crystallize overnight. This first crop of crystals was recrystallized twice more from methanol to produce the (+) salt (note: the (-) and (+) salts are so named because of their respective rotations; **25a**). The mother liquor from the first crop was evaporated down to a solid and crystallized three times from 95% ethanol to generate the (-) salt **25b**. Despite the reported "in-house" success of this procedure, it proved to be a cumbersome procedure and a severe

bottleneck. Multiple runs of this reaction were required in order to produce several grams of each diastereomer. Several grams were required because the majority of compound weight is made up in the strychnine-resolving agent, which is eventually discarded in favor of the phosphorus ester. Eventually, the desired products were isolated in low yield (10-20% compared with the 45% previously reported), however, these recoveries were offset by the excellent purity as demonstrated by the ^{31}P NMR analysis and the specific rotations (see Table 4.1).

With the resolved methylstrychninium-*O*,*O*,*S*-dimethyl phosphorodithioate salts (**25a** and **25b**) in hand, it was necessary to generate the triflates of (2*R*) and (2*S*) diethyl malate **26*R*** and **26*S***, which would be used to introduce the thiosuccinate ligand via S-displacement at the triflate center (Sn2). Bis-ethyl esterification of (*R*)- and (*S*)-malic acid **29*R*** and **29*S*** was accomplished by bubbling HCl gas through a solution of (*R*)- or (*S*)-malic acid in absolute ethanol. Upon bubbling the gaseous HCl, the solution warmed and the HCl introduction was halted. The reaction was capped and sealed at 0 °C for approximately 48 h. The product, (*R*)- or (*S*)-diethyl malates (**30*R*** and **30*S***) were then purified by Kugelrohr distillation. The spectral properties of each isomer were identical to that reported (Cohen, 1966) with the exception of the specific rotations which were roughly equal and opposite (see Table 4.1). The next step involved the conversion of the diethyl malate hydroxyl group into a good leaving group, in our case a triflate. The purified ester was mixed with 2-6-lutidine (a hindered base) in anhydrous methylene chloride and cooled to -78 °C to reduce elimination reactions. Trifluoromethanesulfonic anhydride was added and the reaction stirred at room temperature. Once this addition was completed, the mixture was gradually warmed to room temperature and mixed with diethyl ether and a

small amount of Celite® to precipitate out the resulting lutidine/ triflate salts. Owing to the high reactivity of the triflates, these compounds were used in the next step without further purification. Previous studies in our group (Berkman 1993a) showed that leaving groups other than triflate were not amenable to this reaction sequence.

Scheme 4.3. Production of Synthetic Intermediates.

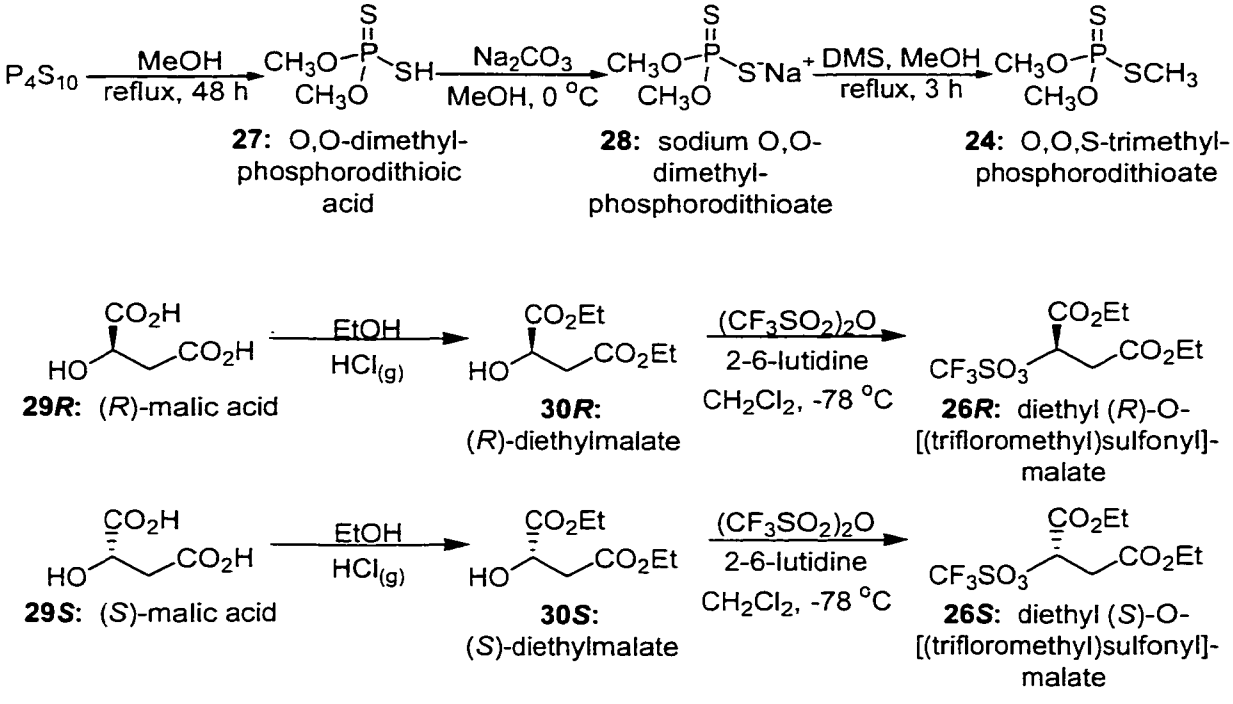

In order to minimize the potential for racemization, a small amount of the (*R*)- and (*S*)-triflates **26*R*** and **26*S*** were removed for spectral analysis and conformation of conversion while the remainder of each isomer was added immediately to a stirring suspension of either the (+) or (-) methyl strychninium salts **25a** and **25b** in acetonitrile that had been chilled to 0 °C. Once the addition of the respective triflate was completed the mixtures were allowed to come to room temperature and stirred for approximately two

hours. When the reaction had reached completion as demonstrated by TLC, diethyl ether and a small amount of Celite® was added to crash out the resulting triflate/strychninium salts. The mixtures were then filtered and dried down to a light tan oil containing putative, stereochemical pure isomalathion and approximately 10-20% of the O-alkylated side product. Each isomalathion isomer was then separated from its corresponding O-alkylated side product by silica gel chromatography (hexane/diethyl ether, 1:1) to give a colorless oil.

4.2-Malathion

The (*R*) and (*S*) triflates of diethyl malate **26*R*** and **26*S*** were added dropwise to stirring mixtures of the sodium *O,O*-dimethyl phosphorodithioate salt **28**, in THF, chilled to 0 °C to generate (*S*)- and (*R*)-malathion (**6*S*** and **6*R***) respectively (Scheme 4.4). These mixtures were then brought to room temperature and allowed to stir for approximately two hours until TLC indicated the reaction was complete. The mixtures were then partitioned between diethyl ether and water. After separation of the aqueous and organic layers, the aqueous layer was extracted two more times with diethyl ether. The ether layers were then combined, extracted with brine, dried over sodium sulfate, and concentrated to an oil. This was then purified by silica gel chromatography (hexane/diethyl ether, 1:1) to give a colorless oil.

Scheme 4.4. Synthesis of Malathion and Isomalathion.

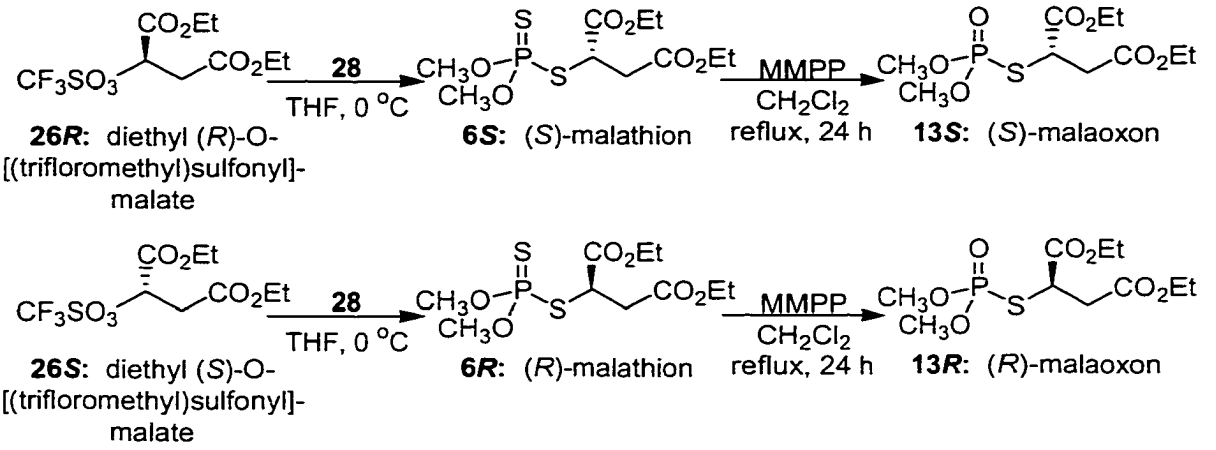

4.3-Malaoxon

(*R*)- and (*S*)-malaoxon **13*R*** and **13*S*** were also prepared for structural and inhibitory comparisons. To accomplish this, a portion of both the (*R*)- and (*S*)-malathion **6*R*** and **6*S*** samples were dissolved in methylene chloride and added to a stirring suspension of monoperoxyphthalic acid, magnesium salt (MMPP) in methylene chloride at room temperature (Scheme 4.4). The mixtures were then heated at reflux for 24 h and cooled to room temperature, and partitioned between diethyl ether and saturated sodium bicarbonate solution. Once the organic layer was separated, the aqueous layer was extracted twice more with diethyl ether. The organic layers were then combined, dried over sodium sulfate, and condensed to a colorless oil. The crude (*R*)-and (*S*)-malaoxon samples were then individually purified via gravity chromatography using silica (hexane/diethyl ether, 1:2).

4.4-ITP Stereoisomers

A modification of the pathway outlined in Scheme 4.2 was used to generate highly enantioenriched samples of the stereoisomers of a novel **i**soparathion **t**hiosuccinate **p**hosphorothiolate (ITP) compound **31**. Specifically, the diastereomeric methylstrychninium salt of isoparathion methyl **32a** and **32b** obtained from the demethylation of parathion methyl **7** by (-)-strychnine is followed by repetitive fractional recrystallization. The resolved (-) or (+) methyl strychninium salts **32a** and **32b** are mixed with THF and the resulting suspension chilled to 0 °C. The (*R*)- and (*S*)- triflates of diethyl malate **26*R*** and **26*S*** dissolved in THF at 0 °C are then added dropwise to the stirring mixtures. Once the addition of the respective triflate was completed the mixtures were allowed to come to room temperature and stirred for approximately two more hours. When the reaction had reached completion, as demonstrated by TLC, diethyl ether and a small amount of Celite® was added to precipitate the resulting triflate/strychninium salts. The mixtures were then filtered and dried down to an oil containing putative, stereochemical pure ITP. Each ITP isomer was then purified via flash chromatography on silica gel (diethyl ether/petroleum ether, 2:1) to give a colorless oil. During these studies it was observed that the stereoisomers of this particular compound were prone to undergo hydrolysis in protic solvents and during chromatography. Consequently, a small amount (< 5 %) of *p*-nitrophenol was detected in all samples. Repeated attempts to further purify the stereoisomers by flash chromatography resulted in significantly decreased yields.

Scheme 4.5. Synthesis of ITP Stereoisomers via Strychnine Resolution of Parathion Methyl.

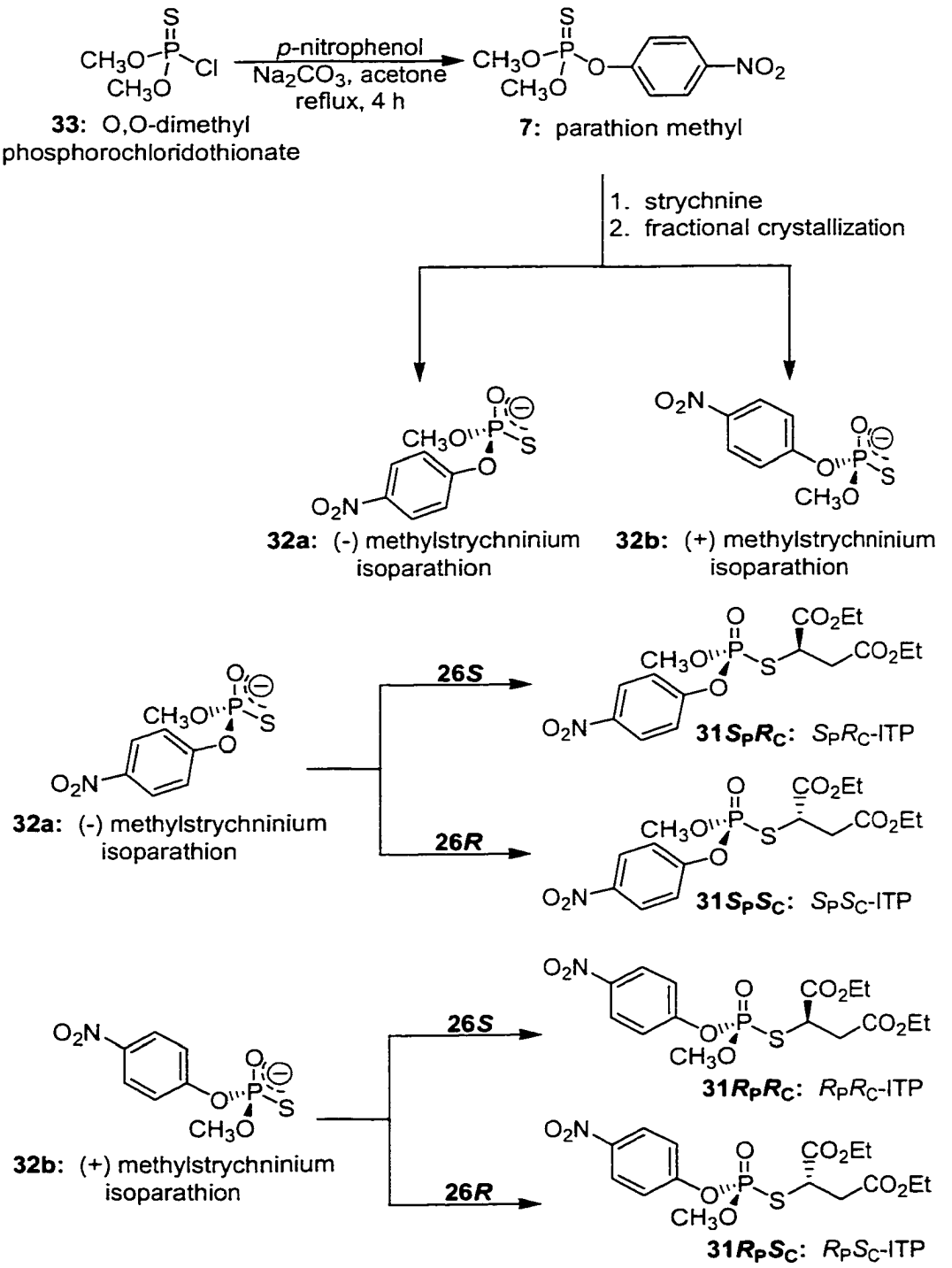

In order to attain the ITP stereoisomers by this method, multigram quantities of *O,O*-dimethyl-*p*-nitrophenoxy phosphorothionate (parathion methyl, **7**) was required. Parathion methyl is prepared by mixing *O,O*-dimethyl phosphorochloridothionate **33,** dissolved in anhydrous acetone, with anhydrous sodium carbonate. *p*-Nitrophenol is then added to the mixture and the resulting suspension is heated to reflux for approximately 4 h. When the reaction is complete, as demonstrated by TLC, the mixture is cooled to room temperature, filtered through a plug of Celite®, and evaporated to an oil. The oil is dissolved in diethyl ether, washed twice with saturated sodium carbonate and brine, dried over sodium sulfate, followed by evaporation of the excess solvent. The crude product is then purified by flash chromatography using silica (diethyl ether/petroleum ether, 1:3) to give a colorless oil.

Purified parathion methyl **7** was then refluxed in a equimolar solution of (-)-strychnine and methanol for approximately 24 hours which results in chemoselective removal of a methyl group from an oxygen ester (O-Me cleavage). Diastereomeric crystals of the methylstrychninium-isoparathion methyl salts (**32a** and **32b**) were deposited both on cooling of the reaction mixture and upon selective fractional crystallization. These diastereomeric crystals were then dissolved in a minimum of hot methanol and allowed to crystallize overnight. The first crop of crystals was recrystallized twice more from methanol to produce the (-) salt **32a**. The mother liquor from the first crop was evaporated down to a solid and crystallized three times from acetonitrile to generate the (+) salt **32b**.

4.5-Spectral Characterization

Once the isolation and purification of each compound was completed a full structural and stereochemical characterization was undertaken. Spectral data can sometimes provide excellent markers of chemical structure and stereochemical purity and, ^{1}H, ^{13}C, and ^{31}P (when applicable) NMR spectral analysis was conducted on each compound. As a number of the compounds were stereoisomers, the NMR spectral data was useful in confirming and comparing structures, but not absolute configuration assignment. While ^{31}P NMR was used to assess contamination by diastereomers, polarimetry was conducted on each chiral sample to estimate and verify its enantioenrichment (see Table 4.1).

The ^{31}P NMR data listed in Table 3 demonstrates what a powerful tool ^{31}P NMR can be. As there is a considerable difference in the chemical shift as one goes from a P=S to a P=O, it is quite easy to follow the course of a reaction. Furthermore, as each phosphorus atom in a phosphorus containing molecule produces only one sharp definitive peak with a chemical shift that is directly related to the phosphorus atom's immediate environment, phosphorus containing impurities are easily spotted.

Table 4.1. Spectral Data.

Compound	$[\alpha]_D^{24}$	^{31}P NMR δ
6*R* (*R*)-malathion	+79.7 (1.25)	96.15
6*S* (*S*)-malathion	-80.0 (1.25)	96.15
7 parathion methyl	-	66.09
13*R* (*R*)-malaoxon	+51.5 (0.59)	28.30
13*S* (*S*)-malaoxon	-49.2 (0.63)	28.30
12*RR* (R_PR_C)-isomalathion	+42.0 (0.57)	58.30
12*RS* (R_PS_C)-isomalathion	-57.5 (0.63)	56.91
12*SR* (S_PR_C)-isomalathion	+58.9 (0.67)	56.90
12*SS* (S_PS_C)-isomalathion	-44.2 (0.62)	58.27
25a (+) methylstrychninium O,S-dimethyl phosphorodithioate	+16.2 (0.64)	78.87
25b (-) methylstrychninium O,S-dimethyl phosphorodithioate	-13.4 (0.63)	78.79
30*S* (*S*)-diethyl malate	-9.82 (0.55)	-
30*R* (*R*)-diethyl malate	+9.59 (1.35)	-
26*S* (*S*)-O-(Trifluoromethanesulfonyl)-diethylmalate	+32.6 (1.39)	-
26*R* (*R*)-O-(Trifluoromethanesulfonyl)-diethylmalate	-30.1 (1.71)	-
32a (-) methylstrychninium isoparathion	-22.9 (0.45)	55.85
32b (+) methylstrychninium isoparathion	+23.0 (0.10)	55.85
31*RR* (R_PR_C)-ITP	+13.0 (1.10)	23.76
31*RS* (R_PS_C)- ITP	-16.3 (0.91)	23.68
31*SR* (S_PR_C)- ITP	+16.0 (0.86)	23.67
31*SS* (S_PS_C)- ITP	-12.9 (1.00)	23.75

Chapter 5

RESULTS AND DISCUSSION

5.1-Determination of the Kinetic Properties of rMAChE and EEAChE.

To ensure that optimal substrate concentrations were used during these studies, the rate of ATCh-I hydrolysis, v, was determined for a series of substrate concentrations, [S], for both EEAChE and rMAChE. The average of 20 experiments (n = 20) per enzyme is graphically represented in Figure 5.1. The values from the logarithmic portion of the graph generated from each experiment were subjected to Lineweaver-Burk, Eadie-Hofstee, and Woolf analysis to determine the apparent Michaelis-Menten constants (K_m apparent) and the value of V_{max} for both enzymes. These three methods of analysis were chosen to facilitate direct comparison of the kinetic parameters obtained with those found in a wide spectrum of the contemporary literature. The mean and standard deviation of the values obtained from each of these methods of analysis are listed in Tables 5.1 and 5.2 for EEAChE and rMAChE, respectively. The values of K_m apparent generated are within reasonable agreement of the 46 μM value published by others using more rigorous methods of analysis (Hosea 1996).

Figure 5.1. Concentration Dependence of Acetylthiocholine Hydrolysis for EEAChE and rMAChE.

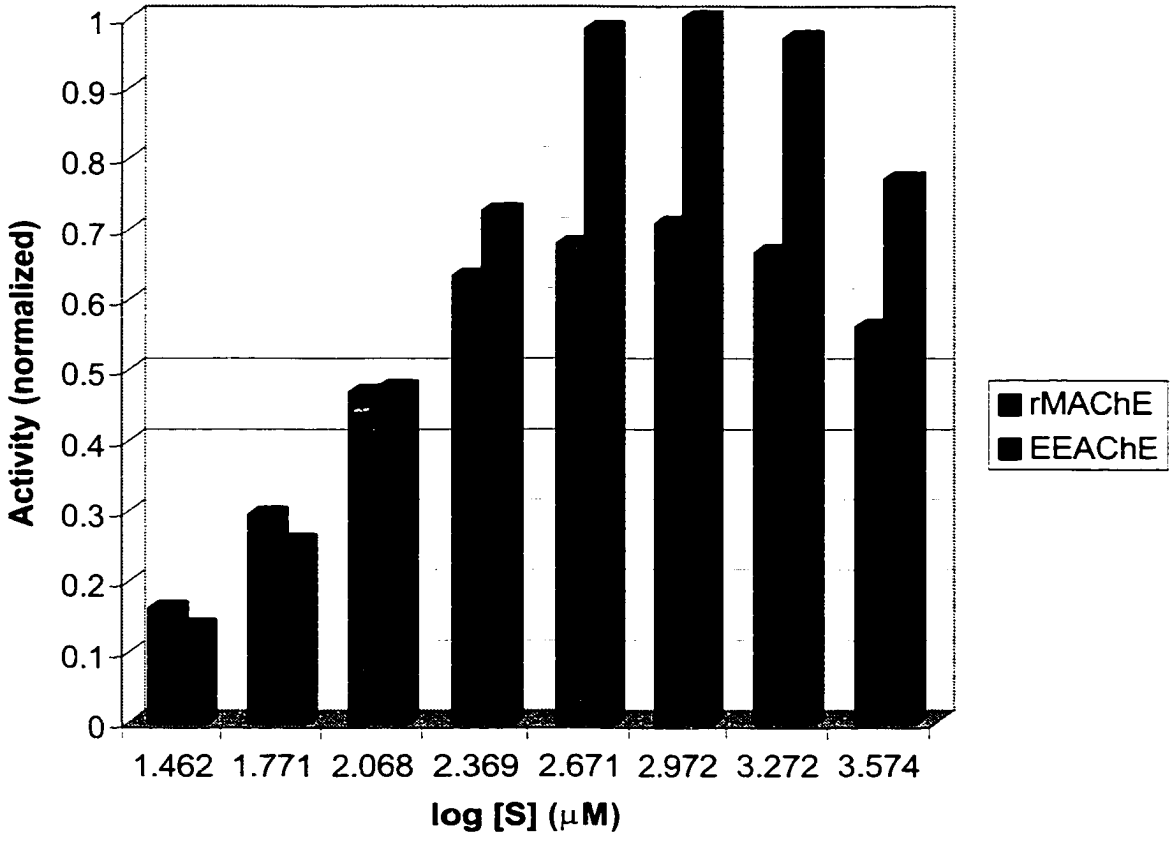

Table 5.1. Apparent Michaelis-Menten Kinetic Constants for the Hydrolysis of ATCh-I by EEAChE[a].

Method	K_m Apparent (μM)	V_{max} (s^{-1})	R^2
Lineweaver-Burk	215 ± 48	222 ± 48	0.999
Eadie-Hofstee	200 ± 26	213 ± 24	0.991
Woolf	205 ± 30	214 ± 15	0.992

[a] n = 20

Table 5.2. Apparent Michaelis-Menten Kinetic Constants for the Hydrolysis of ATCh-I by rMAChE[a].

Method	K_m Apparent (μM)	V_{max} (s^{-1})	R^2
Lineweaver-Burk	93 ± 5	81 ± 3	0.994
Eadie-Hofstee	84 ± 4	77 ± 3	0.996
Woolf	79 ± 7	75 ± 4	0.999

[a]n = 20

It is important to note that, as demonstrated by the data presented in Figure 5.1, enzyme activity decreases slightly at very high substrate concentration. This phenomenon, termed substrate inhibition, is well documented for AChE (Quinn 1987; Taylor 1994) and a number of other enzymes including fumarase and ribonuclease exhibit this process (Aldridge 1975). The process has been proposed to occur directly at the active center (Froede 1986) or indirectly through interactions with a peripheral site which are believed to either induce conformational changes to the active center of the enzyme allosterically (Barak 1994; 1995; Ordentlich 1995; Velan 1996; Marchot 1998; 1999; Radic 2000) or by formation of a "steric blockade" of the entrance to the active site (Rosenberry 1996; 1999; Szegletes 1998; 1999; Mallender 1999; 2000). Studies using ligands selective for the peripheral anionic site combined with site-specific mutagenesis suggest that the binding site for substrate inhibition may consist of structural elements that overlap with, or are the same as, those that make up the peripheral anionic site (Radic 1991; 1994; Shafferman 1992; Duran 1994; Bourne 1995; 1999; Velan 1996; Marchot 1999).

The phenomenon contrasts with the apparent substrate activation that has been observed for BuChE (Radic 1993; Vellom 1993). It has been demonstrated through the use

of site-specific mutagenesis that replacement of residue Phe297 of rMAChE with an isoleucine residue (F297I) not only eliminates the substrate inhibition observed with ATCh-I for the wild type enzyme, but also confers some elements of substrate activation seen for BuChE (Vellom 1993). It has been proposed that the physiological role of substrate inhibition may be an essential element in the regulation of the residence time of ACh in the synaptic cleft. A sensor site, such as the peripheral anionic site on AChE, could trigger an inhibitory response to the initially high concentration of ACh near the presynaptic membrane. This could allow ACh to diffuse into the synaptic cleft to interact with the receptor prior to its hydrolysis by an AChE (Shafferman 1992).

5.2-Inhibition of rMAChE and EEAChE by DFP.

The neurotoxic compound DFP was evaluated as an inhibitor of EEAChE and rMAChE to provide a frame of reference with better known OP compounds and to serve as an external standard during the development of the microplate assays outlined in Methods 3 and 4 of Section 7.3.3. Despite its lack of a center of asymmetry, the decision to use DFP was based upon the extensive body of literature available for the compound, the well documented postinhibitory properties of the compound (i.e. inhibition of AChE with DFP *eventually* leads to an aged enzyme), and the commercial availability of the compound. The kinetic parameters k_i, K_D, and k_p were determined experimentally using Eqn. 2 (Section 2.3.1) and are listed in Table 5.3. The values obtained are in excellent agreement with those previously reported for HuAChE and *Tc*AChE (Millard 1999b).

Table 5.3. Concentration Dependent Kinetic Data for the Inhibition of rMAChE and EEAChE by DFP[a].

Enzyme Source	k_i ($\times 10^3$ M^{-1} min^{-1})	K_D (μM)	k_p (min^{-1})
rMAChE	29 ± 5	51 ± 7	1.5
EEAChE	12 ± 3	34 ± 6	0.4
TcAChE[b]	20 ± 1	70 ± 20	1.5
HuAChE[b]	50 ± 1	13 ± 2	0.6

[a]n = 11
[b](Millard 1999b)

In addition, the kinetic parameters for both spontaneous reactivation and reactivation in the presence of an oxime (2-PAM and TMB-4) were determined experimentally using Eqn 7 (Section 7.3.3) and the results obtained are listed in Table 5.4.

Table 5.4. Reactivation Data for rMAChE and EEAChE Inhibited by DFP[a].

Enzyme Source	k_3 (spon) min^{-1} ($\times 10^{-3}$)	% spontaneous reactivation	K_3 (2-PAM) min^{-1} ($\times 10^{-3}$)	% 2-PAM reactivation	k_3 (TMB-4) min^{-1} ($\times 10^{-3}$)	% TMB-4 reactivation
rMAChE	0.3 ± 0.1	<1	5.2 ± 2	3.1	9.8 ± 3	6.5
EEAChE	0.8 ± 0.2	<1	6.9 ± 1	5.7	14 ± 6	8.4

[a]n = 8

The results confirm the observation that DFP is only a moderately potent inhibitor of AChE. This is due primarily to the steric properties of the isopropyl ligands hindering the compounds approach to the active site within the spatial confines of the enzyme (Gallo 1991). In contrast, the data presented in Table 5.4 demonstrates the irreversible nature of

DFP inhibition. As discussed in Section 2.3, the effect is believed to be due, in part, to the dimensional constraints imposed by the gorge structure obstructing the access of potentially reactivating nucleophiles (Ashani 1995; Wong 2000).

5.3-Inhibition of EEAChE by the Stereoisomers of Isomalathion

To examine the stereoselective inhibition of EEAChE, the inhibition kinetics profiles of the individual stereoisomers of isomalathion were determined in a concentration dependent manner as described in Methods 3 and 4 of Section 7.3.3 using Eqn. 2 and the kinetic parameters determined are presented in Table 5.5. A 4-fold difference in anti-AChE potency was found between the strongest isomer, S_PR_C -isomalathion, and weakest isomer, S_PS_C isomalathion. The isomalathion stereoisomers with *R* configuration at the asymmetric carbon displayed greater inhibitory potency toward EEAChE than those with the *S* configuration at the asymmetric carbon. However, the attenuation of the inhibition reaction by the stereogenic carbon was further modulated by the chirality of the phosphorus-containing portion of the molecule. The difference in inhibitory strength when changing the configuration at carbon from *R* to *S* was 4.7-fold when the configuration at phosphorus was *S*. In contrast, the difference was only 1.5-fold when comparing the two isomers that had the *R* configuration at phosphorus. In a similar fashion, the carbon stereocenter attenuated the effect on inhibitory potency exerted by the stereochemical orientation of the phosphorus. A comparison between the isomers that had *S* or *R* configuration at the phosphorus demonstrate a 1.8-fold difference in inhibitory potency when the stereochemical orientation of the carbon is *R*, but only a 1.2-fold difference in inhibitory potency is observed for the stereoisomers with the *S* configuration at carbon.

These observations demonstrated that the carbon and phosphorus asymmetric centers of isomalathion act independently during the inhibition of EEAChE and are consistent with the observations obtained during previous studies (Berkman 1994). That the stereochemical orientation of the carbon has less of an effect on the inhibitory potency of an OP compound with two stereocenters relative to the influence of the configuration at phosphorus is also consistent with the observations of others (Ordentlich 1999).

Table 5.5. Concentration Dependent Kinetic Data for the Inhibition of EEAChE by Isomalathion Stereoisomers[a].

Isomer	k_i ($\times 10^3$ M^{-1} min^{-1})	K_D (μM)	k_p (min^{-1})
R_PR_C	25 ± 10	7.8 ± 3	0.20
R_PS_C	17 ± 4	8.2 ± 2	0.14
S_PR_C	44 ± 12	32 ± 8	1.4
S_PS_C	12 ± 3	250 ± 56	3.0

[a] n = 20

The kinetic parameters K_D and k_P were also determined for the interactions of the individual isomalathion stereoisomers with EEAChE (Table 5.5). As reported for the stereoisomers of malaoxon (Berkman 1994), the k_i values typically paralleled the dissociation constants, K_D, such that the isomer with the greater affinity for the active site was the stronger inhibitors. An example of this is displayed by the 7.8-fold stronger

affinity for (or weaker disassociation from) the active site determined for the *S*, *R* isomer versus it's *S*, *S* counterpart and was a 3.7-fold more potent inhibitor. However, as implied by Eqn. 2 a compound's affinity for the active site is not the only determinant of inhibition. A comparison of the K_D values obtained for the *R*, *R* isomer and the *S*, *S* isomer would lead one to expect a 32-fold difference in inhibitory potency. This is in contrast to the 2.1-fold difference in inhibitory potency observed for the two isomers. These observations can, in part, be rationalized by the unusual magnitude of k_p (3.0) for the *S*, *S* isomer. The reactivity of the compound toward the enzyme, k_p, partially compensates for the poor affinity toward the active site.

The values determined for the kinetic parameter k_p during the inhibition of EEAChE by *R*, *R* and *R*, *S* isomalathion stereoisomers are nearly identical, consistent with the results reported for the inhibition of RBAChE by malaoxon (Berkman 1994). This is in contrast with the more than 2.1-fold difference observed in the k_p values determined for the *S*, *S* and *S*, *R* isomers. That the stereochemistry of the carbon significantly influenced the phosphorylation only when the *S*, *S* and *S*, *R* isomers of isomalathion were used as the inhibitors suggest that the thiosuccinyl ligand remains attached following inhibition by these isomers as depicted in Path B of Scheme 5.1. Conversely, the lack of significant variance in the observed k_p values for the *R*, *R* and *R*, *S* can be rationalized if the thiosuccinyl ligand is the primary leaving group thus negating its ability to exert stereochemical influence over the reaction as depicted in Path A of Scheme 5.1.

Scheme 5.1. Proposed Mechanisms for the Inhibition of AChE by Isomalathion.

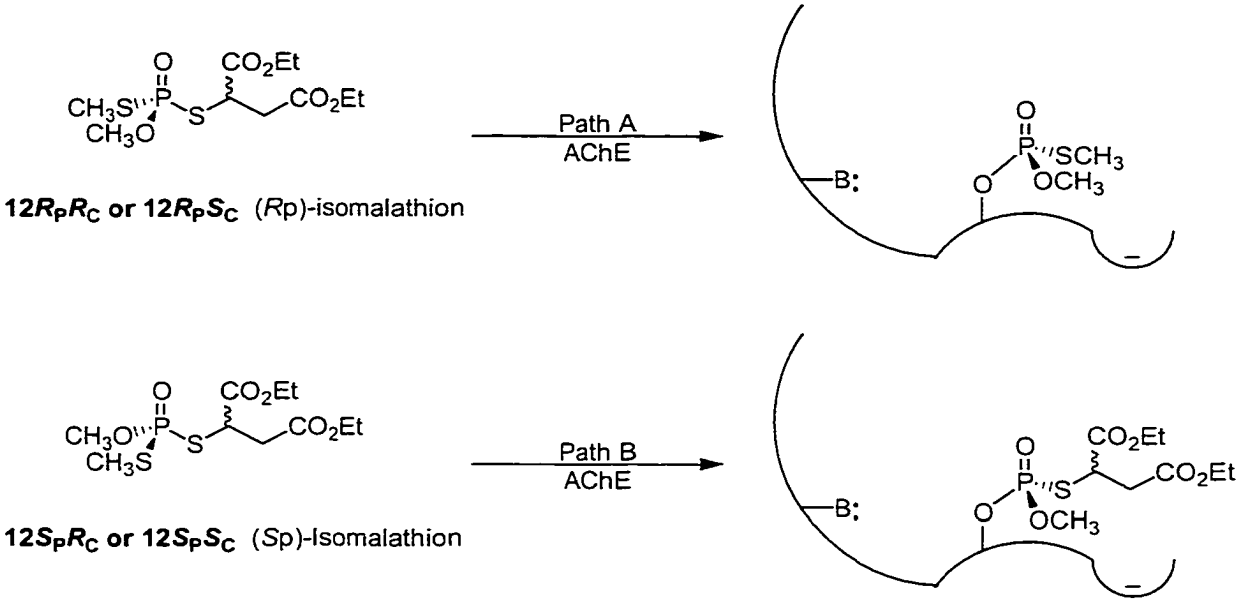

12R_PR_C or 12R_PS_C (*R*p)-isomalathion

12S_PR_C or 12S_PS_C (*S*p)-Isomalathion

The time-dependent method for determining the bimolecular rate constant of inhibition (k_i) against EEAChE was also performed for the isomalathion stereoisomers. The values are presented in Table 5.6. The values generated by this method show the same inhibition trend and stereoisomer preference but the concentration dependent data (Table 5.5), does differ significantly in key elements (Figure 5.2). First, it is noteworthy that the rank order of inhibitory potency ($S_PR_C > R_PR_C > S_PS_C > R_PS_C$) is conserved between the two methods.

Table 5.6. Time Dependent Kinetic Data for the Inhibition of EEAChE by the Isomalathion Stereoisomers[a].

Isomer	k_i ($\times 10^3$ M^{-1} min^{-1})
R_PR_C	21 ± 3
R_PS_C	0.63 ± 1
S_PR_C	144 ± 6
S_PS_C	3 ± 1

[a] n = 10

Figure 5.2. Comparison of the Bimolecular Rate Constants of Inhibition ($k_i \times 10^3$ M^{-1} min^{-1}) Obtained by the Concentration Dependent Method and Time Dependent Method for the Inhibition of EEAChE by the Stereoisomers of Isomalathion.

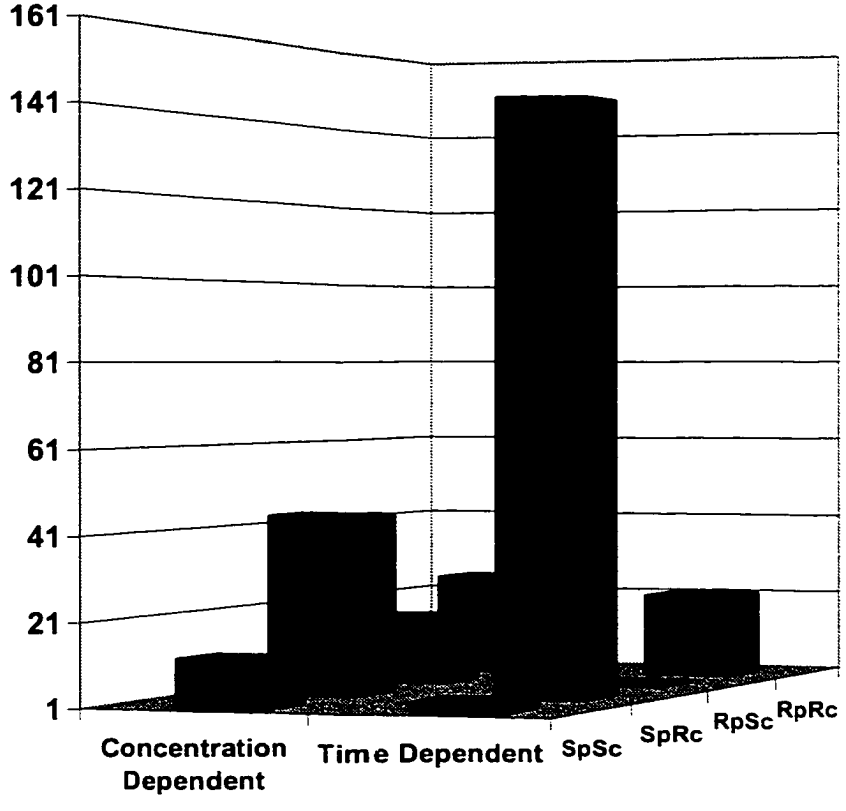

During the course of the time-dependent experiments it was observed that EEAChE inhibited by the stereoisomers containing the *S* configuration at phosphorus consistently provided linear data similar to that shown in Figure 5.3 (Panel A). In contrast, the data obtained by this method of analysis for EEAChE inhibited by the isomers that were *R* configuration at phosphorus was consistently non-linear despite repeated variance of the

inhibitor concentration and numerous attempts to attenuate the conditions of the study (Figure 5.3, Panel B). These differences in inhibitory behavior provide further evidence that the isomers of isomalathion interact with EEAChE by two distinctly different mechanisms dependent upon the stereochemical orientation of the phosphorus. Further, these results were so intriguing that a detailed kinetic analysis of the phenomenon was conducted which is detailed in a subsequent section.

Figure 5.3. Comparison of the Data Obtained from the Inhibition of EEAChE by Isomalathions (Panel A) and the R_P Isomalithion (Panel B) During the Time Dependent Method of Analysis.

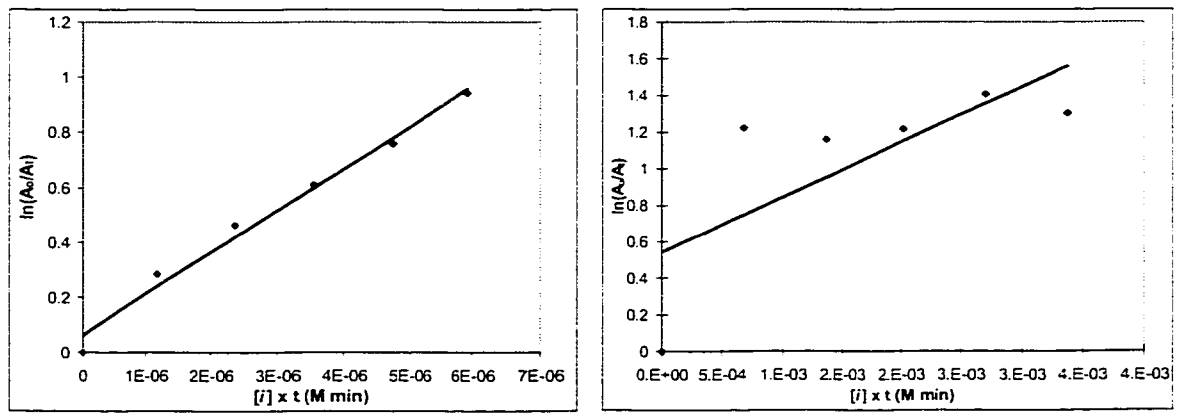

Panel A. Panel B.

5.4-Inhibition of rMAChE by the Stereoisomers of Isomalathion

To explore the possibility of species-dependent variations in stereoselectivity (Lee 1978; Wallace 1991), inhibition of rMAChE by the isomalathion stereoisomers was investigated. Further, a recombinant source of mammalian AChE was sought as recent studies have demonstrated the presence of other esterases in the tissue homogenates traditionally used during anti-AChE assays that can directly influence the kinetic parameters obtained from them (Mortensen 1998; Moretto 2000). Also, observations by members of our group have identified a number of impurities present in the commercial preparations of EEAChE that may affect the outcome of studies preformed with this source (George 2000). In addition to the well-documented purity of rMAChE, its extensive characterization and the prevalence of this enzyme source in the contemporary literature facilitates direct comparison of results obtained from it.

The kinetic parameters k_i, K_D, and k_p for the inhibition of rMAChE by the isomalathion stereoisomers were determined experimentally using Eqn. 2 and the results obtained are presented in Table 5.7. The 40-fold difference in anti-AChE potency between the weakest isomer (S_PS_C isomalathion) and the most potent isomer (R_PR_C isomalathion) was considerably greater than that observed for EEAChE. That rMAChE demonstrated a greater ability to discriminate between the stereoisomers was not unexpected as species-dependent, stereoselective inhibition against varying sources of AChE has been observed for the fonofos oxon enantiomers (Lee 1978). The results from the inhibition of AChE obtained from several different sources by the stereoisomers of isomalathion are represented in Figure 5.4 for comparison.

Table 5.7. Concentration Dependent Kinetic Data for the Inhibition of rMAChE by the Isomalathion Stereoisomers[a].

Isomer	k_i ($\times 10^3$ M^{-1} min^{-1})	K_D (μM)	k_p (min^{-1})
R_PR_C	190 ± 34	0.89 ± 0.3	0.17
R_PS_C	42 ± 6	9.3 ± 2	0.39
S_PR_C	32 ± 4	150 ± 30	4.8
S_PS_C	4.8 ± 2	770 ± 80	3.7

[a] n = 20

Figure 5.4. Comparison of the Bimolecular Rate Constants of Inhibition ($k_i \times 10^3$ M^{-1} min^{-1}) for AChE from Different Sources Inhibited by the Stereoisomers of Isomalathion[a].

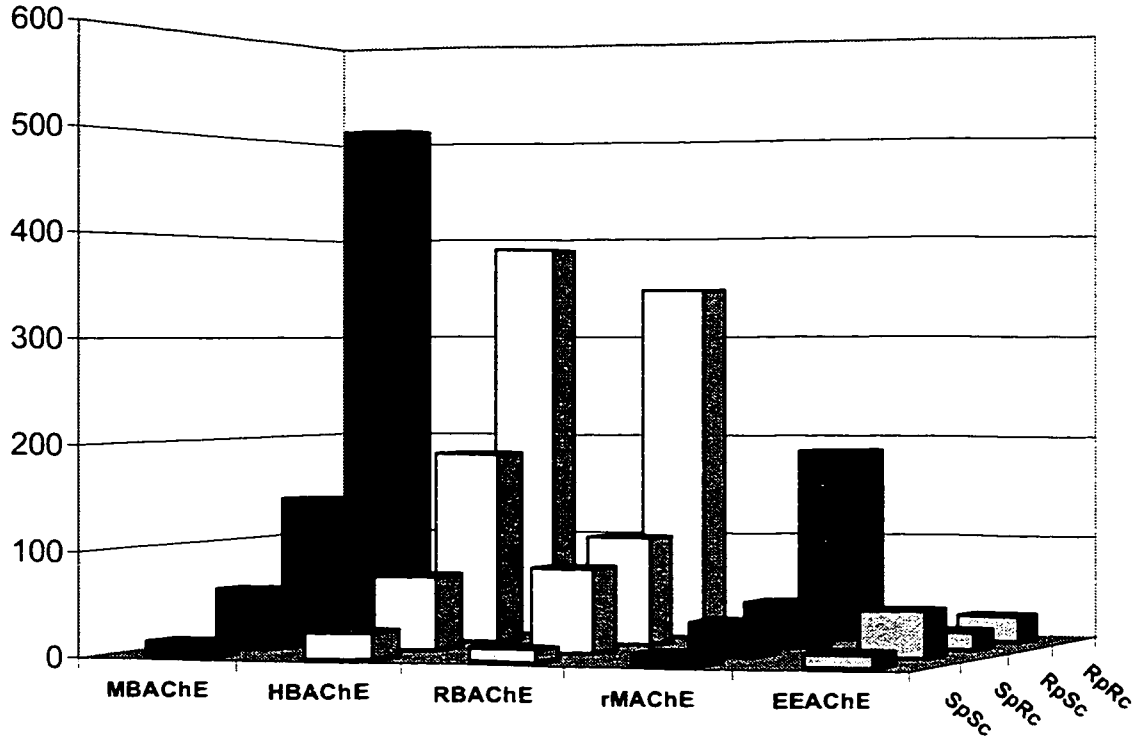

[a]Mouse brain AChE (MBAChE); hen brain AChE (HBAChE) (Jianmongkol 1999); rat brain AChE (RBAChE) (Berkman 1993a)

Both R_PR_C- and R_PS_C-isomalathion were more potent inhibitors of rMAChE than the corresponding isomers with *S* configuration at phosphorus. This trend in inhibitory potency has been observed for a number of OP compounds that are structurally equivalent including *S* isoparathion methyl (Ryu 1991), the chemical warfare agents sarin and soman (Millard 1999b; Ordentlich 1999; Spruit 2000), and a series of chiral organophosphonates

(Hosea 1995; Hosea 1996; Wong 2000). It has been demonstrated that the acyl pocket region of the enzymes active site is primarily responsible for dictating the enantiomeric preference displayed by AChE. Specifically, site-specific mutagenesis and crystallographic studies combined with molecular docking experiments have implicated Phe295 and Phe297 of mammalian AChE as dominant residues (Hosea 1995; Hosea 1996; Millard 1999b; Ordentlich 1999; Wong 2000). It has been proposed that the influence of these residues is due to their ability to sterically hinder the approach of one stereoisomer relative to another thereby reducing the compounds ability to achieve the orientation necessary for optimal phosphonyl transfer (Hosea 1995; Hosea 1996). It has also been demonstrated that in addition to governing the stereoselectivity of AChE with respect to the phosphorus chirality that, at least for soman, this region plays a role in determining the enzyme's ability to discriminate between stereoisomers that only differ in the orientation of their stereogenic carbon (Ordentlich 1999).

As observed for EEAChE, the inhibition of rMAChE was dependent upon the stereochemical orientation of both the phosphorus atom and the asymmetric carbon present in the isomalathion stereoisomers. A 6-fold difference in inhibitory potency is observed for the isomers that were *R* at carbon when the orientation of the phosphorus was switched from *R* to *S* while an 8.8-fold difference observed when the configuration at carbon was *S*. In contrast, changing the orientation of the asymmetric carbon from *R* to *S* resulted in a 4.5-fold difference in inhibitory potency when the orientation at the phosphorus was *R* while a difference of 6.7-fold was observed between the isomers that were *S* at phosphorus.

The k_p values obtained for the inhibition of rMAChE by the R_PR_C and R_PS_C isomalathion isomers were very similar in magnitude, consistent with the results obtained

with EEAChE. In contrast, the k_p values obtained from the inhibition of rMAChE by the S_PS_C and S_PR_C were considerably different than those obtained from there respective enantiomers. These observations provide further evidence that there are two distinct mechanisms for the inhibition of AChE by the stereoisomers of isomalathion dependent, primarily, upon the stereochemical orientation of the phosphorus atom.

Previously, it had been suggested that inhibition of AChE by the four isomalathion isomers proceeded via a common mechanism (i.e. displacement of the thiosuccinyl ligand with inversion of the phosphorus configuration (Berman 1989a)). If this hypothesis is correct, then the putative (*S*)- or (*R*)-O,S-dimethylphosphorothiolated AChE adduct should be the result of the inhibition reaction. These AChE conjugates should then be identical to the phosphorylated enzymes that would result from inhibition by (*S*)- or (*R*)-isoparathion methyl as depicted in Scheme 5.2.

Scheme 5.2. Convergent Mechanisms for the Inhibition of AChE by Isomalathion and Isoparathion Methyl.

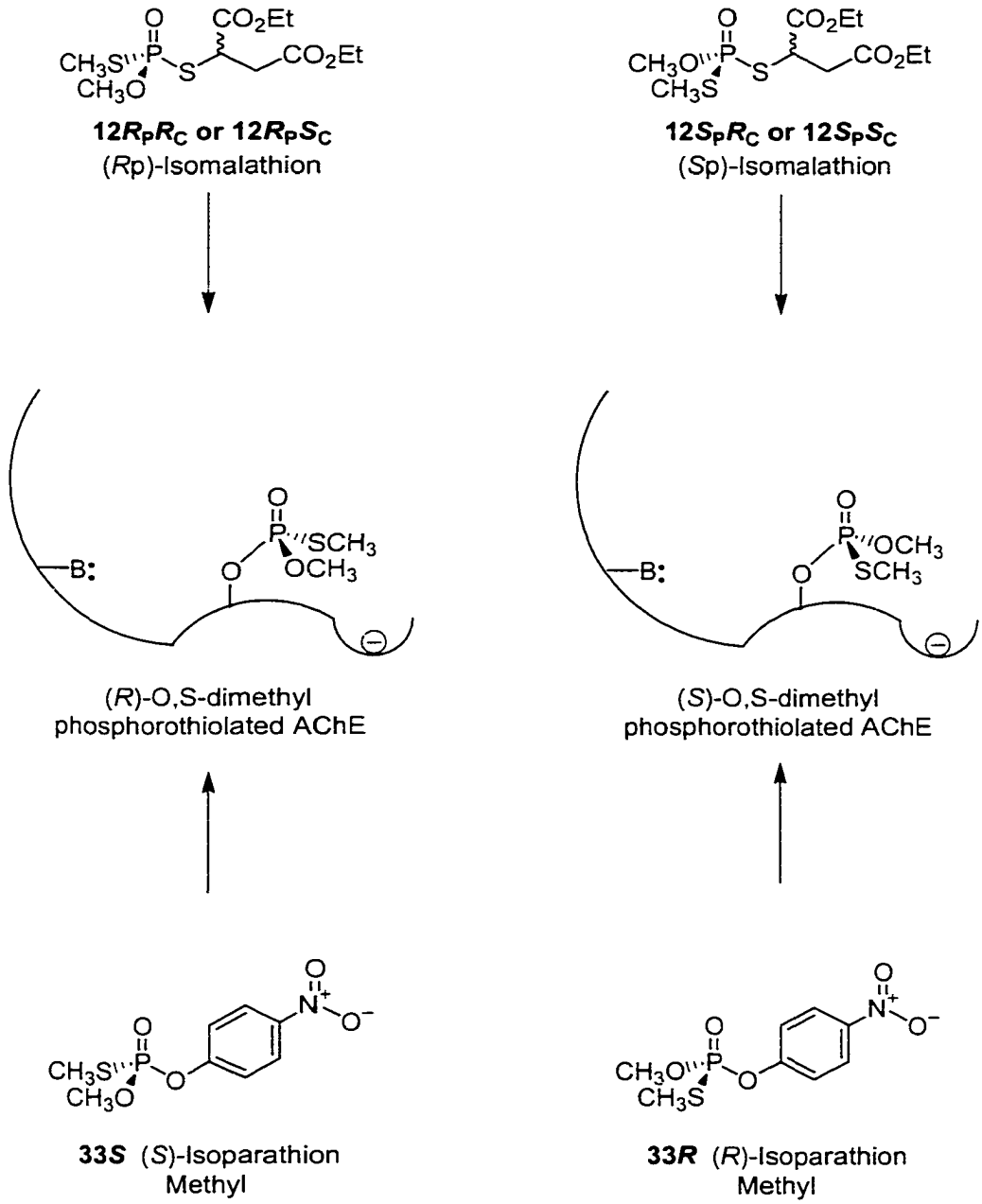

5.5-Reactivation of EEAChE and rMAChE inhibited by the Stereoisomers of Isomalathion

If, as suggested by Scheme 5.2, the inhibition of AChE by isoparathion methyl and isomalathion proceeds by a convergent mechanism then the reactivation profiles (reversible removal of phosphorus group) of AChE inhibited by these two compounds should be comparable. In order to clarify the mechanistic ambiguity of these processes and attempt to identify the stereochemical influences upon reactivation, the rate constants for both spontaneous reactivation and reactivation in the presence of the oximes 2-PAM and TMB-4 were determined experimentally for both EEAChE and rMAChE using Eqn. 7. The results obtained from these studies are listed in Tables 5.8 and 5.9 and are presented graphically in Figures 5.5 and 5.6.

Table 5.8. Reactivation Data for EEAChE Inhibited by the Stereoisomers of Isomalathion[a].

Isomer	k_3 (spon) min^{-1} ($\times 10^{-3}$)	% spontaneous reactivation	k_3 (2-PAM) min^{-1} ($\times 10^{-3}$)	% 2-PAM reactivation	k_3 (TMB-4) min^{-1} ($\times 10^{-3}$)	% TMB-4 reactivation
R_PR_C	5.3 ± 1	32	74 ± 19	85	79 ± 4	89
R_PS_C	2.2 ± 1	28	61 ± 20	72	76 ± 15	87
S_PR_C	0.3 ± 1	<1	1.4 ± 1	8	3 ± 1	11
S_PS_C	0 ± 1	<1	1.2 ± 1	1.5	2.5 ± 1	4

[a] n = 16

Figure 5.5. Reactivation Rate Constants ($k_3 \times 10^{-3}$ min^{-1}) for EEAChE Inhibited by the Stereoisomers of Isomalathion.

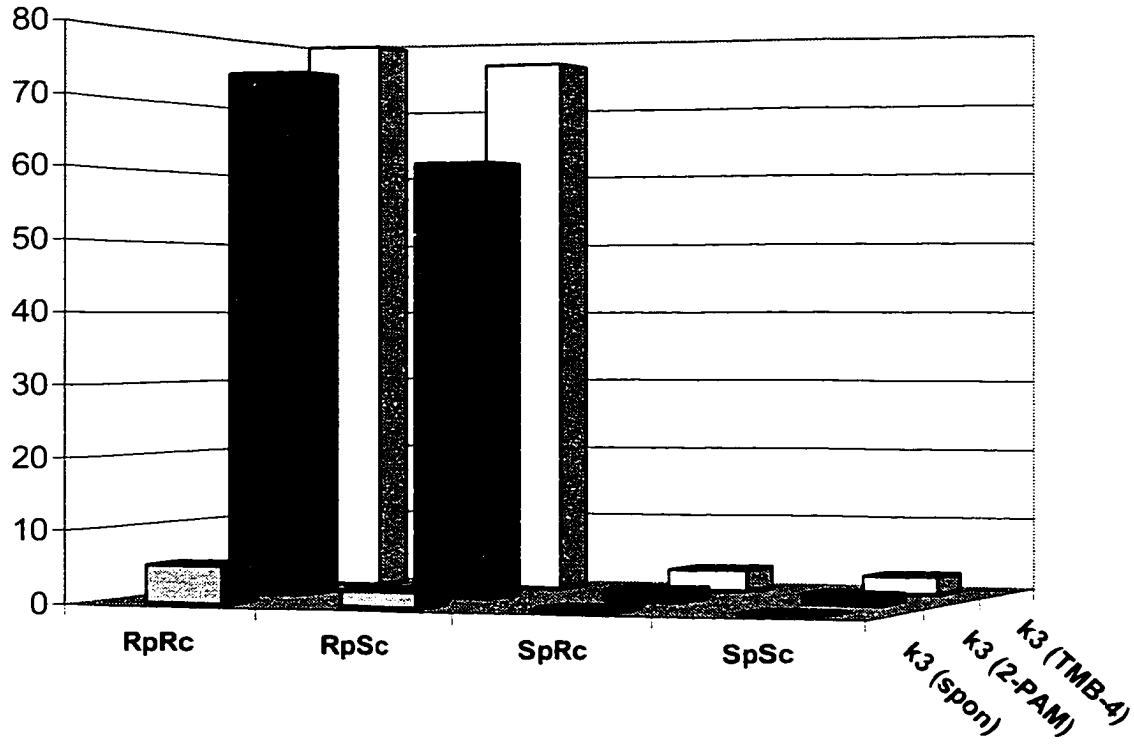

Table 5.9. Reactivation Data for rMAChE Inhibited by the Stereoisomers of Isomalathion[a].

Isomer	k_3 (spon) min^{-1} ($\times 10^{-3}$)	% spontaneous reactivation	k_3 (2-PAM) min^{-1} ($\times 10^{-3}$)	% 2-PAM reactivation	k_3 (TMB-4) min^{-1} ($\times 10^{-3}$)	% TMB-4 reactivation
R_PR_C	14 ± 4	32	38 ± 6	82	80 ± 10	98
R_PS_C	4.2 ± 2	18	31 ± 5	73	76 ± 11	97
S_PR_C	1.8 ± 1	9	9.2 ± 3	13	10 ± 3	15
S_PS_C	0 ± 1	<1	0.9 ± 1	1.7	1.2 ± 1	2.3

[a]n = 8

Figure 5.6. Reactivation Rate Constants ($k_3 \times 10^{-3}$ min^{-1}) for the Reactivation of rMAChE Inhibited by the Stereoisomers of Isomalathion.

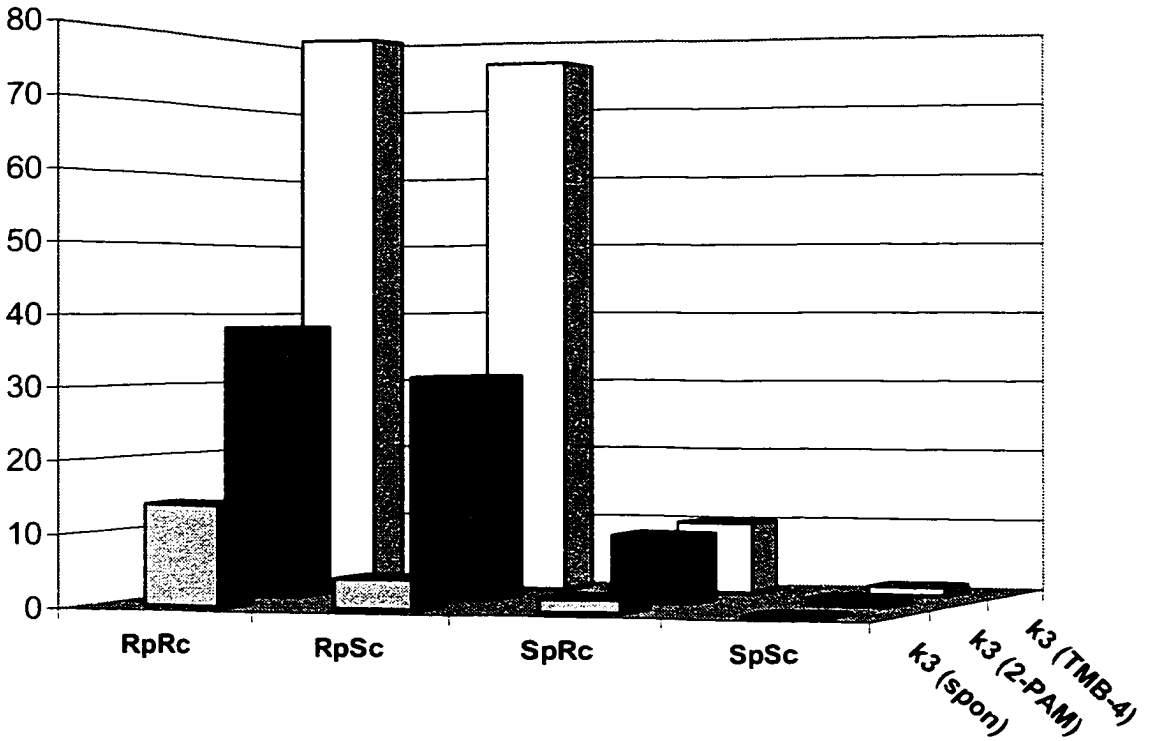

Following 20 h of inhibition with each of the isomalathion isomers, the EEAChE and rMAChE samples were diluted 100-fold with 0.1 M phosphate buffer to halt further inhibition. The spontaneous reactivation rate constants, k_3, were calculated from the slope of the initial portion (0-10 min) of the graph generated by plotting *ln(100/%inhibition)* vs. *time*. Rate constants for oxime-mediated reactivation, k_3 (2-PAM) and k_3 (TMB-4), were determined in a similar fashion with the exception that the solution used to halt inhibition was 0.1 mM of the oxime used.

By 60 min, both spontaneous and oxime mediated reactivation reached a plateau that was assigned the total percent reactivation relative to uninhibited enzyme. Enzyme activity was monitored for up to 24 h and in all cases only negligible increases in enzyme activity (>2%) relative to the control was observed.

The k_3 values for EEAChE inhibited by R_PR_C or R_PS_C isomalathion obtained in the presence of 2-PAM, k_3 (2-PAM), were 14- and 30-fold greater than those obtained for spontaneous reactivation. It is interesting that TMB-4 proved to be slightly more effective reactivating agent than 2-PAM for EEAChE inhibited by these isomers generating k_3 (TMB-4) values that were 15- and 36-fold greater than the k_3 for spontaneous reactivation. A similar reactivation rate trend was observed for rMAChE inhibited by the isomalathion isomers. The k_3 (2-PAM) values obtained were 3- and 7.4-fold greater than the k_3 for spontaneous reactivation while the k_3 (TMB-4) values obtained were 5.7- and 18-fold greater. That both spontaneous and oxime-mediated reactivation rates for these two diastereomers are so similar in magnitude suggests that the resultant phosphorylated enzymes were chemically and stereochemically equivalent.

This is in stark contrast with the results obtained from EEAChE and rMAChE inhibited by S_PR_C or S_PS_C isomalathion. These samples proved to be refractory to both spontaneous and oxime mediated reactivation and showed only negligible amounts of total returned activity following treatment with the oximes. The small amount of reactivation that was detected is most likely due to the 1-3 % contamination by the respective enantiomers that led to reactivateable enzyme.

A comparison of this data with the spontaneous and oxime-mediated reactivation rates reported for the inhibition of several sources of AChE by the stereoisomers of

isoparathion methyl suggest some intriguing mechanistic implications. EEAChE and rMAChE inhibited with the 1*R*-isomalathion stereoisomers had k_3 values that were not significantly different from each other and are similar to the k_3 values for enzyme inhibited with the configurationally equivalent (*S*)-isoparathion methyl (Berkman 1993b; Jianmongkol 1999), which suggests that both R_P-isomalathions and (*S*)-isoparathion methyl generate the R_P O,S-dimethyl phosphate adduct upon reaction with AChE as depicted in Scheme 5.2.

In contrast, AChE inactivated by S_PR_C or S_PS_C isomalathion had significantly different k_3 values from enzyme inhibited with the configurationally equivalent (*R*)-isoparathion methyl (Berkman 1993b; Jianmongkol 1999). As observed with other sources of AChE, EEAChE and rMAChE inhibited with either of the S_P-isomalathion stereoisomers were found to be intractable to reactivation, even though the enzyme inhibited with the corresponding (*R*)-isomer of isoparathion methyl could be reactivated with a measurable rate. These surprising results indicate the S_P-isomalathions do not yield the expected O,S-dimethyl phosphorylated AChE adducts with loss of diethyl thiosuccinyl as the primary leaving group. Rather, they suggests that the S_P-isomalathions inhibit AChE by a different mechanism from that of the R_P-isomalathions with loss of thiomethyl as the primary leaving group to yield an inhibited enzyme containing a diethyl thiosuccinyl ligand capable of undergoing further reactions that render the enzyme refractory to reactivation (Berkman 1993a; Berkman 1993b; Jianmongkol 1999).

Methoxy was discounted as the primary leaving group in the inhibition of AChE by S_PS_C isomalathion for the following reasons. First, thiomethyl is predicted to be a better leaving group than the methoxy ligand. It is known that methanethiol ($pK_a = 10.0$) is a

stronger acid than methanol (pK_a = 15.5), and its conjugate base is therefore better able to delocalize the resultant negative charge (Vollhardt 1999). Second, Thompson *et al.* demonstrated that inhibition of AChE with methamidophos proceeds primarily with loss of thiomethyl instead of the methoxy group as depicted in Scheme 5.3 (Thompson 1982).

Scheme 5.3. Mechanism for the Inhibition of AChE by Methamidophos.

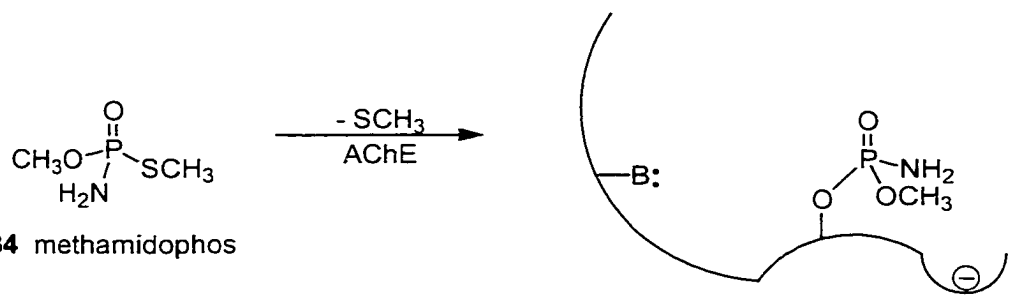

34 methamidophos

Several of the postinhibitory processes that are possible following inhibition of AChE by either of the two S_P-isomalathion stereoisomers are represented in Scheme 5.4. In path A, displacement of the thiosuccinyl ligand via a general base catalyzed mechanism is shown while path B depicts an intramolecular phosphorylation by a second enzyme residue and path C represents the β-elimination of diethyl fumarate or diethyl maleate. Another alternative to these mechanisms is occlusion of the approach of incoming nucleophiles (H_2O or oxime) owing to steric crowding by the thiosuccinyl ligand. If the succinyl thiolester-phosphorus bond were cleaved by the action of water or oxime, the remaining phosphoryl conjugate would become charged and therefore would be unable to undergo reactivation by nucleophiles.

Scheme 5.4. Possible Non-Reactivatable Pathways for S_P Isomalathion.

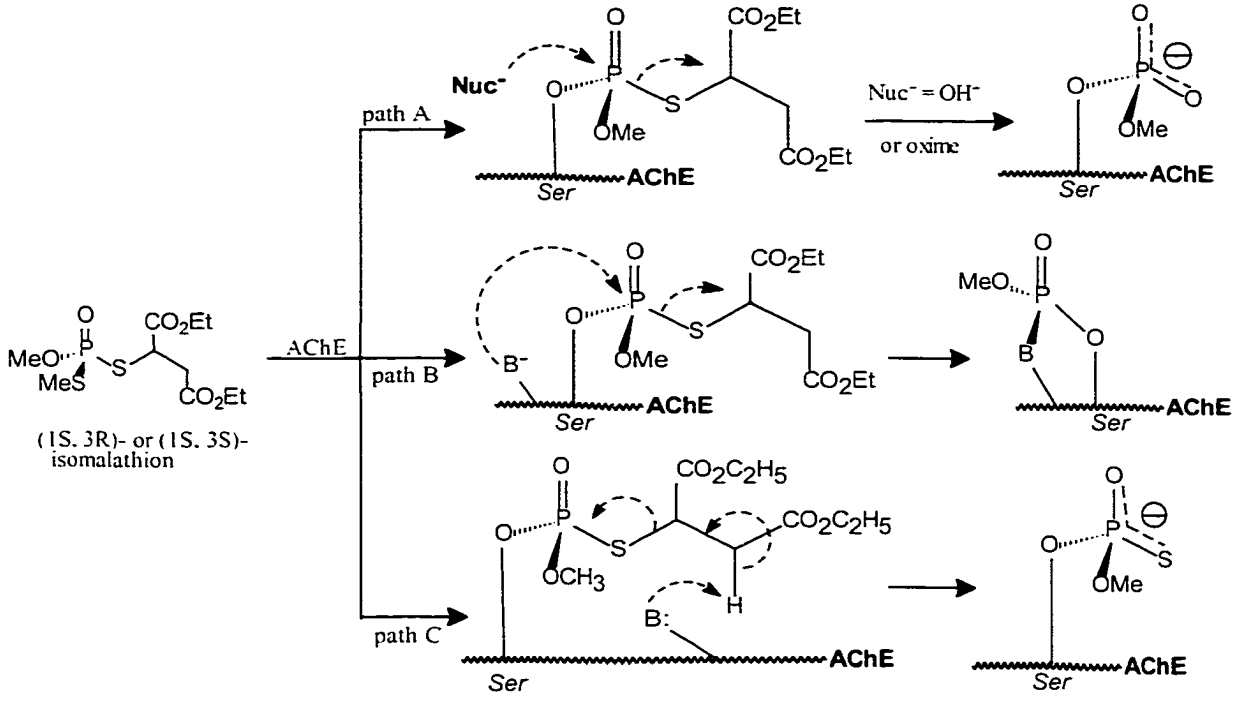

Path A and B also generate diethyl thiosuccinate and path C produces diethyl fumarate/maleate.

With the aid of our collaborators, Dr. Rudy J. Richardson and co-workers at the University of Michigan in Ann Arbor, a study was carried out to determine the identity of the adduct that renders AChE refractory towards reactivation when inhibited with S_PS_C isomalathion. Using matrix-assisted laser desorption/ionization time-of-flight mass spectrometry (MALDI-TOF-MS), the hypothesis was tested that inactivation of AChE by S_PS_C isomalathion proceeds with loss of thiomethyl as the primary leaving group, and loss of thiosuccinate as the secondary leaving group (Doorn 2000). The results of the study demonstrated that the identity of the adduct that renders EEAChE refractory or resistant towards reactivation after inhibition with S_PS_C isomalathion was in fact the O-methyl phosphate adduct as predicted by path A of Scheme 5.4. A peak with mass corresponding

to the active site peptide containing the catalytic Ser with a covalently bound O-methyl phosphate adduct was found in the mass spectra of treated but not control samples. Identities of the modified active site peptide and adduct were confirmed using reflectron MALDI-TOF-MS, and peaks corresponding to loss of adduct as phosphorous/phosphoric acid methyl ester were observed (Figure 5.7). The results demonstrate that inhibition of EEAChE by S_PS_C isomalathion proceeds with loss of thiomethyl instead of diethylthiosuccinyl as the primary leaving group followed by rapid expulsion of diethyl thiosuccinyl as the secondary leaving group to yield an aged enzyme.

Figure 5.7. Representative MALDI-TOF-MS Spectra of Digested EEAChE Separated by HPLC Prior to Inhibition (panel A) and Following Inhibition (panel B) with S_PS_C Isomalathion.

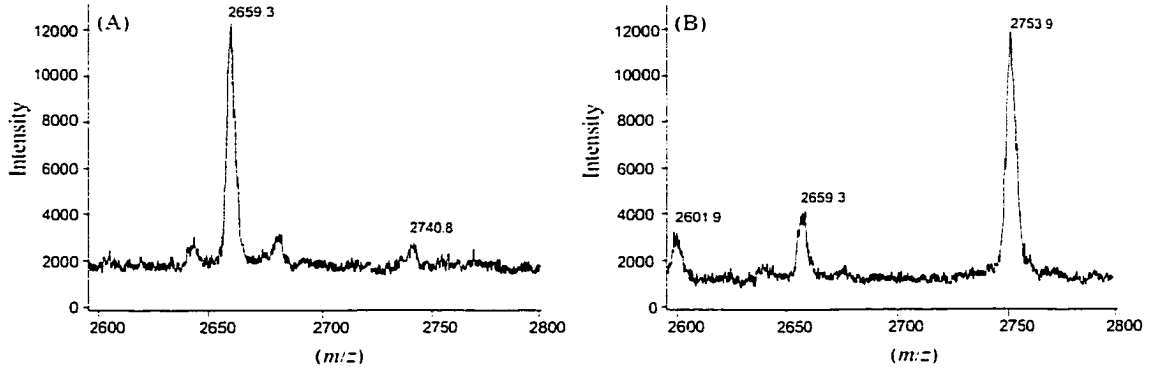

Panel A Panel B

Table 5.10 displays the average masses of the measured and theoretical protonated molecular ion (MH^+) corresponding to peptides of interest. Figure 5.7 shows representative MALDI-TOF-MS spectra of digested EEAChE separated with HPLC. Panel A of Figure

5.7 shows a peak with mass corresponding to that of the unmodified active site peptide (2659.3 Da) containing the catalytic Ser found in the control sample. Panel B of Figure 5.7 shows the peak with a mass corresponding to that of the active site peptide (2753.9 Da) containing the catalytic Ser with an O-methyl phosphate adduct found in the sample treated with S_PS_C isomalathion. Acid-catalyzed hydrolysis of the OP adduct in the HPLC mobile phase may be responsible for presence of unmodified active site peptide.

Table 5.10. Masses of Theoretical and Observed MH^+ for Unmodified and Modified Active Site Peptides of EEAChE[a].

preparation	peptide[b]	theoretical	Δ m (theoretical)[c]	observed	Δ m (observed)[c]
unseparated	unmodified	2657.0		2659.3	
	modified	2751.0	94.0	2753.9	94.6
HPLC separated	unmodified	2657.0		2658.0 (± 0.9)[d]	
	modified	2751.0	94.0	2751.9 (± 1.0)[d]	93.9 (± 1.3)

[a]Conditions used for the preparation and analysis of the active site peptide containing the catalytic Ser were as described in Doorn 2000.

[b]Active site peptide containing the catalytic Ser in the control (unmodified) and S_PS_C isomalathion-treated (modified) samples.

[c]Difference in mass between modified and unmodified active site peptide which takes into account the Ser proton lost in the phosphorylation reaction.

[d]Mean ± SE (n = 4 or 5 experiments for unmodified and modified samples, respectively).

The data generated by this study provides the first direct chemical identification of the OP adduct formed following inhibition of EEAChE with S_PS_C isomalathion. The identity of the adduct resulting from inhibition of EEAChE with S_PS_C isomalathion as determined by MALDI-TOF-MS is strikingly different from that predicted by the conventional mechanism of inhibition and aging (Scheme 5.2). That the HPLC and MALDI-TOF-MS analysis of peptides of electric eel enzyme did not reveal any peaks with mass representing the active site peptide with an O,S-dimethyl phosphate or O-methyl thiophosphate adduct is further evidence that that inhibition of EEAChE by S_PS_C isomalathion proceeds with loss of thiomethyl instead of diethylthiosuccinyl as the primary leaving group followed by rapid expulsion of diethyl thiosuccinyl as the secondary leaving group to yield an aged enzyme as depicted in Path A of Scheme 5.4.

5.6-Inhibition of EEAChE by the ITP Stereoisomers

To further examine the stereoselective inhibition of EEAChE, and define the correlation between stereochemistry and the leaving group differences, the inhibitory profiles of the individual ITP stereoisomers were determined in a concentration-dependent manner as described in Methods 3 and 4 of Section 7.3.3 using Eqn. 2. The kinetic data that was collected is presented in Table 5.11.

A 7.9-fold difference in anti-AChE potency was found between the strongest isomer, R_PR_C-ITP, and weakest isomer, S_PS_C-ITP. The ITP stereoisomers with R_C configuration displayed greater inhibitory potency toward EEAChE than those that had the S_C configuration, similar to the results obtained from the inhibition off EEAChE by the stereoisomers of isomalathion. However, the attenuation of the inhibition reaction by the stereogenic carbon was further modulated by the chirality of the phosphorus-containing portion of the molecule. The difference in inhibitory strength when changing the configuration at carbon from R_C to S_C was 4-fold when the configuration at phosphorus was *S*. In contrast, the difference was 4.8-fold when comparing the two isomers that had the *R* configuration at phosphorus. In a similar fashion, the carbon stereocenter attenuated the effect on inhibitory potency exerted by the stereochemical orientation of the phosphorus. A comparison of the isomers that had *S* or *R* configuration at the phosphorus demonstrate a 1.8-fold difference in inhibitory potency when the stereochemical orientation of the carbon is *R*, but only a 1.2-fold difference in inhibitory potency is observed for the stereoisomers with the *S* configuration at carbon. These observations suggested that the carbon and phosphorus asymmetric centers of ITP isomers act independently during the inhibition of EEAChE and are consistent with the observations obtained during the analysis of EEAChE

inhibited by the isomalathion stereoisomers. That the stereochemical orientation of the carbon has less of an effect on the inhibitory potency by an OP compound with two stereocenters relative to the influence of the configuration at phosphorus is also consistent with the observations obtained during the analysis of EEAChE inhibited by the isomalathion stereoisomers.

Table 5.11. Concentration Dependent Kinetic Data for the Inhibition of EEAChE by the ITP Stereoisomers[a].

Isomer	k_i ($\times 10^3$ M^{-1} min^{-1})	K_D (μM)	k_p (min^{-1})
R_PR_C	110 ± 12	15 ± 9	1.6
R_PS_C	23 ± 6	3 ± 1	0.07
S_PR_C	56 ± 13	12 ± 4	0.66
S_PS_C	14 ± 5	26 ± 4	0.36

[a]n = 20

The kinetic parameters K_D and k_P were also determined for the interactions of the individual ITP stereoisomers with EEAChE. As observed for the stereoisomers of isomalathion, the k_i values typically paralleled the disassociation constants, K_D, such that the isomer with the greater affinity for the active site was the stronger inhibitors. An example of this is displayed by the 2.2-fold stronger affinity for (or weaker disassociation from) the active site determined for the S_PR_C-isomer versus its S_PS_C counterpart and was a

4-fold more potent inhibitor. However, as implied by Eqn. 2 a compound's affinity for the active site is not the only determinant of inhibition. A comparison of the K_D values obtained for the R_PR_C-isomer and the S_PS_C-isomer would lead one to expect less than a 2-fold difference in inhibitory potency. Yet the two isomers demonstrate a 7.8-fold difference in inhibitory potency. These observations can, in part, be rationalized by the relative magnitude of k_p (1.6) for the R_PR_C- isomer. The reactivity of the compound toward the enzyme, k_p, partially compensates for its comparatively low affinity toward the active site.

The values determined for the kinetic parameter k_p during the inhibition of EEAChE by R_PR_C- and R_PS_C- stereoisomers are considerably different (1.6 vs. 0.07, respectively). These observations are in contrast with those obtained from the inhibition of EEAChE by the stereoisomers of isomalathion, which demonstrated nearly identical k_p values for the corresponding isomers. This suggests that unlike the isomalathion stereoisomers, inhibition of EEAChE by R_PR_C- and R_PS_C-ITP *is* dependent upon the stereochemical orientation of the asymmetric carbon present in the thiosuccinyl portion of the molecule. This is further demonstrated by the fact that the isomers with *R* configuration at carbon are, for EEAChE, the strongest pair of inhibitors and have the highest k_p values.

The time-dependent method for determining the bimolecular rate constant of inhibition was also performed to compare with the concentration dependent method and the values obtained are presented in Table 5.12. The values generated by both methods are in good general agreement (time-dependent values proportionally lower) and are contrasted graphically in Figure 5.8. In particular, it is noteworthy that the rank order of inhibitory potency ($R_PR_C > S_PR_C > R_PS_C > S_PS_C$) is conserved between the two methods.

Table 5.12. Time Dependent Bimolecular Rate Constants of Inhibition ($k_i \times 10^3$ M^{-1} min^{-1}) for the Inhibition of EEAChE by the ITP Stereoisomers[a].

Isomer	k_i ($\times 10^3$ M^{-1} min^{-1})
R_PR_C	66 ± 4
R_PS_C	9 ± 1
S_PR_C	17 ± 5
S_PS_C	5 ± 1

[a]n = 10

Figure 5.8. Comparison of the Bimolecular Rate Constants of Inhibition ($k_i \times 10^3$ M^{-1} min^{-1}) Obtained by the Concentration Dependent Method and Time Dependent Method for the Inhibition of EEAChE by the ITP Stereoisomers

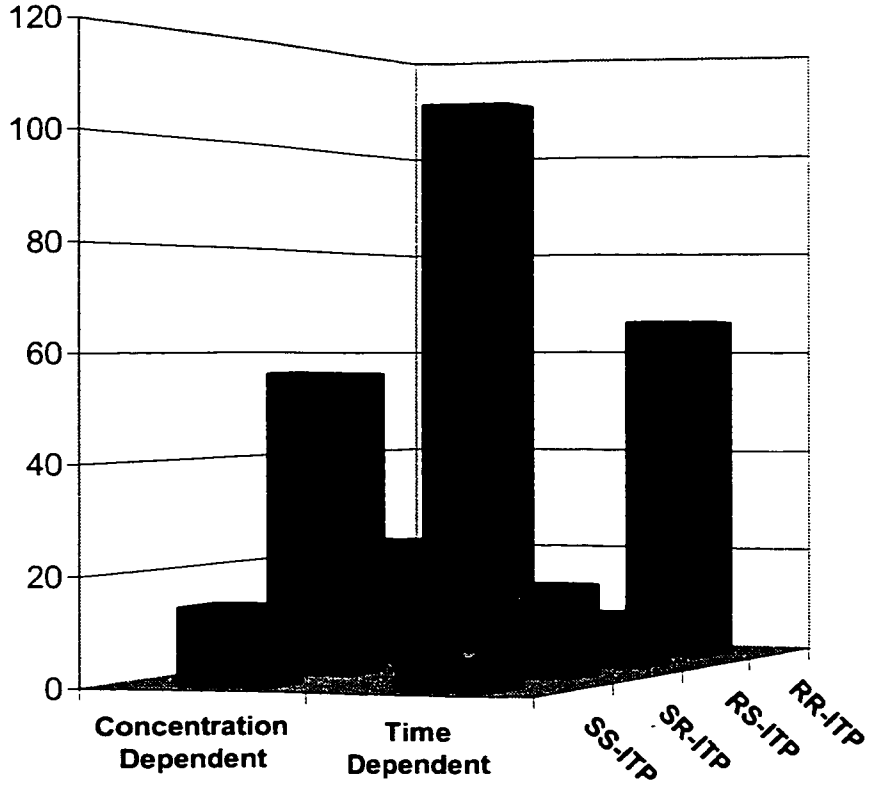

5.7-Inhibition of rMAChE by the ITP Stereoisomers

For comparison with EEAChE inhibited by the ITP stereoisomers and with the data obtained from the inhibition of rMAChE by the stereoisomers of isomalathion the stereodependent inhibition of rMAChE by the ITP isomers was determined in a concentration dependent manner using Methods 3 and 4 of Section 7.3.3 and Eqn. 2. In addition, the stereodependent inhibition profiles of rat cerebellum AChE (RCAChE) and

rat spine AChE (RSAChE) inhibited by the ITP isomers were determined (numeric data not shown) for further comparison. The results obtained from rMAChE are listed in Table 5.13 and are contrasted with the values obtained from the inhibition of RCAChE, RSAChE, and EEAChE graphically in Figure 5.9.

Table 5.13. Concentration Dependent Kinetic Data for the Inhibition of rMAChE by the ITP Stereoisomers[a].

Isomer	k_i ($\times 10^3$ M^{-1} min^{-1})	K_D (μM)	k_p (min^{-1})
R_PR_C	220 ± 17	36 ± 5	8.0
R_PS_C	110 ± 12	15 ± 4	1.6
S_PR_C	82 ± 8	25 ± 5	2.0
S_PS_C	9 ± 4	73 ± 13	0.68

[a] n = 20

The k_i values from the inhibition of rMAChE by the ITP stereoisomers were roughly 2-fold greater than those observed during the inhibition of EEAChE. The one exception to this trend is the k_i value obtained for the inhibition of rMAChE by the S_PS_C isomer, which was only two thirds the value obtained from the inhibition of EEAChE by the same isomer. A 23.7-fold difference in anti-AChE potency was found between the strongest isomer, R_PR_C-ITP, and weakest isomer, S_PS_C-ITP. This difference is three times greater that observed during the inhibition EEAChE by the same isomers. That rMAChE is

better able to discriminate between the stereoisomers than EEAChE is consistent with the data obtained during the study of the interactions of isomalathion stereoisomers with the same enzyme sources. The ITP stereoisomers with R_P configuration displayed greater inhibitory potency toward rMAChE than those that had the S_P configuration, similar to the results obtained from the inhibition of rMAChE by the stereoisomers of isomalathion. Attenuation of the inhibition reaction by the stereogenic phosphorus was also modulated by the chirality of the asymmetric carbon present in the molecule. The difference in inhibitory strength when changing the configuration at carbon from R_P to S_P was 11.8-fold when the configuration at carbon was *S*. In contrast, the difference was 2.2-fold when comparing the two isomers that had the *R* configuration at carbon. In a similar fashion, the phosphorus stereocenter attenuated the effect on inhibitory potency exerted by the stereochemical orientation of the carbon. A comparison of the isomers that had *S* or *R* configuration at carbon demonstrate only a 2-fold difference in inhibitory potency when the stereochemical orientation of the phosphorus is *R*, but an 8.8-fold difference in inhibitory potency is observed for the stereoisomers with the *S* configuration at phosphorus. These observations demonstrated that the carbon and phosphorus asymmetric centers of ITP isomers act independently during the inhibition of rMAChE and are consistent with the observations obtained during the analysis of EEAChE and rMAChE inhibited by the isomalathion stereoisomers. That the stereochemical orientation of the carbon has less of an effect on the inhibitory potency of an OP compound with two stereocenters relative to the influence of the configuration at phosphorus is also consistent with the observations obtained during the analysis of EEAChE and rMAChE inhibited by the isomalathion stereoisomers.

The kinetic parameters K_D and k_P were also determined for the interactions of the individual ITP stereoisomers with rMAChE. In contrast with the observations obtained for the stereoisomers of isomalathion, the k_i values did not typically parallel the disassociation constants, K_D. An example of this is shown by the following data. The R_PS_C isomer had a 2.4-fold stronger affinity for (or weaker disassociation from) the active site than determined for the R_PR_C but surprisingly, the R_PR_C isomer was a 2-fold more potent inhibitor. These observations can, in part, be rationalized by the extremely high value of k_p (8.0) observed for the R_PR_C- isomer. The reactivity of the compound toward the enzyme, k_p, partially compensates for its comparatively low affinity for toward the active site.

The values determined for the kinetic parameter k_p during the inhibition of rMAChE by R_PR_C and R_PS_C stereoisomers are different by 5-fold. These observations are in contrast with those obtained from the inhibition of rMAChE by the stereoisomers of isomalathion, which demonstrated nearly identical k_p values for the corresponding isomers. This suggests that, unlike the isomalathion stereoisomers, inhibition of rMAChE by R_PR_C- and R_PS_C-ITP *is* dependent upon the stereochemical orientation of the asymmetric carbon present in the thiosuccinyl portion of the molecule consistent with observations obtained for EEAChE inhibited by the ITP stereoisomers.

Figure 5.9. Bimolecular Rate Constants ($k_i \times 10^3$ M^{-1} min^{-1}) for the Inhibition of AChE from Different Sources by the ITP Stereoisomers.

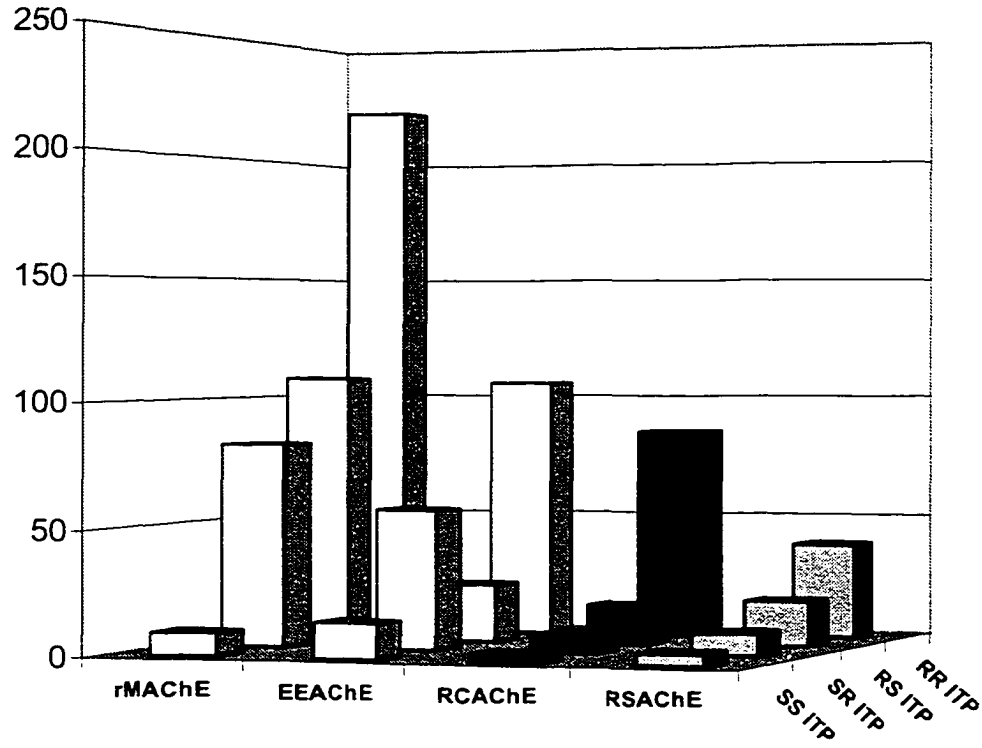

The data from the inhibition of EEAChE and rMAChE imply that the ITP stereoisomers are interacting with these sources of AChE in a manner that is distinct from the mechanisms observed for the isomalathion stereoisomers despite their inherent structural similarities. This is surprising considering the observed values for the kinetic parameter k_i for both sets of stereoisomers are very similar in both rank order and magnitude as demonstrated in Figure 5.10.

Figure 5.10. Comparison of the Bimolecular Rate Constants ($k_i \times 10^3$ M^{-1} min^{-1}) Determined for the Inhibition of EEAChE and rMAChE by the ITP Stereoisomers and the Stereoisomers of Isomalathion.

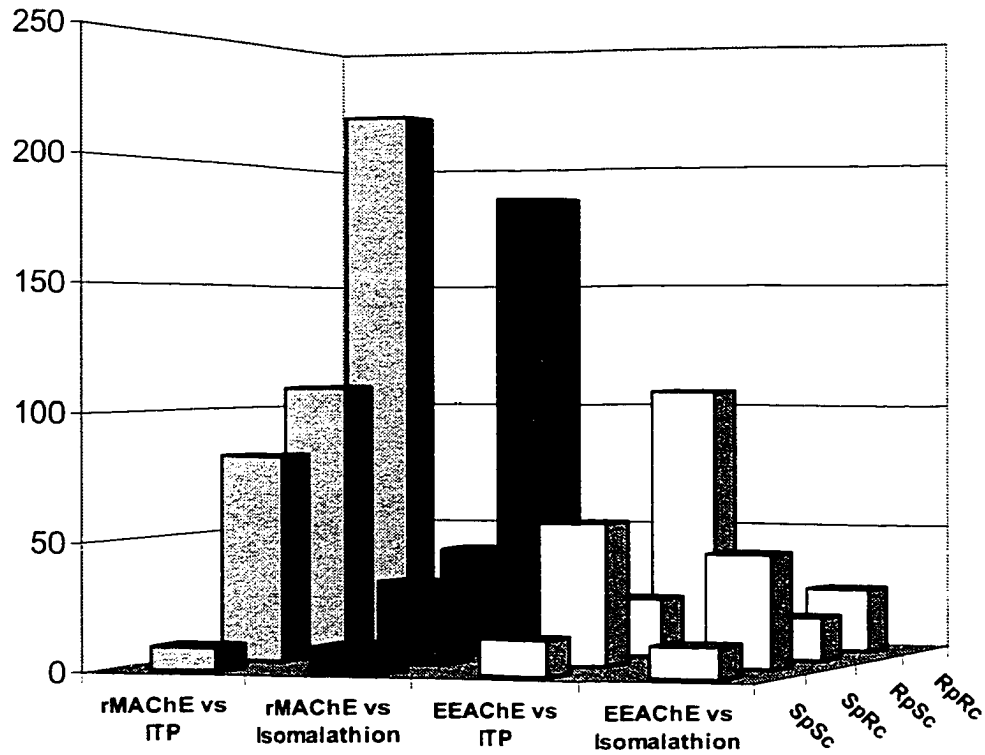

An examination of the general ITP structure reveals that, like the isomalathion stereoisomers, there are two potential leaving groups present in the molecule. Therefore, inhibition of AChE by the ITP stereoisomers has the potential to generate two different phosphorylated adducts as depicted in Paths A and B of Scheme 5.5. The kinetic data presented in Sections 5.3-5.5 combined with the MALDI-TOF-MS analysis of EEAChE presented in Section 5.5 provide compelling evidence for the hypothesis that the inhibition of AChE by the stereoisomers of isomalathion occurs via different mechanisms dependent

upon the stereochemical orientation of the phosphorus moiety (see Scheme 5.1). That the two groups of stereoisomers demonstrated subtle differences in the observed kinetic parameters K_D and k_P warranted further investigation.

Scheme 5.5. Possible AChE Adducts Resulting from Inhibition by the ITP Stereoisomers.

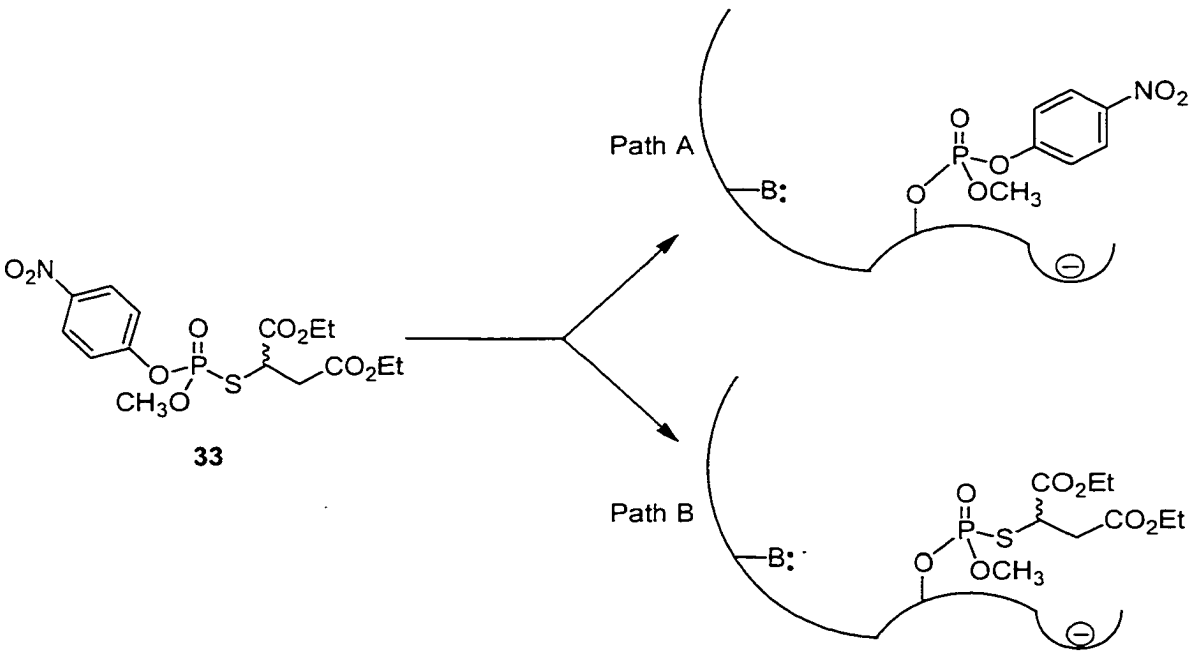

5.8-Reactivation of EEAChE and rMAChE inhibited by the ITP Stereoisomers

If, as suggested by the inhibition kinetic data in the two previous sections, the inhibition of AChE by the ITP and isomalathion stereoisomers proceeds by divergent mechanisms, then the reactivation profiles of AChE inhibited by paths A and B (Scheme 5.5) should be quite different. In an attempt to clarify the mechanistic ambiguity of these processes and to identify the stereochemical influences upon reactivation the rate constants for both spontaneous reactivation and reactivation in the presence of the oximes 2-PAM and TMB-4 were determined experimentally for both EEAChE and rMAChE using Eqn. 7. The results obtained from these studies are listed in Tables 5.14 and 5.15 and are presented graphically in Figures 5.11 and 5.12.

Following 20 h of inhibition with each of the ITP isomers, the EEAChE and rMAChE samples were diluted 100-fold to halt further inhibition. The spontaneous reactivation rate constants, k_3, were calculated from the slope of the initial portion (0-10 min) of the graph generated by plotting *ln(100/%inhibition)* vs. *time* as described previously. Rate constants for oxime-mediated reactivation, k_3 (2-PAM) and k_3 (TMB-4), were determined in a similar fashion with the exception that the solution used to halt inhibition was 0.1 mM of the oxime used.

By 60 min, both spontaneous and oxime mediated reactivation reached a plateau that was assigned the total percent reactivation relative to uninhibited enzyme. Enzyme activity was monitored for up to 24 h and in all cases only negligible (> 2 %) increases in enzyme activity, relative to the control, were observed.

Table 5.14. Reactivation Data for EEAChE Inhibited by the ITP Stereoisomers[a].

Isomer	k_3 (spon) min^{-1} ($\times 10^{-3}$)	% spontaneous reactivation	k_3 (2-PAM) min^{-1} ($\times 10^{-3}$)	% 2-PAM reactivation	k_3 (TMB-4) min^{-1} ($\times 10^{-3}$)	% TMB-4 reactivation
R_PR_C	13 ± 2	27	148 ± 20	93	179 ± 27	97
R_PS_C	19 ± 5	35	49 ± 13	67	48 ± 15	69
S_PR_C	0.6 ± 1	4	202 ± 30	95	189 ± 33	91
S_PS_C	2.3 ± 1	15	55 ± 14	72	73 ± 13	79

[a]n = 16

Figure 5.11. Rate Constants ($k_3 \times 10^{-3}$ min^{-1}) for the Reactivation of EEAChE Inhibited by the ITP Stereoisomers.

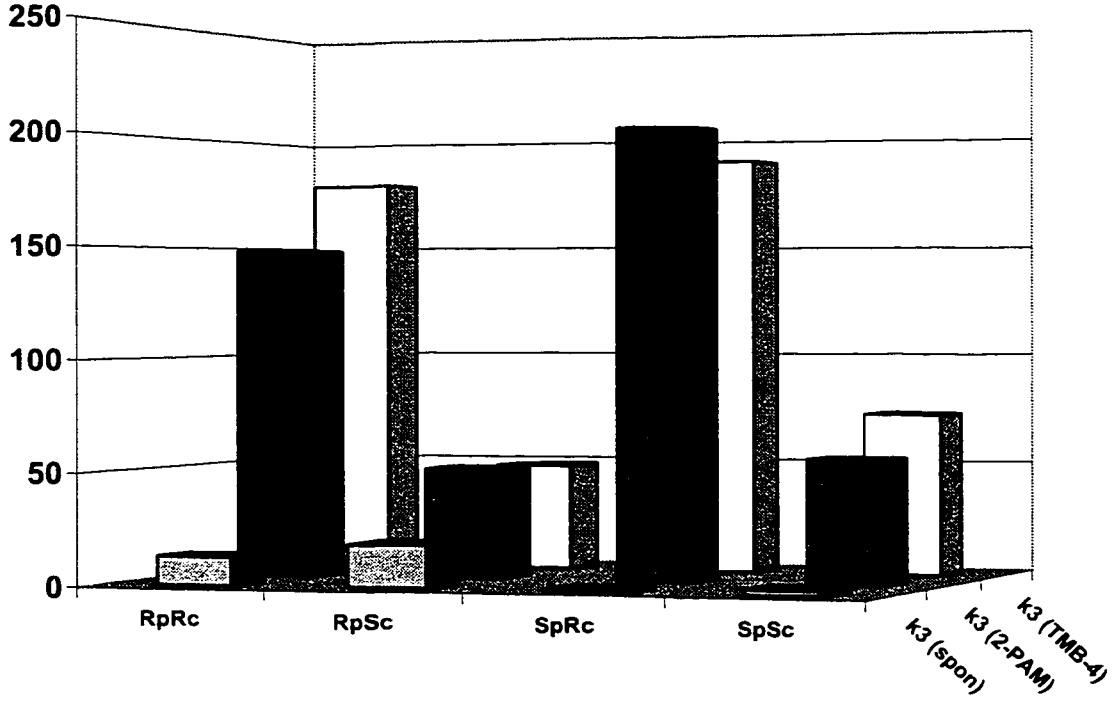

Table 5.15. Reactivation Data for rMAChE Inhibited by the ITP Stereoisomers.

Isomer	k_3 (spon) min^{-1} ($\times 10^{-3}$)	% spontaneous reactivation	k_3 (2-PAM) min^{-1} ($\times 10^{-3}$)	% 2-PAM reactivation	k_3 (TMB-4) min^{-1} ($\times 10^{-3}$)	% TMB-4 reactivation
R_PR_C	3 ± 1	9	137 ± 15	91	163 ± 17	95
R_PS_C	5 ± 2	15	43 ± 6	52	40 ± 13	61
S_PR_C	0.8 ± 1	3	190 ± 8	98	189 ± 11	97
S_PS_C	8.2 ± 3	27	41 ± 7	61	70 ± 10	80

[a] n = 8

Figure 5.12. Rate Constants ($k_3 \times 10^{-3}$ min^{-1}) for the Reactivation of rMAChE Inhibited by the ITP Stereoisomers.

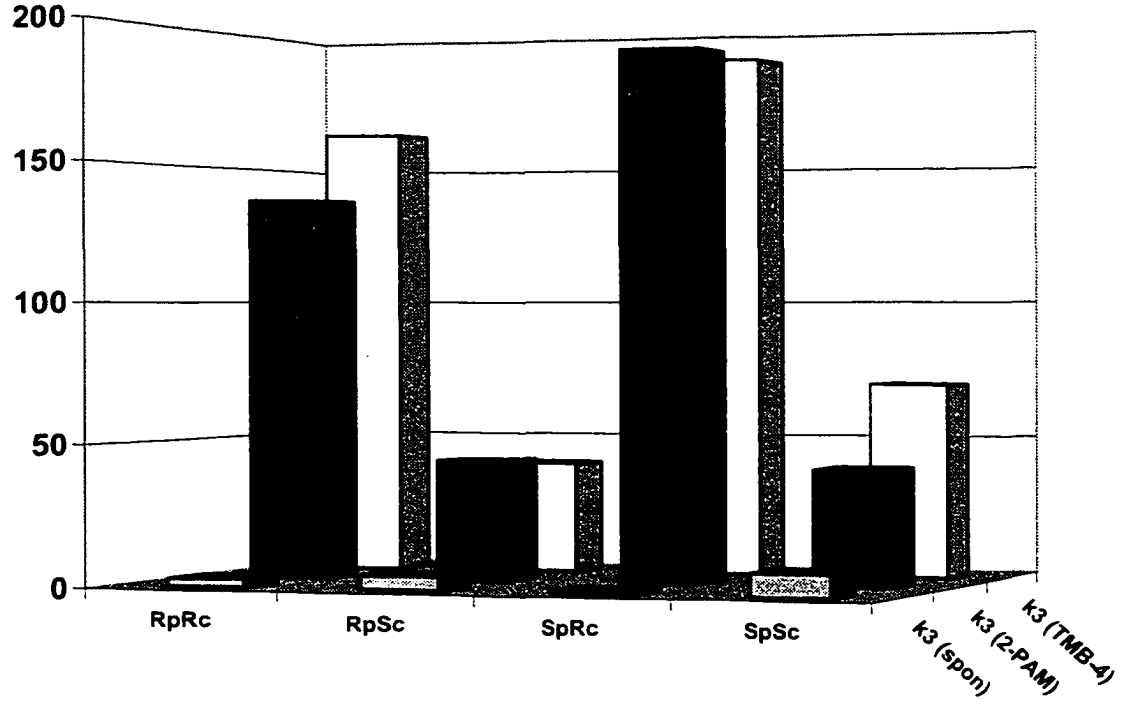

The k_3 values for EEAChE inhibited by the R_PR_C or S_PR_C ITP stereoisomers obtained in the presence of 2-PAM, k_3 (2-PAM), were 11.4- and 336-fold greater than those obtained for spontaneous reactivation. In the presence of the oxime TMB-4, these isomers generated k_3 (TMB-4) values that were 13.8- and 315-fold greater than the k_3 for spontaneous reactivation. A similar trend was observed for rMAChE inhibited by the same isomers. The k_3 (2-PAM) values obtained were 46- and 237- fold greater than the k_3 for spontaneous reactivation while the k_3 (TMB-4) values obtained were 54- and 236-fold greater. That both the spontaneous and oxime-mediated reactivation rates for these two diastereomers are so similar in magnitude for both enzyme sources suggests that the resultant phosphorylated enzymes undergo similar mechanisms of reactivation.

This is in stark contrast with the results obtained from EEAChE and rMAChE inhibited by R_PS_C or S_PS_C ITP stereoisomers. For both enzyme sources these isomers demonstrated very limited spontaneous and oxime mediated reactivation and demonstrated only a partial return of activity following treatment with the oximes.

While these results are fairly consistent with the values of k_p and K_D obtained from the inhibition of EEAChE and rMAChE by the ITP stereoisomers, they contrast surprisingly with the kinetic behavior observed for the isomalathion stereoisomers with the same enzyme sources. It was assumed that replacing the thiomethyl moiety present in the isomalathion stereoisomer with a functionality that was a better leaving group would result in a set of compounds that would demonstrate similar, if not enhanced, kinetic behavior. That the kinetic parameters observed for the ITP stereoisomers are so divergent from those of the isomalathion stereoisomers suggests that this assumption was based upon an

oversimplification of the processes that influence the tendency of a compound to demonstrate anti-AChE potency and to undergo the postinhibitory reaction of aging.

It is possible that the steric and electrostatic differences between the two ligands cause the molecules to assume different orientations thus altering their interactions with the enzyme. That the k_i values obtained for the ITP stereoisomers are comparable in both magnitude and stereochemical preference to the isomalathions and other structurally equivalent asymmetric OP compounds implies the ITP stereoisomers initial approach to, and interactions with, the active site of the enzyme follow a mechanism that is common to these types of compounds. However, comparison of the kinetic parameters K_D, k_p, and k_3 (both spontaneous and oxime-mediated) obtained form the inhibition of EEAChE and rMAChE by the ITP stereoisomers and the isomalathions reveal distinct differences. These differences may be the result of slight perturbations in the architecture of the enzyme's active site.

In the case of the isomalathion stereoisomers it was shown that the primary leaving group was either the thiomethyl ligand or the thiosuccinyl ligand depending primarily upon the stereochemical orientation of the phosphorus moiety. The enhanced displacement reactivity of the *p*-nitrophenoxy ligand present in the ITP stereoisomers relative to that of the thiosuccinyl ligand may result in greater competition between these two potential leaving groups. This may result in two distinct sets of phosphorylated enzymes following inhibition by a single ITP isomer, the populations of which are dependent upon the stereochemical orientation of the phosphorus moiety (see Scheme 5.5).

This hypothesis might explain the observed k_3 values obtained from the inhibition of EEAChE and rMAChE by the ITP stereoisomers. Very little spontaneous reactivation

was observed for both enzyme sources regardless of which isomer was used for the inhibition reaction. In contrast, at least some oxime-mediated reactivation was observed in all cases, the magnitude of which was directly related to the stereochemical orientation of the asymmetric carbon. If the ITP stereoisomers assume an orientation with the phosphonyl oxygen positioned within the putative oxyanion hole and the phosphorylated serine apical to the position that was occupied by the ejected leaving group, as suggested by the crystal structures of AChEs inhibited by other OP compounds (Millard 1999a; Millard 1999b; Ordentlich 1999), then the stereochemical orientation about the phosphorus moiety of the OP-AChE adduct is essentially "locked" into place following the inhibition reaction (Hosea 1995; Wong 2000). As the ITP stereoisomers contain two potential leaving groups, one of which possesses a center of asymmetry, this alignment imposed by the structural constraints of the enzymes active site implies that six unique AChE conjugates are possible following the inhibition of AChE. If these putative adducts were to undergo the postinhibitory reactions of reactivation or aging, it is feasible that they would do so in a stereodependent manner as the three dimensional orientation of the ligands present could directly impact the accessibility of the reactivating nucleophiles (H_2O or oxime) to the phosphorylated active site. Conversely, the steric bulk of the remaining ligands combined with their inherent stereochemical orientation may perturb the optimal alignment of the phosphonyl oxygen within the putative oxyanion hole due to the dimensional constraints imposed by the gorge structure, thus reducing the susceptibility of the phosphorylated enzyme to nucleophilic attack (Ashani 1995; Wong 2000). A schematic representation of these possibilities is shown in Scheme 5.6. Note that for the purpose of illustration the view presented in Scheme 5.6 is looking down the P=O bond.

Scheme 5.6. Possible Inhibitory and Postinhibitory Mechanisms for the Inhibition of AChE by the ITP Stereoisomers.

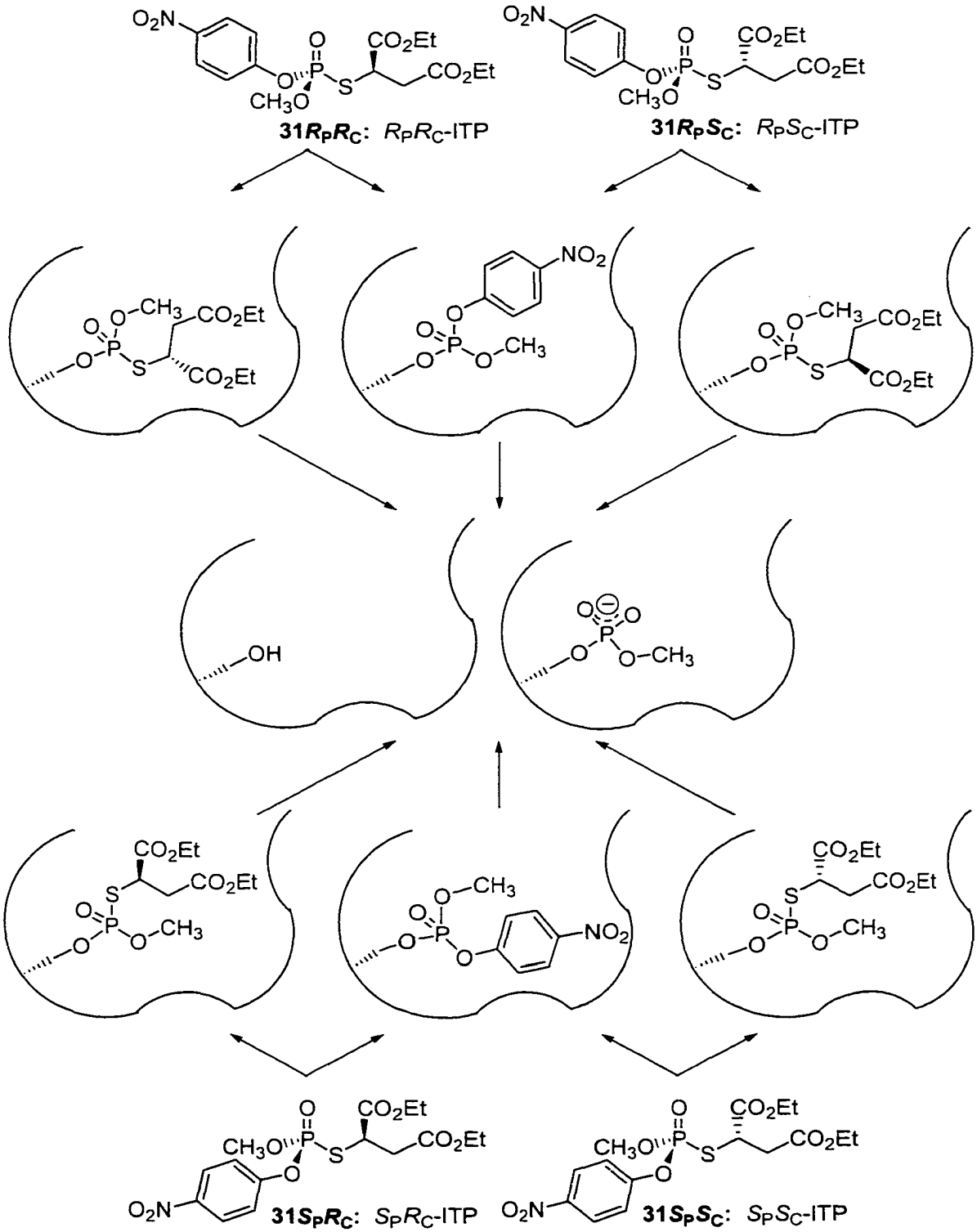

5.9-Observation of Abnormal Kinetics

As mentioned previously, during the time-dependent determination of the rate constant of inhibition for the stereoisomers of isomalathion versus EEAChE, it was observed that the R_P isomers afforded consistently abnormal data as depicted in Panel B of Figure 5.3. These observations were so intriguing that a detailed kinetic analysis of this phenomenon was conducted on the R_PS_C isomer of isomalathion. The averages of three individual assays at six different inhibitor concentrations are represented graphically in Figure 5.13 and a comparison of the results obtained is presented in Table 5.16.

Table 5.16. Comparison of the Kinetic Parameters Obtained at Different Concentrations of R_PS_C Isomalathion.

Experiment	$[i]$	Relative $[i]$ $[i]_o/[i]_A$	k_{obs}	Relative k_{obs} $(k_{obs})_o/(k_{obs})_A$	k_i	Relative k_i $(k_i)_o/(k_i)_A$	y Intercept
A	4.07×10^{-5}	1	-4.60×10^{-3}	1	628	1	1.89
B	1.42×10^{-4}	3.49	-6.51×10^{-3}	1.42	106	0.168	1.86
C	2.76×10^{-4}	6.78	-8.84×10^{-3}	1.92	74	0.117	1.86
D	4.60×10^{-4}	11.30	-1.20×10^{-2}	2.60	60	0.095	1.86
E	1.42×10^{-3}	34.87	-2.12×10^{-2}	4.60	34	0.054	1.77
F	2.76×10^{-3}	67.78	-2.97×10^{-2}	6.46	24	0.039	1.58

Figure 5.13. Comparison of the k_{obs} at Different Concentrations of R_PS_C Isomalathion

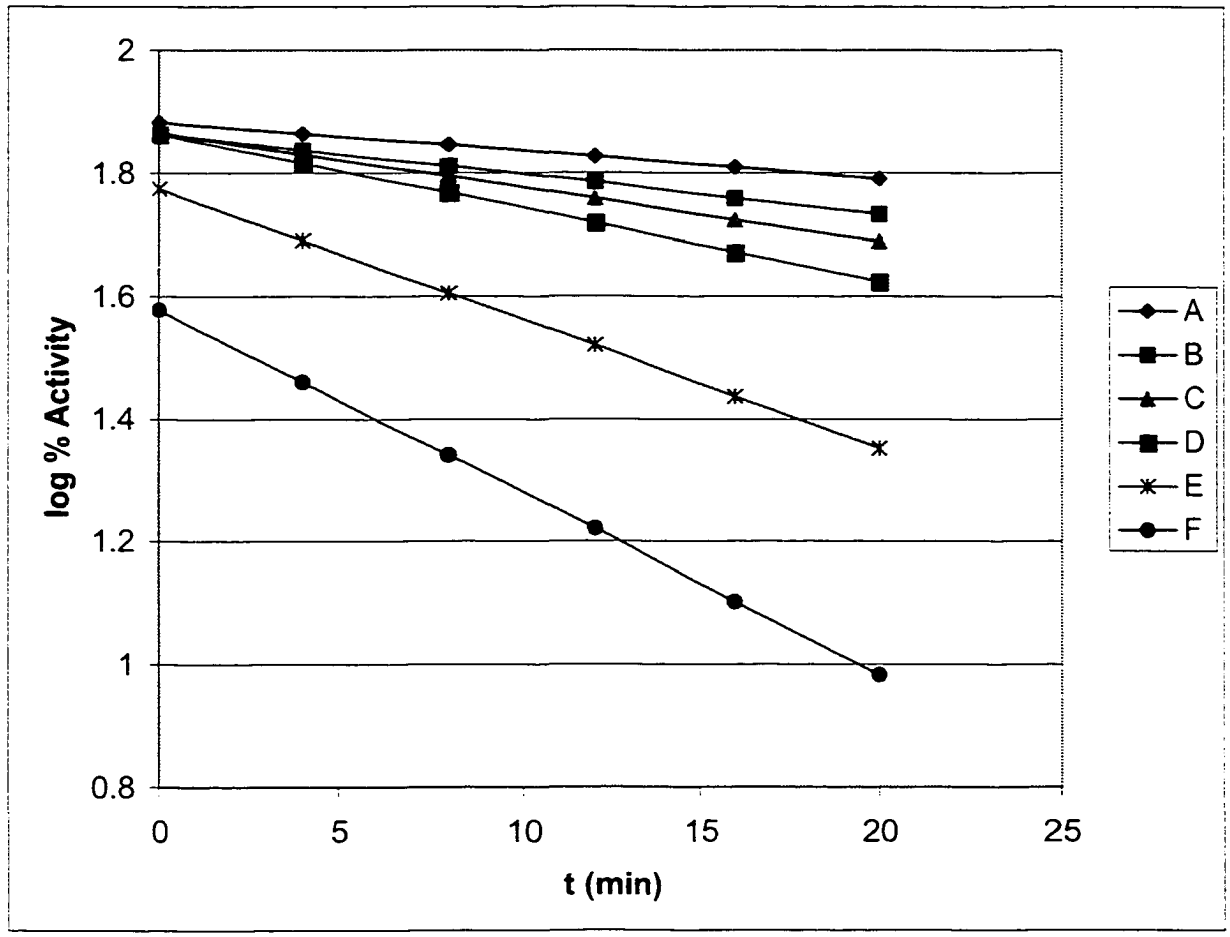

It is interesting to note that although the rate of inhibition is first order, the lines do not converge at 100% activity as would be expected. Another interesting characteristic of the data is that the first order rates are not linearly related to the concentration of the inhibitor. Similar kinetics have been noted for the compounds coroxon and haloxon (Aldridge 1969, 1975). More recently it has been demonstrated that paraoxon and methyl paraoxon also exhibit this behavior at extremes of concentration (Kardos 2000). The intercepts on the vertical access indicate a considerable degree of inhibition, which must be produced very quickly. The same inhibition was obtained when the inhibitor and substrate

are added either together or the substrate was added first. Such findings suggest a rapid equilibrium process, which is usually characteristic of reversible inhibition.

Another theoretical explanation for this phenomenon is that the inhibitor and substrate react together to produce a reversible inhibitor. However, this is unlikely for the following reasons: (1)-if the inhibitor is added to the enzyme just after or together with the substrate the same inhibition is obtained, (2)-if the substrate and the inhibitor are preincubated before the enzyme is added, the inhibition is independent of the time of the incubation, and (3)-the reversible inhibition decreases with increasing concentrations of substrate. These factors suggest that the explanation of the unexpected kinetic behavior must be made on the basis of the compound being the active inhibitor. It has also been suggested that these results may be caused by rapid reactivation of the inhibited enzyme. However, this possibility was discounted by the observation of similar kinetics for the S_PS_C isomalathion isomer, a compound that has been demonstrated to age rapidly (Doorn 2000).

Another possible explanation for the abnormal kinetic behavior observed during the inhibition of AChE by a number of compounds involves a second binding site on the protein that is distinct from the active site. Reversible binding to this other site is thought to impede subsequent phosphorylation of the active site by either causing steric occlusion of the gorge entrance or through allosteric modification of the enzymes function thereby decreasing the reactivity of the active site. The existence of a peripheral binding site was first suggested by Changeux (Changeux 1966) and was later implicated as causing the abnormal kinetic behavior observed by Aldridge and Reiner for the compounds coroxon and haloxon (Aldridge 1969, 1975). Numerous studies using site-specific mutagenesis have since established the existence of a peripheral binding site that binds ligands such as

propidium and fasciculin (Shafferman 1992; Barak 1994; Radic 1994; Velan 1996). However, the exact mechanism by which these compounds inhibit the hydrolysis of ACh remains ambiguous (and the source of much debate) as they have demonstrated elements indicative of both steric occlusion and allosteric modulation (Taylor 1975, 1994; Berman 1980; Radic 1984, 1991, 1995, 1999, 2000; Barak 1995; Bourne 1995; Rosenberry 1996, 1999; Velan 1996; Szegletes 1998, 1999; Mallender 1999, 2000).

5.10-Conclusions

1. The synthetic route proposed by Berkman *et al.* (1993b) was demonstrated to be a reliable method for the generation of the individual stereoisomers of isomalathion.
2. Combination of key reactions from the syntheses of isomalathion and isoparathion methyl was demonstrated to be an effective method to generate the individual stereoisomers of a new stereoisomeric isoparathion thiosuccinate phosphorothiolate (ITP) compound.
3. Comparison of the inhibitory kinetic profiles for the isomalathion stereoisomers vs. EEAChE and rMAChE demonstrated both stereoselectivity in inhibitory potency of the stereoisomers and species-dependent variations in stereoselectivity.
4. The postinhibitory kinetic profiles for the isomalathion stereoisomers vs. EEAChE and rMAChE demonstrated that, as suggested by examination of the kinetic parameters K_D and k_p, the stereochemical orientation of the phosphorus atom directly affects both the mechanisms of inhibition and the postinhibitory mechanisms associated with aging or nonreactivation.
5. MALDI-TOF-MS analysis of EEAChE inhibited by the isomalathion stereoisomers confirmed the presence of two distinct mechanisms of inhibition dependent upon the stereochemical orientation of the phosphorus atom (i.e. loss of the thiosuccinyl or thiomethyl ligand).
6. The inhibitory kinetic profiles for the ITP stereoisomers vs. EEAChE and rMAChE were similar in both magnitude and rank order of inhibitory potency

to those observed for the isomalathion stereoisomers and other structurally equivalent asymmetric OP compounds. This implies the ITP stereoisomers initial approach to, and interactions with, the active site of the enzyme follow a mechanism that is common to these types of compounds.

7. The spontaneous and oxime-mediated reactivation rates for EEAChE and rMAChE inhibited by the R_PR_C or S_PR_C ITP stereoisomers were similar in magnitude for both enzyme sources. This suggests that the resultant phosphorylated enzymes undergo similar mechanisms of reactivation.

8. The spontaneous and oxime-mediated reactivation rates obtained from EEAChE and rMAChE inhibited by R_PS_C or S_PS_C ITP stereoisomers were similar in magnitude for both enzyme sources, but were considerably lower than those observed for their corresponding enantiomers (R_PR_C or S_PR_C ITP). This suggests the OP-AChE adducts that result from inhibition by this pair of diastereomers are different from those generated by the inhibition of AChE by the R_PR_C or S_PR_C ITP stereoisomers.

Chapter 6

FUTURE WORK

Stereoselective inhibition of other α/β-hydrolases

As AChE is a member of the α/β-hydrolase superfamily, it would be of biochemical and toxicological interest to determine whether related enzymes are stereoselectively inhibited by the ITP and isomalathion stereoisomers. In particular, it would be interesting to determine whether the difference in mechanism of AChE inactivation between the R_P and the S_P isomers is conserved for other α/β-hydrolases. Such a study would further our understanding of the mechanistic commonalities and differences that exist among the members of this enzyme superfamily and would provide information about other potential targets of OP poisoning.

Stereoselective Inhibition of Carboxylesterases

The mammalian toxicity of commercial malathion preparations is believed to be attenuated by the isomalathion content through inhibition of carboxylesterases. The stereodependent inhibitory profile of the isomalathion stereoisomers vs. these enzymes should be examined and contrasted with their corresponding anti-AChE potencies. This type of analysis may provide a better understanding of the toxicological profiles of the individual stereoisomers and aid in the identification of the contribution of each

stereoisomer to the overall toxicity of a racemic mixture. The ITP and isomalathion stereoisomers may also provide a means to pharmacologically characterize the polymorphic variants that have been demonstrated for a number of esterases.

Stereoselective inhibition of other AChE's

Site-specific mutagenesis of AChE has generated a number of mutants in resent years. The ITP and isomalathion stereoisomers may be valuable tools for the examination of reactivity in relation to the geometric confines of the active center of AChE. A combined understanding of the structure of AChE and its mutants with the enantiomeric selectivity they display for OP compounds constitutes a powerful approach for delineating the orientation of the reactants involved in OP inhibition and reactivation of AChE. Also, an examination of the inhibition and reactivation profiles of AChE from other sources inhibited by the ITP or isomalathion stereoisomers may reveal novel species-dependent variations in the mechanisms of inhibition and reactivation.

MALDI-TOF-MS Characterization of the Adducts Formed by the Inhibition of AChE by the ITP Stereoisomers

The inhibitory and postinhibitory kinetic profiles of EEAChE and rMAChE inhibited by the ITP stereoisomers suggest that, as observed for the isomalathions, the mechanisms of inhibition and nonreactivation are determined by the stereochemical orientation of the particular isomer. However, the postinhibitory data obtained from inhibition of EEAChE and rMAChE by the ITP stereoisomers were considerably different from that obtained with the isomalathion stereoisomers. MALDI-TOF-MS characterization of AChE inhibited by the ITP stereoisomers would allow direct chemical determination of

the adducts formed, and would elucidate the ambiguity concerning the identity of the primary leaving group. It would also further our understanding of the mechanism of ITP inhibition of AChE.

Molecular Docking Studies

The availability of the X-ray crystal structures for a number of AChE's and other esterases allows molecular modeling of the ITP and isomalathion stereoisomers within the active sight of the enzymes. Molecular docking studies would lend further insight into the proposed stereochemically determined shift in primary leaving group that is suggested by the inhibitory and postinhibitory kinetic data that has been determined for the two sets of stereoisomers. Analysis of the results obtained from such studies combined with those from MALDI-TOF-MS characterization of the adducts formed by the inhibition of AChE by the ITP and isomalathion stereoisomers would increase our understanding of the structural features of the AChE active site and gorge that influence the mechanisms of inhibition and nonreactivation.

Immunological Characterization of AChE Inhibited by the ITP and Isomalathion Stereoisomers

The processes of inhibition and aging of AChE following treatment with the ITP or isomalathion stereoisomers may result in a modification of the enzymes three-dimensional structure. Perturbations of the enzyme's native structure may cause the enzyme to be "mis-recognized" by an organism's immune system. In addition to possibly eliciting deleterious immunological effects *in vivo*, the resultant formation of antibodies against the modified

enzyme may provide a means of detecting and/or purifying AChE that has been exposed to an OP compound.

Further Evaluation of the Abnormal Kinetic Behavior Observed During the Inhibition of EEAChE

The abnormal kinetics observed during the inhibition of EEAChE should be more rigorously investigated. As discussed in Section 5.9, the results obtained with high concentrations of the inhibitor were significantly different than the results obtained for the same inhibitor at lower concentrations (see Table 5.16 and Figure 5.13). This trend was observed for all OP inhibitors screened during this study, including DFP and S_PS_C isomalathion, which implies that the phenomenon is due to some inherent property of AChE. The data further suggests that R_PS_C isomalathion is interacting with a site on the enzyme that is distinct from the active site. However, it is not possible to ascertain from this data whether this secondary interaction occurs at the peripheral anionic site or some other region of the enzyme. In order to delineate this ambiguity, it will be necessary to repeat the kinetic analysis of these inhibitors in the presence and absence of AChE peripheral site inhibitors such as fasciculin, gallamine, D-tubocurarine, and propidium.

Chapter 7

EXPERIMENTAL

7.1-General

Commercially available reagents were purchased from Aldrich Chemical Co., Milwaukee, WI. All solvents and reagents were purified when necessary by standard literature methods. Melting points were determined on a Fisher-Johns melting point apparatus. Analytical thin-layer chromatography (TLC) was conducted on E. Merck aluminum-backed, 0.2 mm silica gel 60 F_{254}, TLC plates. Flash chromatography was performed with Kieselgel 60, 230-400 mesh (Merck). Elemental analyses were performed by Midwest Microlab Ltd., Indianapolis, IN.

Proton (^{1}H), carbon (^{13}C), and phosphorus (^{31}P) NMR spectra were recorded on a Varian VXR 400-NMR instrument in deuterated chloroform ($CDCl_3$) unless specified otherwise. Pertinent proton frequencies are tabulated in the following order: chemical shift (* in ppm), multiplicity (s, singlet; d, doublet; t, triplet; q, quartet; m, multiplet), coupling constant (*J* in hertz), and the number of hydrogens. Proton and carbon frequencies of spectra obtained are relative to chloroform (^{1}H, 7.24 ppm; ^{13}C, 77.0 ppm) as an internal standard unless specified otherwise. Phosphorus chemical shifts are relative to phosphoric acid (H_3PO_4) in $CDCl_3$ as an external standard.

Caution: *The OP chemicals synthesized and used in this study are hazardous anticholinesterases and should be handled by trained personnel in a well-ventilated hood. The OP chemicals described are hydrolyzed by 3 M NaOH to render them inactive as AChE inhibitors.*

7.2-Synthesis

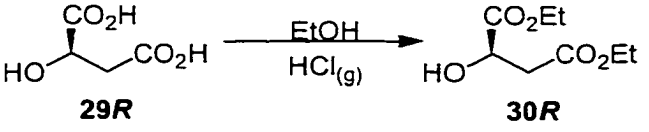

29*R* **30*R***

(*R*)-Diethyl malate (30*R*). This synthesis has been described previously (Cohen 1966) and is presented here with slight modification. HCl gas was bubbled through a solution of (*R*)-malic acid (20 g, 150 mmol) in 200 mL of absolute ethanol for 20 min. The solution was then capped, sealed, and stored at 0 °C for 48 h. Purification via Kugelrohr distillation (80 °C at 0.6 mm Hg) gave a colorless oil (26.95 g, 94 % yield). $[\alpha]_D^{24} = +9.59°$ ($c = 0.55$, $CHCl_3$). ^1H NMR δ 1.27 (t, $J = 7.2$ Hz, 3 H), 1.31 (t, $J = 7.2$ Hz, 3 H), 2.75-2.90 (m, 2 H), 4.18 (q, $J = 7.1$ Hz, 2 H), 4.28 (q, $J = 7.2$ Hz, 2 H), 4.49 (t, $J = 5.3$ Hz, 1 H). ^{13}C NMR δ 14.0, 38.7, 60.9, 61.9, 67.2, 170.4, 173.

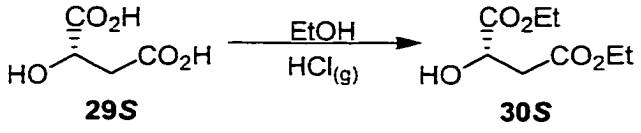

29*S* **30*S***

(*S*)-Diethyl malate (30*S*). Prepared as described for **30*R*** starting with (*S*) malic acid **29*S*** (20 g, 150 mmol). Purification via Kugelrohr distillation (80 °C at 0.6 mm Hg) gave a colorless oil (27.40 g, 96 % yield). $[\alpha]_D^{24} = -9.98°$ (c = 1.35, $CHCl_3$). The NMR spectral data of this material was identical to that of (*R*)-diethyl malate (**30*R***).

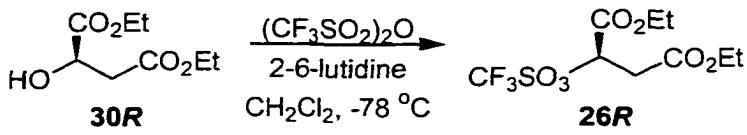

(R)-O-(Trifluoromethanesulfonyl)-diethyl malate (26*R*). This synthesis has been described previously (Berkman 1993) and is presented here with slight modification. Trifluoromethanesulfonic anhydride (2.00 mL, 11.9 mmol) was dissolved in 10 mL CH_2Cl_2 under an $Ar_{(g)}$ blanket and chilled to -78 °C. In a separate flask, (*R*)-diethyl malate (**30*R***) (2.00 g, 10.6 mmol) and 2,6-lutidine (1.24 mL, 10.6 mmol) were dissolved in 10 mL CH_2Cl_2 at room temperature, and added dropwise to the anhydride solution over 15 minutes. After the addition was complete, the reaction mixture was brought to 0 °C for 1 hour and then allowed to warm slowly to room temperature until TLC indicated the consumption of (*R*)-diethyl malate. The reaction mixture was concentrated to an oil followed by the addition of ether to precipitate the lutidinium salt. The salt was filtered *in vacuo* and washed three times with 50 mL ether. The filtrate was concentrated to an oil (3.47 g, 100% crude yield). $[\alpha]_D^{24} = -30.1°$ (c = 1.71, $CHCl_3$). ^{1}H NMR: δ 1.29 (t, J = 7.2 Hz, 3 H), 1.34 (t, J = 7.2 Hz, 3 H), 3.06 (d, J = 5.7 Hz, 2 H), 4.22 (dq, J = 2.1, 7.2 Hz, 2 H), 4.33 (dq, J = 2.1, 7.2 Hz, 2 H), 5.49 (t, J = 6.0 Hz, 1 H). ^{13}C NMR δ 13.8, 19.9, 36.8, 61.8, 63.2, 78.8, 112.5, 116.2, 120.5, 124.7, 166.0, 167.5.

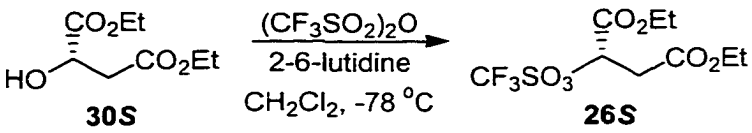

(*S*)-O-(Trifluoromethanesulfonyl)-diethyl malate (26*S*). Prepared as described for **26*R*** starting with (*S*)-diethyl malate (**30*S***, 2.00 g, 10.6 mmol) $[\alpha]_D^{24} = +32.6°$ (c = 1.39, $CHCl_3$). Workup provided an oil (3.47 g, 100% crude yield). The NMR spectral data of this material was identical to that of (*R*)-O-(Trifluoromethanesulfonyl)-diethyl malate (**26*R***).

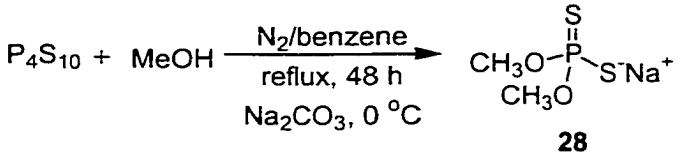

28

Sodium O,O-dimethyl phosphorodithioate (28). This synthesis has been described previously (Berkman, 1993) and is presented here with slight modification. Methanol (22 ml) was added dropwise to a stirring suspension of phosphorus pentasulfide (30 g, 67 mmol) in benzene (120 mL), at room temperature. The mixture was then heated to reflux for 48 h, cooled to room temperature, filtered, and the remaining solvent removed *in vacuo* to afford a greenish oil. The crude product was then used immediately for the conversion to sodium O,O-dimethyl phosphorodithioate. O,O-Dimethyl phosphorodithioic acid (**27**) was reacted with an equimolar amount of sodium carbonate in methanol at 0 °C. Following filtration and concentration of the solvent, crystallization was induced with ethyl ether (45 g, 92% yield). ^{1}H NMR δ 3.43 (d, J = 14.4 Hz, 6 H). ^{13}C NMR δ 52.8 (d, J = 9 Hz). ^{31}P NMR δ 117.6.

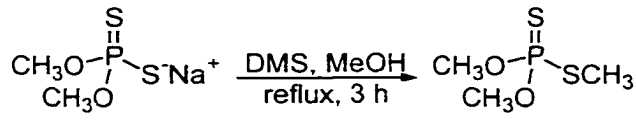

28 **24**

O,O,S-Trimethyl phosphorodithioate (24). As described previously (Umetsu 1977), dimethyl sulfate (25 g, 194 mmol) was added dropwise to a stirring solution of sodium-O,O-dimethyl phosphorodithioate (**28**; 35 g, 194 mmol) in 100 mL of methanol previously chilled to 0 °C. The mixture was then heated to reflux for 3 h and cooled to room temperature. The solution was then filtered and concentrated to an oil. Purification via Kugelrohr distillation (40 °C at 0.6 mm Hg) gave a colorless oil (30.07 g, 90% yield). ^{1}H NMR δ 3.89 (d, J = 14.1 Hz, 6 H), 2.23 (d, J = 14.2 Hz, 3 H). ^{13}C NMR δ 52.8 (d, J = 9 Hz), 5.4 (d, J = 9 Hz). ^{31}P NMR δ 100.4

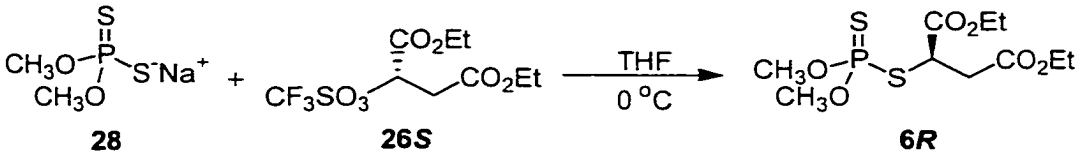

(*R*)-Malathion (6*R*). This synthesis has been described previously (Berkman, 1993) and is presented here with slight modification. Triflate **26*S*** (3.47 g; 10.6 mmol) was dissolved in 20 mL THF and chilled to 0 °C under $Ar_{(g)}$. In a separate flask,sodium O,O-dimethyl-phosphorodithioate **28** (2.86 g, 15.9 mmol) was dissolved in 10 mL THF, chilled to 0 °C and added dropwise to the triflate solution over 15 minutes. The reaction mixture was allowed to warm slowly to room temperature, stirred for 2 h, and partitioned between 50 mL ethyl ether and 50 mL water. The ether layer was separated and the aqueous layer re-extracted with ether (3 × 50 mL). The organic layers were combined, dried over sodium sulfate, and concentrated to an oil. Purification via chromatography using silica (hexane:EtOAc, 9:1 → 1:1) gave a colorless oil (2.64 g, 80% yield). $[\alpha]_D^{24} = +79.7°$ (c = 1.25, $CHCl_3$). ^{1}H NMR δ 1.22 (t, J = 7.2 Hz, 3 H), 1.25 (t, J = 7.2 Hz, 3 H), 2.84 (dd, J = 5.4, 17.1 Hz, 1 H), 3.00 (dd, J = 9.0, 17.1 Hz, 1 H), 3.77 (dd, J = 3.0, 15.3 Hz, 6 H), 4.03-4.22 (m, 5 H). ^{13}C NMR δ 13.9, 14.0, 37.7, 37.8, 45.0 (d, J = 5 Hz), 54.2 (d, J = 6 Hz), 61.1, 62.0, 169.9, 170.0. ^{31}P NMR: δ 96.2.

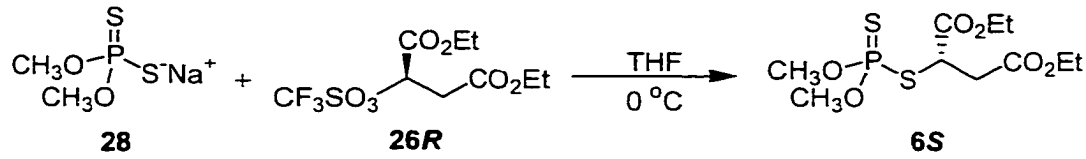

(*S*)-Malathion (6*S*). Prepared as described for **6*R*** starting with triflate **26** (3.47 g; 10.6 mmol). Purification via chromatography using silica (hexane:EtOAc, 9:1 - 1:1) gave a colorless oil (2.79 g, 84% yield). $[\alpha]_D^{24} = -80.0°$ (c = 1.25, $CHCl_3$). The NMR spectra of **6*S*** were identical to that of **6*R***.

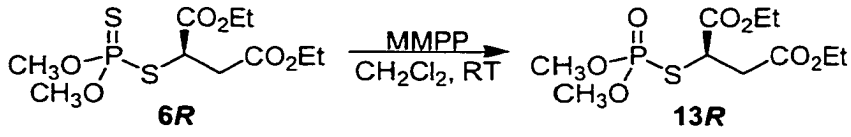

(*R*)-Maloxon (13*R*). This synthesis has been described previously (Berkman, 1993) and is presented here with slight modification. (*R*)-Malathion (**6*R***) (0.20 g, 0.606 mmol) was dissolved in 3 mL of CH_2Cl_2 and added to a stirring suspension of 80% monoperoxyphthalic acid, magnesium salt (0.187 g, 0.606 mmol), in 2 mL of CH_2Cl_2 at room temperature. The mixture was heated to reflux for 24 h, cooled to room temperature, and partitioned between 20 mL of ethyl ether and 20 mL of saturated sodium bicarbonate solution. The aqueous layer was extracted with 20 mL of ether, and the organic layers were combined, extracted with brine, dried over sodium sulfate, and concentrated to an oil. Purification via flash chromatography using silica gel (ethyl ether:petroleum ether, 2:1) gave a colorless oil (0.098 g, 52% yield). R_f = 0.13 (ethyl ether:petroleum ether, 2:1). $[\alpha]_D^{24}$ = + 51.5° (*c* = 0.59, $CHCl_3$). ^{1}H NMR δ 1.23 (t, *J* = 7.0 Hz, 3 H), 1.27 (t, *J* = 7.0 Hz, 3 H), 2.90 (dd, *J* = 5.1, 17.1 Hz, 1 H), 3.06 (dd, *J* = 8.7, 17.1 Hz, 1 H), 3.81 (dd, *J* = 5.1, 12.9 Hz, 6 H), 4.08-4.24 (m, 5 H). ^{13}C NMR δ 13.9, 14.0, 38.2, 42.4 (d, *J* = 5 Hz), 54.1, 54.2, 61.1, 62.1, 169.8, 170.1. ^{31}P NMR δ 28.3.

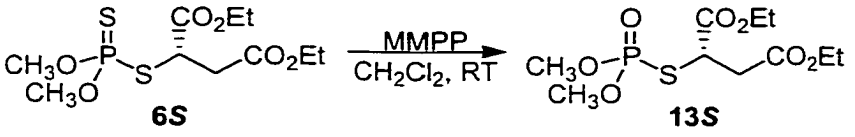

(*S*)-Maloxon (13*S*). Prepared as described for **13*R*** starting with (*S*)-malathion **6*S*** (0.20 g, 0.606 mmol). Purification via flash chromatography using silica gel (ethyl ether:petroleum ether, 2:1) gave a colorless oil (0.114 g, 60 % yield). R_f = 0.13 (ethyl ether:petroleum ether, 2:1). $[\alpha]_D^{24}$ = -49.2° (c = 0.63, $CHCl_3$). The NMR spectra of **13*S*** were identical to that of **13*R***.

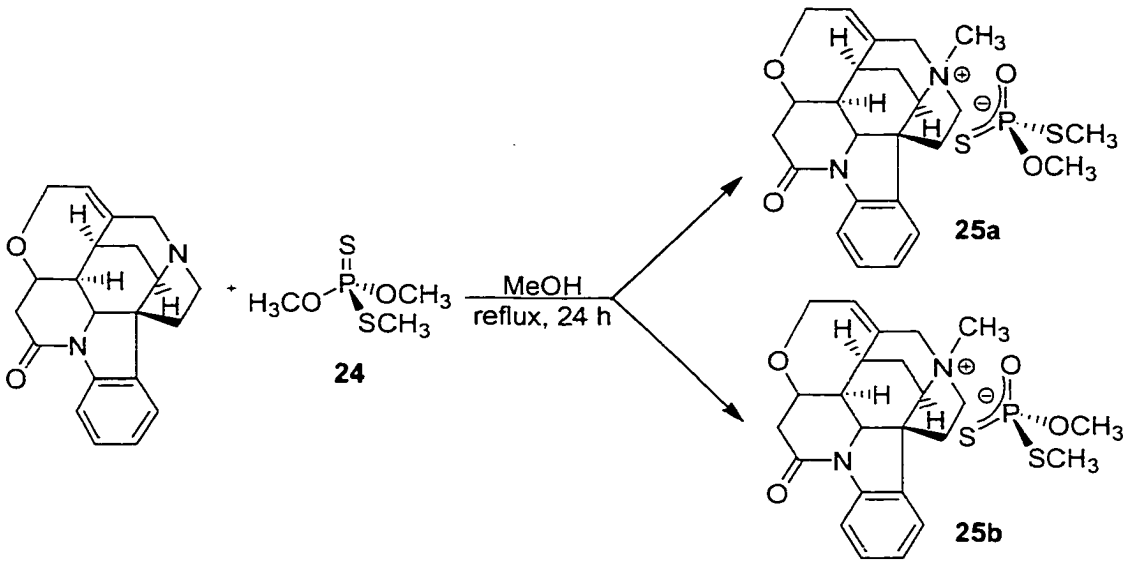

Strychnine-O,O,S-trimethylphosphorodithioate salt (25a and 25b). This procedure has been reported previously (Hilgetag 1969) but is repeated here with slight modifications. Strychnine (25.2 g, 75 mmol) was added to a stirring solution of O,O,S-trimethyl phosphorodithioate **24** (13.0 g, 75 mmol) in 180 mL of methanol. The reaction mixture was brought to reflux for 24 h. Upon cooling, the first crop of crystals (*R*/+) precipitated and were filtered, washed with methanol, and recrystallized twice from methanol. Data for **25a**: mp = 202-203 °C. $[\alpha]_D^{24} = +16.2°$ (c = 0.64, MeOH). ^{1}H NMR δ 1.38 (dt, J = 3.1, 10.7 Hz, 1 H), 1.56 (d, J = 14.8 Hz, 1 H), 1.97 (d, J = 2.8 Hz, 1 H), 2.02 (d, J = 14.1 Hz, 3 H), 2.14 (dt, J = 7.6, 13.7 Hz, 1 H), 2.44-2.59 (m, 2 H), 2.97 (dd, J = 8.2, 17.8 Hz, 1 H), 3.27 (s, 3 H), 3.30 (s, 1 H), 3.44 (d, J = 14.6 Hz, 3 H), 3.56-3.76 (m, 3 H), 3.95-4.25 (m, 5 H), 4.35 (dt, J = 3.2, 8.3 Hz, 1 H), 6.28 (s, 1 H), 7.12 (t, J = 7.6 Hz, 1 H), 7.25 (t, J = 7.7 Hz, 1 H), 7.37 (d, J = 7.6 Hz, 1 H), 7.78 (d, J = 8.1, 1 H). ^{13}C NMR δ 13.5 (d, J = 3 Hz), 24.2, 28.9, 38.8, 40.7, 46.0, 48.83, 52.8, 53.1 (d, J = 3 Hz), 54.4, 58.4, 61.6,

64.2 (d, J = 10 Hz), 74.7, 76.4, 115.8, 122.9, 125.4, 129.1, 129.9, 132.7, 135.6, 140.7, 171.3. ^{31}P NMR δ 78.87. The mother liquor was stored at 0 °C and gave a second crop that was recrystallized in 95% ethanol. The mother liquor was concentrated *in vacuo* to a solid and recrystallized in 95% ethanol to give a third crop of crystals. The second and third crop were combined and recrystallized once more in 95% ethanol (*S*/-). Data for **25b**: mp = 253 °C. $[\alpha]_D^{24}$ = -13.5° (c = 0.63, MeOH). ^{1}H NMR δ 1.36 (d, J = 10.7 Hz, 1 H), 1.55 (d, J = 15.7 Hz, 1 H), 1.91 (d, J = 12.2 Hz, 1 H), 2.01 (d, J = 14.1 Hz, 3 H), 2.12 (dt, J = 7.8, 13.7 Hz, 1 H), 2.44-2.57 (m, 2 H), 2.96 (dd, J = 8.2, 18.1 Hz, 1 H), 3.27 (s, 4 H), 3.44 (d, J = 14.5 Hz, 3 H), 3.53-3.76 (m, 3 H), 3.93-4.25 (m, 5 H), 4.34 (dt, J = 3.1, 8.3 Hz, 1 H), 6.28 (s, 1 H), 7.12 (t, J = 7.6 Hz, 1 H), 7.24 (t, J = 7.6 Hz, 1 H), 7.36 (d, J = 7.6 Hz, 1 H), 7.76 (d, J = 8.1 Hz, 1 H). ^{13}C NMR δ 13.4 (d, J = 3 Hz), 24.2, 28.9, 38.8, 40.7, 46.1, 52.8, 53.1 (d, J = 3 Hz), 54.4, 58.4, 61.6, 63.9 (d, J = 10 Hz), 74.7, 76.4, 115.8, 123.0, 125.5, 129.1, 130.0, 132.7, 135.6, 140.7, 171.3. ^{31}P NMR δ 78.79.

General procedure for the synthesis of isomalathion stereoisomers (12R_PR_C, R_PS_C, S_PR_C, and S_PS_C) from strychnine-O,S-dimethyl phosphorodithioate salts (25a and 25b). To a chilled (0 °C) solution of triflate (1.23 g, 3.8 mmol) in 25 mL of CH_3CN, the (+ or -) strychnine-O,S-dimethyl phosphorodithioate salt (1.75 g, 3.45 mmol) is added all at once. The solution is brought to room temperature and vigorously mixed for 2 h. The solution is then diluted two-fold with ethyl ether to precipitate the strychninium triflate salt. The mixture is filtered and the filtrate was concentrated *in vacuo* to an oil. Purification by gravity chromatography using silica (hexane:EtOAc, 9:1 - 1:1) gave a colorless oil.

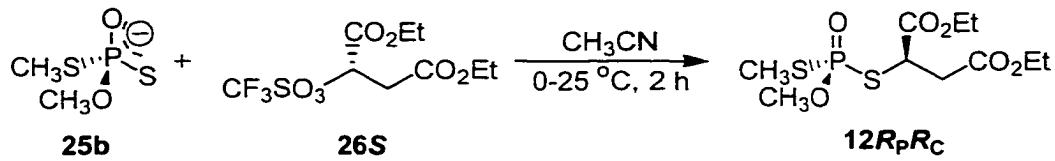

25b **26*S*** **12R_PR_C**

R_PR_C*-Isomalathion (12R_PR_C).** To a chilled (0 °C) solution of triflate **26*S (1.23 g, 3.8 mmol) in 25 mL of CH_3CN, the (–) strychnine-O,S-dimethyl phosphorodithioate salt **25b** (1.75 g, 3.45 mmol) is added all at once. The solution is brought to room temperature and vigorously mixed for 2 h. The solution is then diluted two-fold with ethyl ether to precipitate the strychninium triflate salt. The mixture is filtered and the filtrate concentrated *in vacuo* to an oil. Purification by gravity chromatography using silica (hexane:EtOAc, 9:1 – 1:1) gave a colorless oil (0.86 g, 75 % yield). $[\alpha]_D^{24} = +42.0°$ (c = 0.57, $CHCl_3$). ^{1}H NMR δ 1.23 (t, J = 7.1 Hz, 3 H), 1.27 (t, J = 7.1 Hz, 3 H), 2.36 (d, J = 16.9 Hz, 3 H), 2.97 (dd, J = 5.2 , 17.2 Hz, 1 H), 3.08 (dd, J = 8.9 , 17.1 Hz , 1 H), 3.84 (d, J = 13.6 Hz, 3 H), 4.08-4.25 (m, 5 H). ^{13}C NMR δ 13.4, 14.1, 38.1, 38.2, 43.2 (d, J = 10 Hz), 53.9 (d, J = 3 Hz), 61.1, 62.2, 169.9, 170.0. ^{31}P NMR δ 58.30. $C_{10}H_{20}O_6PS_2$ (m+1) requires 331.0439; found 331.0438.

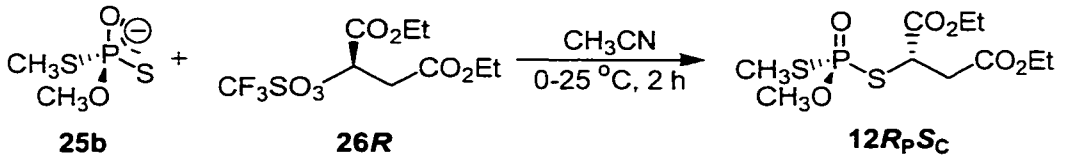

25b **26*R*** **12R_PS_C**

R_PS_C* -Isomalathion (12R_PS_C).** To a chilled (0 °C) solution of triflate **26*R (1.34 g, 4.16 mmol) in 25 mL of CH_3CN, the (–) strychnine-O,S-dimethyl phosphorodithioate salt **25b** (1.91 g, 3.77 mmol) is added all at once. The solution is brought to room temperature and vigorously mixed for 2 h. The solution is then diluted two-fold with ethyl ether to precipitate the strychninium triflate salt. The mixture is filtered and the filtrate concentrated *in vacuo* to an oil. Purification by gravity chromatography using silica (hexane:EtOAc, 9:1 – 1:1) gave a colorless oil (0.94 g, 76 % yield). $[\alpha]_D^{24}$ = - 57.5° (*c* = 0.63, $CHCl_3$). ^{1}H NMR δ 1.23 (t, *J* = 7.1 Hz, 3 H), 1.27 (t, *J* = 7.1 Hz, 3 H), 2.37 (d, *J* = 16.8 Hz, 3 H), 2.94 (dd, *J* = 5.2, 17.1 Hz, 1 H), 3.08 (dd, *J* = 8.8, 17.1 Hz, 1 H), 3.85 (d, *J* = 13.7 Hz, 3 H), 4.09-4.26 (m, 5 H). ^{13}C NMR δ 13.1, 13.2, 14.1, 38.0, 43.4 (d, *J* = 5 Hz), 54.1 (d, *J* = 11 Hz), 61.1, 62.2, 169.9, 171.0. ^{31}P NMR δ 56.91. $C_{10}H_{20}O_6PS_2$ (m+1) requires 331.0439; found 331.0440.

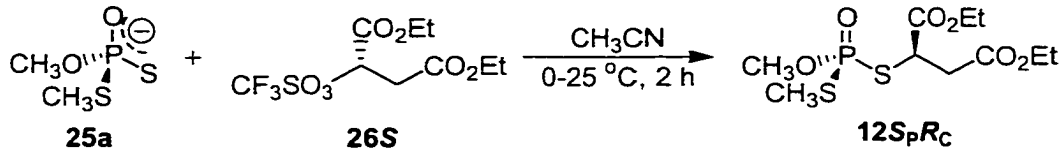

25a **26*S*** **12S_PR_C**

S_PR_C* -Isomalathion (12S_PR_C).** To a chilled (0 °C) solution of triflate **26*S (1.19 g, 3.69 mmol) in 25 mL of CH_3CN, the (–) strychnine-O,S-dimethyl phosphorodithioate salt **25a** (1.57 g, 3.10 mmol) is added all at once. The solution is brought to room temperature and vigorously mixed for 2 h. The solution is then diluted two-fold with ethyl ether to precipitate the strychninium triflate salt. The mixture is filtered and the filtrate concentrated *in vacuo* to an oil. Purification by gravity chromatography using silica (hexane:EtOAc, 9:1 - 1:1) gave a colorless oil (0.78 g, 76 % yield). $[\alpha]_D^{24} = +58.9°$ (c = 0.67, $CHCl_3$). The NMR spectra of **12S_PR_C** were identical to that of **12R_PS_C**. $C_{10}H_{20}O_6PS_2$ (m+1) requires 331.0439; found 331.0437.

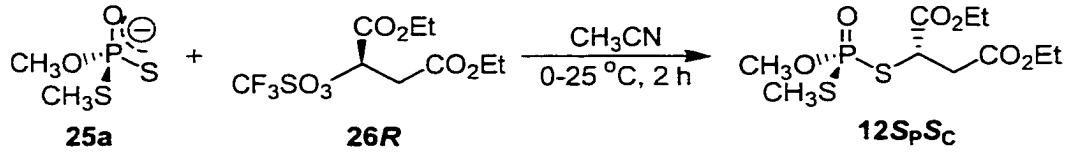

S_PS_C* -Isomalathion (12*S_PS_C*).** To a chilled (0 °C) solution of triflate **26*R (1.11 g, 3.44 mmol) in 25 mL of CH_3CN, the (–) strychnine-O,S-dimethyl phosphorodithioate salt **25a** (1.58 g, 3.13 mmol) is added all at once. The solution is brought to room temperature and vigorously mixed for 2 h. The solution is then diluted two-fold with ethyl ether to precipitate the strychninium triflate salt. The mixture is filtered and the filtrate concentrated *in vacuo* to an oil. Purification by gravity chromatography using silica (hexane:EtOAc, 9:1 – 1:1) gave a colorless oil (0.61 g, 59 % yield). $[\alpha]_D^{24} = -44.2°$ (*c* = 0.62, $CHCl_3$). The NMR spectra of **12*S_PS_C*** were identical to that of **12*R_PR_C***. $C_{10}H_{20}O_6PS_2$ (m+1) requires 331.0439; found 331.0441.

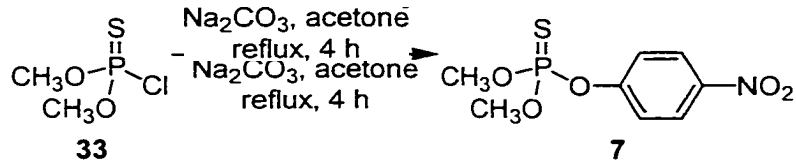

O,O-Dimethyl-p-nitrophenoxy phosphorothionate (Parathion Methyl) (7).

This synthesis (Fletcher et al., 1950) is reported here with some modification. *p*-Nitrophenol (13.86 g, 100 mmol) and sodium carbonate (11.62 g, 110 mmol) were added to a vigorously stirring solution of O,O-dimethyl phosphorochloridothioate (16.00 g, 100 mmol) in 100 mL of freshly distilled acetone. The resulting suspension was brought to reflux for approximately 3 h until consumption of the starting material was observed by TLC. The mixture was then cooled to room tempera0ture, filtered through a bed of Celite®, and the excess solvent removed by rotary evaporation. The resulting oil was then suspended in 100 mL of ethyl ether, washed twice with saturated sodium carbonate and brine, and dried over sodium sulfate. After filtration, the solution was concentrated to an oil and the crude product was purified by flash chromatography (ethyl ether:petroleum ether, 3:1) to yield a colorless oil (20 g, 76%). R_f = 0.46 (ethyl ether:petroleum ether, 3:1). ^{1}H NMR δ 3.84 (d, J = 14.1 Hz, 6 H), 7.29 (d, J = 8.3 Hz, 2 H), 8.20 (d, J = 8.3 Hz, 2 H). ^{13}C NMR δ 54.5 (d, J = 5 Hz), 121.5, 125.9, 145.5 (d, J = 6 Hz), 154.1. ^{31}P NMR δ 66.09.

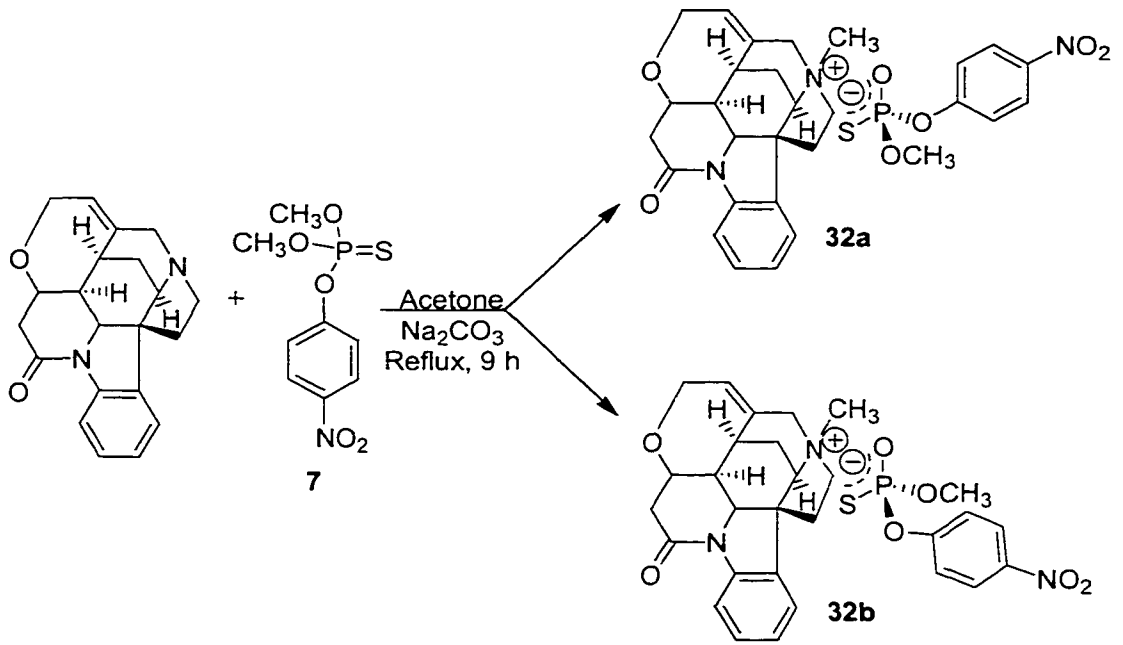

Strychnine-isoparathion methyl salt (32a and 32b). This procedure has been reported previously (Hilgetag 1969) but is repeated here with slight modifications. (-)-Strychnine (2.54 g, 7.07 mmol) was added to a stirring solution of parathion methyl (2.02 g, 7.7 mmol) in 100 mL of methanol and the resulting mixture heated to reflux for 9 h. Upon cooling, the first crop of crystals (**32a**, as prisms) precipitated and were filtered, washed with methanol, and recrystallized twice from methanol. The mother liquor was concentrated to a solid which was then recrystallized twice from acetonitrile (**32b**, needles).

Data for **32a**: mp = 219 °C. $[\alpha]_D^{24} = -22.9°$ ($c = 0.45$, MeCN). ^{1}H NMR: δ 1.43-1.51 (m, 1 H), 1.57-1.64 (m, 1 H), 2.17-2.33 (m, 2 H), 2.60-2.76 (m, 2 H), 2.96 (dd, J = 8.2, 17.2 Hz, 1 H), 3.34 (s, 1 H), 3.42 (s, 3 H), 3.51 (d, J = 13.2 Hz, 3 H), 3.57-3.76 (m, 4 H), 4.36-4.42 (m, 2 H), 6.36 (s, 1 H), 7.17 (t, J = 7.6 Hz, 1 H), 7.33 (t, J = 7.6 Hz, 1 H), 7.40 (d, J = 9.3 Hz, 2 H), 7.72 (d, J = 7.6 Hz, 1 H), 7.94 (d, J = 8.1 Hz, 1 H), 8.17 (d, J = 9.3 Hz, 2 H). ^{13}C

NMR: δ 23.8, 28.7, 45.9, 52.2, 52.3, 52.5, 54.2, 58.0, 61.3, 63.1, 63.3, 73.9, 75.7, 115.2, 120.4, 120.5, 123.5, 123.9, 124.9, 129.3, 129.3, 133.0, 135.2, 141.5, 141.6, 159.3, 168.8. ^{31}P NMR: δ 55.87. Data for **32b**: mp = 214-216 °C. $[\alpha]_D^{24} = +23.0°$ ($c = 0.1$, MeCN). ^{1}H NMR: δ 1.45-1.49 (m, 1 H), 1.50-1.64 (m, 1 H), 2.08 (s, 2 H), 2.19-2.26 (m, 2 H), 2.60-2.71 (m, 2 H), 2.96 (dd, $J = 8.2$, 17.0 Hz, 1 H), 3.36 (s, 3 H), 3.49 (d, $J = 13.2$ Hz, 3 H), 3.59-3.70 (m, 2 H), 3.94 (d, $J = 13.5$ Hz, 1 H), 4.10-4.25 (m, 4 H), 4.34-4.38 (m, 2 H), 6.31-6.39 (m, 1 H), 7.17 (t, $J = 7.5$ Hz, 1 H), 7.32 (d, $J = 7.9$ Hz, 1 H), 7.38 (d, $J = 9.4$ Hz, 2 H), 7.70 (d, $J = 7.32$ Hz, 1 H), 7.94 (d, $J = 8.1$ Hz, 1 H), 8.16 (d, $J = 9.3$ Hz, 2 H). ^{13}C NMR: δ 23.9, 28.7, 46.0, 52.3, 52.4, 52.6, 54.3, 58.1, 61.4, 63.2, 63.4, 73.9, 75.8, 115.3, 120.4, 120.5, 123.5, 124.0, 125.0, 129.4, 129.4, 133.1, 135.3, 141.6, 159.4, 159.5, 168.9. ^{31}P NMR: δ 55.86.

General procedure for the synthesis of the stereoisomers of 2-[methoxy-(4-nitro-phenoxy)-phosphorylsulfanyl]-succinic acid diethyl ester (31R_PR_C, R_PS_C, S_PR_C, and S_PS_C) from strychnine-isoparathion methyl salt (32a and 32b). To a chilled (0 °C) solution of triflate (1.94 g, 6.02 mmol) in THF, (25 mL) the (+ or -) strychnine-isoparathion methyl salt (3.00 g, 5.02 mmol) is added all at once. The solution is vigorously mixed for 24 h at room temperature and then diluted two-fold with ethyl ether to precipitate the strychninium triflate salt. The mixture is filtered and the filtrate was concentrated *in vacuo* to an oil, The products were purified by flash chromatography using silica (ethyl ether:petroleum ether, 3:1) to give colorless oils.

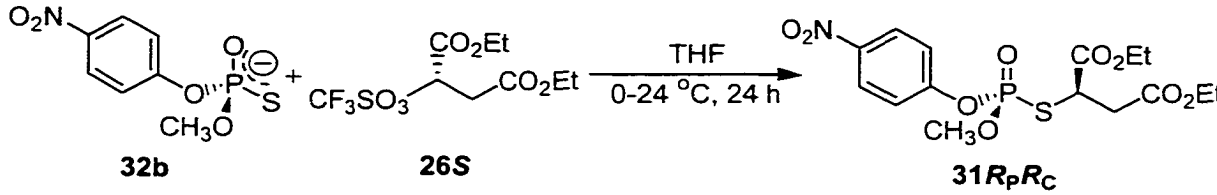

32b **26*S*** **31R_PR_C**

R_PR_C-2-[Methoxy-(4-nitro-phenoxy)-phosphorylsulfanyl]-succinic acid diethyl ester (31R_PR_C). To a chilled (0 °C) solution of triflate **26*S*** (1.94 g, 6.02 mmol) in 25 mL of THF, the (+) strychnine-isoparathion methyl salt **32b** (3.0 g, 5.02 mmol) is added all at once. The solution is brought to room temperature and vigorously mixed for 24 h. The solution is then diluted two-fold with ethyl ether to precipitate the strychninium triflate salt. The mixture is filtered and the filtrate concentrated *in vacuo* to an oil. Purification by flash chromatography using silica (ethyl ether:petroleum ether, 3:1) gave a colorless oil (1.10 g, 48 % yield). $[\alpha]_D^{24} = +13.0°$ (c = 1.10, MeCN). ^{1}H NMR δ 1.19 (t, J = 7.2 Hz, 3 H), 1.20 (t, J = 7.2 Hz, 3 H), 2.89 (dd, J = 5.2, 17.0 Hz, 1 H), 3.04 (dd, J = 8.4 , 17.0 Hz , 1 H), 3.91 (d, J = 12.8 Hz, 3 H), 4.10 (q, J = 7.2 Hz, 2 H), 4.11 (q, J = 7.2 Hz, 2 H), 4.17 (dd, J = 5.2, 8.4 Hz, 1 H), 7.38-7.42 (m, 2 H), 8.19-8.23 (m, 2 H). ^{13}C NMR δ 13.9, 14.0, 38.0, 43.1, 55.0 (d, J = 6 Hz), 61.3, 62.4, 121.2, 121.3, 125.6, 154.5 (d, J = 7 Hz), 162.2, 169.3, 169.7. ^{31}P NMR δ 23.8. $C_{15}H_{21}NO_9PS$ (m+1) requires 422.0674; found 422.0677.

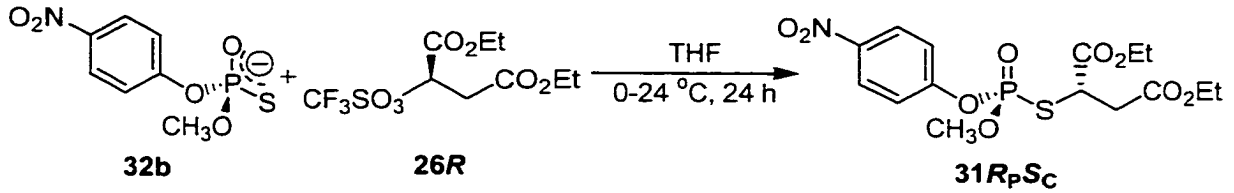

32b **26*R*** **31R_PS_C**

R_PS_C*-2-[Methoxy-(4-nitro-phenoxy)-phosphorylsulfanyl]-succinic acid diethyl ester (31R_PS_C).** To a chilled (0 °C) solution of triflate **26*R (1.94 g, 6.02 mmol) in 25 mL of THF, the (+) strychnine-isoparathion methyl salt **32b** (3.0 g, 5.02 mmol) is added all at once. The solution is brought to room temperature and vigorously mixed for 24 h. The solution is then diluted two-fold with ethyl ether to precipitate the strychninium triflate salt. The mixture is filtered and the filtrate concentrated *in vacuo* to an oil. Purification by flash chromatography using silica (ethyl ether:petroleum ether, 3:1) gave a colorless oil (1.00 g, 47 % yield). $[\alpha]_D^{24} = -16.3°$ ($c = 0.91$, MeCN). ^{1}H NMR δ 1.20 (t, $J = 7.2$ Hz, 3 H), 1.22 (t, $J = 7.2$ Hz, 3 H), 2.89 (dd, $J = 3.9$, 17.2 Hz, 1 H), 3.00 (dd, $J = 7.5$, 17.2 Hz , 1 H), 3.96 (d, $J = 13.6$ Hz, 3 H), 4.10 (q, $J = 7.2$ Hz, 2 H), 4.11 (q, $J = 7.2$ Hz, 2 H), 4.17 (dd, $J = 3.9$, 7.5 Hz, 1 H), 7.38-7.42 (m, 2 H), 8.21-8.25 (m, 2 H). ^{13}C NMR δ 13.8, 13.9, 37.8, 43.1, 55.1 (d, $J = 9$ Hz), 61.2, 62.4, 121.2, 125.6, 154.5 (d, $J = 6$ Hz), 162.2, 169.3, 169.7. ^{31}P NMR δ 23.8. $C_{15}H_{21}NO_9PS$ (m+1) requires 422.0674; found 422.0670.

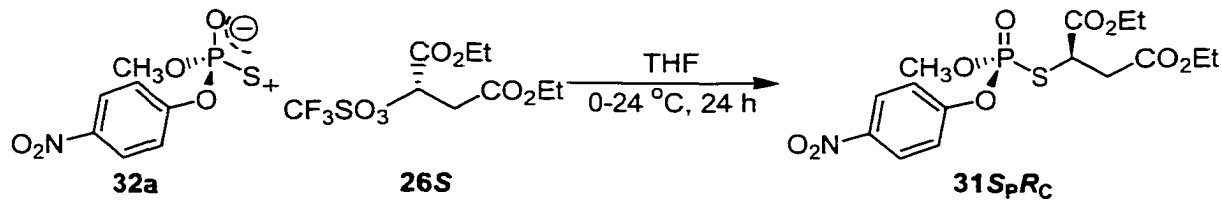

32a **26*S*** **31S_PR_C**

S_PR_C-2-[Methoxy-(4-nitro-phenoxy)-phosphorylsulfanyl]-succinic acid diethyl ester (31S_PR_C). To a chilled (0 °C) solution of triflate **26*S*** (0.65 g, 2.00 mmol) in 25 mL of THF, the (-) strychnine-isoparathion methyl salt **32a** (1.0 g, 1.68 mmol) is added all at once. The solution is brought to room temperature and vigorously mixed for 24 h. The solution is then diluted two-fold with ethyl ether to precipitate the strychninium triflate salt. The mixture is filtered and the filtrate concentrated *in vacuo* to an oil. Purification by flash chromatography using silica (ethyl ether:petroleum ether, 3:1) gave a colorless oil (0.20 g, 57 % yield). $[\alpha]_D^{24} = +16.0°$ ($c = 0.86$, MeCN). The NMR spectra of **31S_PR_C** were identical to that of **31R_PS_C**. $C_{15}H_{21}NO_9PS$ (m+1) requires 422.0674; found 422.0680.

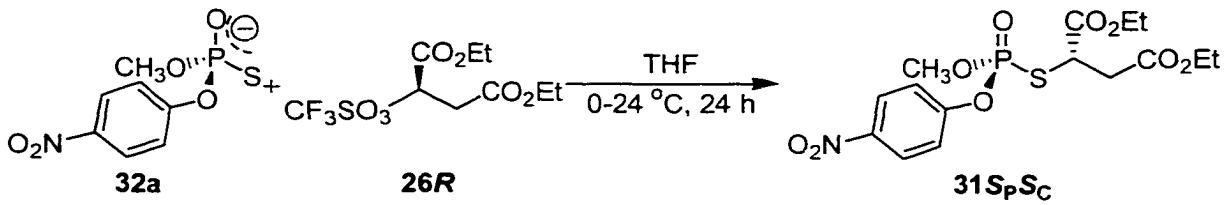

32a **26*R*** **31S_PS_C**

S_PS_C*-2-[Methoxy-(4-nitro-phenoxy)-phosphorylsulfanyl]-succinic acid diethyl ester (31S_PS_C).** To a chilled (0 °C) solution of triflate **26*R (0.65 g, 2.0 mmol) in 25 mL of THF, the (-) strychnine-isoparathion methyl salt **32a** (1.0 g, 1.68 mmol) is added all at once. The solution is brought to room temperature and vigorously mixed for 24 h. The solution is then diluted two-fold with ethyl ether to precipitate the strychninium triflate salt. The mixture is filtered and the filtrate concentrated *in vacuo* to an oil. Purification by flash chromatography using silica (ethyl ether:petroleum ether, 3:1) gave a colorless oil (0.17 g, 49 % yield). $[\alpha]_D^{24} = -12.9°$ (c = 1.0, MeCN). The NMR spectra of **31S_PS_C** were identical to that of **31R_PR_C**. $C_{15}H_{21}NO_9PS$ (m+1) requires 422.0674; found 422.0673.

7.3-Kinetic Analysis

The potency of each stereoisomer as inhibitors of electric eel acetylcholinesterase (EEAChE) and recombinant mouse brain acetylcholinesterase (rMAChE) was determined. As previously mentioned, there are both a time dependent and a concentration dependent method for measuring the bimolecular inhibition constant k_i. Since the concentration dependent method affords k_i , K_D and k_p, this more rigorous method was primarily used. However, the time-dependent method of analysis was also performed in an attempt to verify the accuracy of the kinetic perimeters obtained from the concentration dependent method. The concentration dependent method is based upon equation 2, while the time dependent method is based upon equation 3. Both equations contain the term v, which represents the relative velocity and is equal to A_o/A_t where A_o is the activity of AChE at time equals 0 and A_t is the activity of AChE after t minutes of inhibition.

In order to measure the activity of the enzyme, a colorimetric assay originally developed by Ellman *et al.* (Ellman 1961) was utilized. In this method, acetylthiocholine (ATCh-I) is used as the substrate for AChE instead of ACh. The determination of AChE activity is dependent upon the enzyme-catalyzed hydrolysis of ATCh-I and the subsequent thiocholine-mediated reaction with 5,5'-dithiobis-[2-nitrobenzoic acid] (DTMB or Ellman's reagent), a chromogen, to yield a yellow chromophore (the anion of 5-thio-2-nitrobenzoic acid, see Figure) whose absorbance is measured spectrophotometrically at 412 nm. The rate at which this yellow color is generated is directly proportional to the enzyme's rate of hydrolysis.

7.3.1-Materials

Chemicals. Other chemicals in the enzyme assays were commercially obtained as follows: acetylthiocholine iodide, Aldrich Chemical Company (Milwaukee, WI); diisopropylphorofluoridate (DFP), 5,5′-dithio-[2-nitrobenzoic acid] (DTNB), EEAChE Type V-S, and 1,19-trimethylene-*bis*(4-formylpyridinium bromide) (TMB-4), pyridine-2-aldoxime methiodide (2-PAM), Sigma Chemical Company (St. Louis, MO). Soluble recombinant mouse AChE expressed in HEK-293 cells and purified by affinity chromatography as described previously (Marchot 1996) was a generous gift from Dr. Palmer Taylor (University of California, San Diego, La Jolla, CA). All other chemicals were reagent grade or the highest grade commercially available. Aqueous solutions were prepared in distilled deionized water.

7.3.2-Enzyme and Tissue Preparation

Recombinant Mouse AChE. rMAChE is truncate at its carboxy-terminal end by the insertion of an early stop codon at position 549. This modification allows the enzyme to be expressed into the extra (-)cellular medium as the deleted residues undergo post-transitional modifications, including glycosylation, that dictate their association with the cell membrane. While these modifications have been demonstrated to have a negligible effect on the enzymes activity and specificity relative to the native enzyme, it has been shown that this lack of glycosylation decreases the thermal stability of the expressed AChE (Velan 1993). Our experiments with rMAChE verify these observations of thermal instability. It was established that the enzyme was also particularly sensitive to the effects

of solvents used to dilute inhibitors demonstrating as much as 10% reduction in activity for solutions containing 0.5% (vol/vol) of isopropyl alcohol, ethanol, or ACN (see Figure 7.1).

Figure 7.1. Effect of Solvent on the Activity of AChE

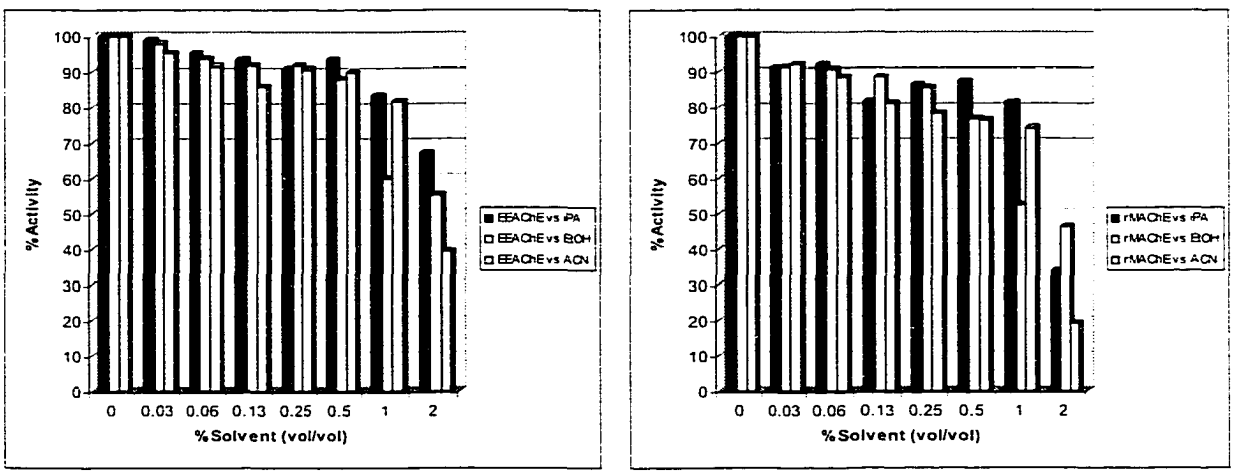

Consequently, prior to use the enzyme was stored at -20 °C. All studies that required an incubation period greater than 1 h (see Reactivation section) were conducted at 4 °C. The highest final concentration of solvent resent in all experiments was less than 0.3 %, and the control reaction in each study contained the same amount of solvent as was present in the inhibited samples.

Stock solutions of rMAChE were prepared by diluting 100 μL of the purified enzyme to a finale volume of 20 mL with 0.1 M phosphate buffer at pH 7.6 and were kept at 4 °C. Working solutions were prepared as needed by diluting the necessary volume of stock solution in pH 7.6 phosphate buffer (0.1 M) to achieve desired activity. Activity of the working solution must be attenuated such that the optical density of the reaction

mixture does not exceed the detection limit of the spectroscopic device used to monitor the reaction during the time scale of the study.

Electric Eel AChE. Stock solutions of EEAChE were prepared by dissolving 5.0 mg of lyophilized enzyme (sigma) in 20 mL of 0.1 M phosphate buffer at pH 7.6 and were kept at 4 °C. Working solutions of EEAChE were prepared as needed by the method outlined for rMAChE above. Gel electrophoresis and Western Blotting experiments demonstrated the presence of contaminants in the commercially available preparations of EEAChE (George 2000). Despite these observations, the enzyme has proven to be very robust to both solvent effects and temperature extremes and has consistently provided reproducible results. These factors combined with the availability of this source have made it the enzyme of choice for conducting all preliminary studies. All tissue homogenate AChE preparations used were prepared as reported previously (Berkman 1993a; Berkman 1993b; Jianmongkol 1996; Jianmongkol 1999).

All studies were conducted in 0.1 M phosphate buffer at pH 7.6 at 24 °C unless noted otherwise. These pH and temperature conditions were chosen for all assays and determinations of kinetic constants to facilitate comparisons with previously published work with the isomalathion stereoisomers, namely inhibition of AChE from rat and hen brain (Berkman 1993a; Berkman 1993b; Jianmongkol 1996; Jianmongkol 1999). It is recognized that the average body temperature of the animals from which the enzyme is obtained is considerably different and the pH optima for substrate hydrolysis, inhibition, and postinhibitory reactions for a given source of AChE may vary (Aldridge 1975).

7.3.3- Methods

Method 1: Time Dependent Determination of k_i. Six cuvettes containing 20 μL ATCh-I solution (75 mM ATCh-I: phosphate buffer pH 7.6) and 2.50 mL of DTNB solution (0.33 mM DTNB, 0.59 mM $NaHCO_3$; phosphate buffer pH 7.6) are placed in a Beckman DU-7500 diode-array spectrophotometer and maintained at 24 °C. Two 480 μL aliquots of working enzyme solution are placed in test tubes and maintained at 24 °C. To the first test tube, 20 μL of the solvent used to dilute the inhibitor is added and this mixture serves as the control (A_o). At $t = 0$, 20 μL of the inhibitor solution is added to the other enzyme aliquot, and vortexed gently. At select time points (t), the residual activity of the two solutions (A_t) is determined by adding 20 μL aliquots of the solutions to the cuvettes and the rate of ATCh-I hydrolysis is monitored at 412 nm (15 sec intervals) for 4 min following the addition of the enzyme. The bimolecular rate constant of inhibition, k_i, is determined as the average of 10 runs by plotting $\ln(A_o/A_t)$ versus the incubation time. The resulting slopes are determined by linear regression based on the equation $\ln(A_o/A_t) = [i]k_i t$ (Aldridge 1950). A_o represents the activity of the uninhibited enzyme ($t = 0$) and A_t is the depressed enzyme activity at time = t following addition of the inhibitor. The final concentrations of the reactants during enzyme assay were: 0.33 mM DTNB, 0.59 mM ATCh-I, and 0.58 mM $NaHCO_3$.

Method 2: Concentration Dependent Determination of k_i, K_D, and k_p. Five test tubes containing 480 μL of working AChE solution are each treated with 20 μL of five progressive inhibitor concentrations ranging from [i] to 10[i]. A sixth test tube is treated

with 20 μL of the solvent used to dilute the inhibitor serves as control. The inhibition was permitted to progress for a specific period of time, t (3 to 30 min dependent upon the concentration and inhibitory potency of the inhibitor used, the temperature at which the experiment is conducted, and the activity of the enzyme solution used), and the remaining enzyme activity (A_t) was determined as described above (Method 1) over a period of 4 min (15-s intervals). The bimolecular reaction constant (k_i), dissociation constant (K_D), and phosphorylation constant (k_p) were determined using the following equation as defined previously (Main, 1964):

$$1/[i] = (\Delta t / \Delta \ln v)k_i - 1/K_D \qquad (2)$$

where:

t = the time of inhibition,

$\ln v = \ln(A_o/A_t)$,

$k_i = k_p/K_D$.

Method 3: Concentration Dependent Determination of k_i, K_D, and k_p. AChE activity was determined spectrophotometrically in 0.10 M sodium phosphate buffer pH 7.6 at 24 °C using the colorimetric method of Ellman *et al.* (1961), which was modified for use in 96-well plates and a temperature-controlled VERSAmax 340 microplate reader (Molecular Devices Corporation, Sunnydale, CA).

Stock solutions of inhibitors were prepared by dissolving the compounds in an appropriate amount of solvent. Working solutions of the inhibitors were prepared by first

diluting an aliquot of the stock inhibitor solution 10-fold with 0.1 M phosphate buffer at pH 7.6 followed by 6 serial dilutions with more phosphate buffer for a total of 7 individual inhibitor solutions with concentrations ranging from [*i*] to 64[*i*]. An eighth solution containing 10% (vol/vol) of the solvent used to dissolve the inhibitor is prepared with 0.1 M phosphate buffer at pH 7.6 to serve as a control.

At $t = 0$, 2 μL aliquots of each solution are then combined with 98 μL of enzyme stock solution in an array similar to that represented in Figure 7.2 using a 96 (-) well plate as the reaction vessel (note that the larger volume should always be added last to insure thorough mixing of the components). The well plate is subjected to intermittent agitation in order to maintain the homogeneity of the resulting mixtures while they are incubated for a discrete period of time (3 to 30 min dependent upon the concentration and inhibitory potency of the inhibitor used, the temperature at which the experiment is conducted, and the activity of the enzyme solution used). The inhibition progress can be monitored by combining 2 μL aliquots from the mixtures with 2 μL of a 75 mM ATCh-I solution in 0.1 M phosphate buffer at pH 7.6 and 196 μL of a standard DTNB solution (0.33 mM DTNB and 0.59 mM $NaHCO_3$ in 0.1 M phosphate buffer at pH 7.6) positioned in a 96 (-) well plate to match the configuration of the first well plate. This 100-fold dilution of the enzyme–inhibitor mixture effectively stops the inhibition reaction and provides the reagents necessary for spectrophotometric monitoring of the residual enzyme activity at 412 nm as per the method of Ellman *et al.*(1961) The 12^{th} row of the well plate contains 2 μL of the ATCh-I solution and 198 μL of the DTNB solution and serves as a blank during the spectaphotometric monitoring.

Residual enzyme activity is calculated by the SOFTmax PRO (slope of absorbance at 412 nm vs. time during the first 4 min) by linear regression following subtraction of control sample. The values obtained for each column are combined with their corresponding inhibitor concentrations using Eqn. 2 and represented graphically. The kinetic parameters k_i, K_D, and k_p are determined as described in Method 2. If the inhibition reactions are monitored at least 4 times during the course of the study it is also possible to use Eqn. 3, as presented in Method 1, to determine k_i in a time-dependent fashion.

Figure 7.2. Well Plate Configuration for Method 3.

	1	2	3	4	5	6	7	8	9	10	11	12
A	Con	Con	Con	Con	Con	Con	Con	Con	Con	Con	Con	Blank
B	[*I*]	[*I*]	[*I*]	[*I*]	[*I*]	[*I*]	[*I*]	[*I*]	[*I*]	[*I*]	[*I*]	Blank
C	2[*I*]	2[*I*]	2[*I*]	2[*I*]	2[*I*]	2[*I*]	2[*I*]	2[*I*]	2[*I*]	2[*I*]	2[*I*]	Blank
D	4[*I*]	4[*I*]	4[*I*]	4[*I*]	4[*I*]	4[*I*]	4[*I*]	4[*I*]	4[*I*]	4[*I*]	4[*I*]	Blank
E	8[*I*]	8[*I*]	8[*I*]	8[*I*]	8[*I*]	8[*I*]	8[*I*]	8[*I*]	8[*I*]	8[*I*]	8[*I*]	Blank
F	16[*I*]	16[*I*]	16[*I*]	16[*I*]	16[*I*]	16[*I*]	16[*I*]	16[*I*]	16[*I*]	16[*I*]	16[*I*]	Blank
G	32[*I*]	32[*I*]	32[*I*]	32[*I*]	32[*I*]	32[*I*]	32[*I*]	32[*I*]	32[*I*]	32[*I*]	32[*I*]	Blank
H	64[*I*]	64[*I*]	64[*I*]	64[*I*]	64[*I*]	64[*I*]	64[*I*]	64[*I*]	64[*I*]	64[*I*]	64[*I*]	Blank

Con = Control
[*I*] = Inhibitor Concentration

The result of this configuration is 11 equivalent and independent experiments, each consisting of 7 different inhibitor concentrations, which are run in parallel. That the individual experiments are run simultaneously nearly eliminates the potential for variability

in the conditions between them. This combined with the volume of data obtained during the experiments greatly enhances the statistical validity of the kinetic parameters obtained by this method.

Method 4: Determination of k_3, The Rate Constant of Spontaneous Reactivation. Aliquots (200 μL) of working enzyme solutions that contain inhibitor concentrations that have caused 90% enzyme inhibition (I_{90}) after a specific period of incubation are isolated. The inhibition reaction is stopped by diluting the samples 100-fold with 0.1 M phosphate buffer at pH 7.6. Effectiveness of 100-fold dilution to retard further inhibition was checked in two ways: (A) results obtained with 100- and 200-fold dilution were comparable, and (B) inhibitory capacity of 100-fold diluted sample was similar to that of inhibitor-free buffer. Immediately following dilution ($t = 0$), and at discrete time points thereafter (t), 1 mL aliquots are added to cuvettes containing 1.5 mL of DTNB solution (0.33 mM DTNB and 0.59 mM $NaHCO_3$ in 0.1 M phosphate buffer at pH 7.6 and 24 °C) and the residual enzyme activity (A_o and A_t, respectively) is determined spectraphotometrically (using Beckman DU-7500) as detailed in Method 1. In parallel, a second set of aliquots from working enzyme solution that has been exposed to the same concentration of solvent as used to dilute the inhibitor in the first sample are diluted with 0.1 M phosphate buffer at pH 7.6 100-fold and their residual enzyme activity and serves as a control for the reaction (A). The rate constant for spontaneous reactivation, k_{3spon}, is calculated from the linear portion of the graph using the following equation (Clothier 1981; Berkman 1993b):

$$\ln(100/\%\text{inhibition}) = k_3 t \quad (7)$$

where % inhibition = $(A - A_t)/(A - A_o) \times 100$.

Enzyme activity was assayed periodically to determine the total % reactivation of enzyme activity after 60 min. Total % reactivation is calculated using the following equation:

$$\%\ \text{reactivation} = 100 - (\%\ \text{inhibition at 60 min}) \quad (8)$$

Method 5: Determination of k_3 (2-PAM or TMB-4), The Rate Constant of Oxime-Mediated Reactivation. This procedure is identical to that described for the determination of spontaneous reactivation Method 4 except that the buffer solution used to dilute the samples also contains an oxime (2-PAM or TMB-4, final concentration, 50 mM). The rate constant for oxime-mediated reactivation k_3 (2-PAM or TMB-4) and the amount of total % reactivation is calculated using the procedures detailed in Method 4.

Method 6: Simultaneous Determination of k_3 Spontaneous, k_3 (2-PAM), and k_3 (TMB-4). Inhibited and control AChE samples obtained during the inhibition studies outlined in Method 3 can be used to determine the postinhibitory kinetic parameters k_{3spon}, $k_{3(2\text{-PAM})}$, and $k_{3(TMB\text{-}4)}$ simultaneously by the following method. Aliquots (30 μL) from samples that contained inhibitor concentrations that caused 90% enzyme inhibition (I_{90}) after a specific period of incubation are isolated. The inhibition reaction is stopped by diluting the samples to a final volume of 3 mL (100-fold) with DTNB solution (0.33 mM DTNB and 0.59 mM $NaHCO_3$ in 0.1 M phosphate buffer at pH 7.6 and 24°C) or with

DTNB solution that also contains the oxime 2-PAM or TMB-4 (final concentration, 0.1 mM) and the initial residual enzyme activity (A_o) is measured immediately (time, $t = 0$) by removing 198 μL aliquots of the resulting mixtures and combining them with 2 μL of a 75 mM ATCh-I solution followed by spectrophotometric monitoring similar to that outlined in Method 3. The residual enzyme activity (A_t) is determined at designated intervals (t) for up to $t = 60$ min. In parallel, the AChE activity in the absence of inhibitor (A) is determined in the same manner to serve as the control. The rate constant of spontaneous and oxime-mediated reactivation for the inhibited AChE (k_3 (spon), k_3 (2-PAM), and k_3 (TMB-4)) and the total %reactivation are determined according to the equations set forth in Method 4.

Figure 7.3. Well Plate Configuration for k_3 Determination (Method 6).

	1	2	3	4	5	6	7	8	9
A	Con (spon)	Con (2-PAM)	Con (TMB-4)	Blank (spon)	Blank (2-PAM)	Blank (TMB-4)	[*i*] (spon)	[*i*] (2-PAM)	[*i*] (TMB-4)
B	Con (spon)	Con (2-PAM)	Con (TMB-4)	Blank (spon)	Blank (2-PAM)	Blank (TMB-4)	[*i*] (spon)	[*i*] (2-PAM)	[*i*] (TMB-4)
C	Con (spon)	Con (2-PAM)	Con (TMB-4)	Blank (spon)	Blank (2-PAM)	Blank (TMB-4)	[*i*] (spon)	[*i*] (2-PAM)	[*i*] (TMB-4)
D	Con (spon)	Con (2-PAM)	Con (TMB-4)	Blank (spon)	Blank (2-PAM)	Blank (TMB-4)	[*i*] (spon)	[*i*] (2-PAM)	[*i*] (TMB-4)
E	Con (spon)	Con (2-PAM)	Con (TMB-4)	Blank (spon)	Blank (2-PAM)	Blank (TMB-4)	[*i*] (spon)	[*i*] (2-PAM)	[*i*] (TMB-4)
F	Con (spon)	Con (2-PAM)	Con (TMB-4)	Blank (spon)	Blank (2-PAM)	Blank (TMB-4)	[*i*] (spon)	[*i*] (2-PAM)	[*i*] (TMB-4)
G	Con (spon)	Con (2-PAM)	Con (TMB-4)	Blank (spon)	Blank (2-PAM)	Blank (TMB-4)	[*i*] (spon)	[*i*] (2-PAM)	[*i*] (TMB-4)
H	Con (spon)	Con (2-PAM)	Con (TMB-4)	Blank (spon)	Blank (2-PAM)	Blank (TMB-4)	[*i*] (spon)	[*i*] (2-PAM)	[*i*] (TMB-4)

Con = Control
Spon = Spontaneous Reactivation samples
2-PAM and TMB-4 = Samples that contain the Respective Oximes
[*i*] = Samples that contain inhibitor

If the samples are configured in a 96 well plate in a fashion similar to that represented in Figure 7.3 it is possible to monitor the progression of spontaneous reactivation and two types of oxime-mediated reactivation simultaneously for eight individual experiments. Further, this configuration is optimized to allow the SOFTmax PRO software to subtract both the inhibitory effect of the oximes themselves and the rate of spontaneous ATCh-I hydrolysis that is caused by the presence of the oximes affording a more accurate determination of the respective kinetic parameters. As with Method 3, the fact that the experiments are run simultaneously greatly diminishes the variance between individual runs thus enhancing the statistical validity of the results obtained.

REFERENCES

Aldridge, W. N. (1950). "Some Properties of Specific Cholinesterases with Particular Reference to the Mechanism of Inhibition by Diethyl P-Nitrophenyl Thiophsophate (E605) and Analogues." *Biochem J* **46**: 451.

Aldridge, W. N. and Davison, A. N. (1952). "The Inhibition of Erythrocyte Cholinesterase by Tri-Esters of Phosphoric Acid." *Biochem J* **51**: 61-70.

Aldridge, W. N., Miles, J. W., Mount, D. L. and Verschoyle, R. D. (1979). "The Toxicological Properties of Impurities in Malathion." *Arch Toxicol* **42**: 95-106.

Aldridge, W. N. and Reiner, E. (1969). "Acetylcholinesterase. Two Types of Inhibition by an Organophosphorus Compound: One the Formation of Phosphorylated Enzyme and the Other Analogous to Inhibition by Substrate." *Biochem J* **115**: 147-162.

Aldridge, W. N. and Reiner, E. (1975). *Enzyme Inhibitors as Substrates*. New York, Elsevier Publishing Co.

Alvarez, A., Alarcon, R., Opazo, C., Campos, E. O., Munoz, F. J., Calderon, F. H., Dajas, F., Gentry, M. K., Doctor, B. P., De Mello, F. G. and Inestrosa, N. C. (1998). "Stable Complexes Involving Acetylcholinesterase and Amyloid-Beta Peptide Change the Biochemical Properties of the Enzyme and Increase the Neurotoxicity of Alzheimer's Fibrils." *J Neurosci* **18**(9): 3213-23.

Alvarez, A., Opazo, C., Alarcon, R., Garrido, J. and Inestrosa, N. C. (1997). "Acetylcholinesterase Promotes the Aggregation of Amyloid-Beta-Peptide Fragments by Forming a Complex with the Growing Fibrils." *J Mol Biol* **272**(3): 348-61.

Ames, R. G., Brown, S. K., Mengle, D. C., Kahn, E., Stratton, J. W. and Jackson, R. J. (1989). "Protecting Agicultural Applicators from over-Exposure to Cholinesterase-Inhibiting Pesticides." *J Soc Occup Med* **39**: 85-92.

Ames, R. G., Steenland, K., Jenkins, B., Chrislip, D. and Russo, J. (1995). "Chronic Neurologic Sequelae to Cholinesterase Inhibition among Agricultural Pesticide Applicators." *Arch Environ Health* **50**(6): 440-4.

Amitai, G., Moorad, D., Adani, R. and Doctor, B. P. (1998). "Inhibition of Acetylcholinesterase and Butyrylcholinesterase by Chlorpyrifos-Oxon." *Biochem Pharmacol* **56**(3): 293-9.

Armstrong, D. J. and Fukuto, T. R. (1987). "Synthesis, Resolution, and Toxicological Properties of the Chiral Isomers of O,S-Dimethyl and -Diethyl Ethylphosphonothioate." *J Agric Food Chem* **35**: 500-503.

Aronstam, R. S., Smith, M. D. and Buccafusco, J. J. (1987). "Clonidine Prevents the Short-Term Down Regulation of Muscarinic Receptors in Mouse Brain Induced by the Acetylcholinesterase Inhibitor Soman." *Neurosci Lett* **78**(1): 107-12.

Aschner, M. (2000). "Interactions between Pesticides and Glia: An Unexplored Experimental Field." *Neurotoxicology* **21**(1-2): 175-80.

Ashani, Y., Radic, Z., Tsigelny, I., Vellom, D. C., Pickering, N. A., Quinn, D. M., Doctor, B. P. and Taylor, P. (1995). "Amino Acid Residues Controlling Reactivation of

Organophosphonyl Conjugates of Acetylcholinesterase by Mono- and Bisquaternary Oximes." *J Biol Chem* **270**(11): 6370-80.

Ashford, N. and Miller, C. S. (1998). *Chemical Exposures: Low Levels and High Stakes.* New York, Wiley.

Axelrad, J. (1998). "An Autoimmune Response Causes Transmissible Spongiform Encephalopathies." *Med Hypotheses* **50**(3): 259-64.

Axelsen, P. H., Harel, M., Silman, I. and Sussman, J. L. (1994). "Structure and Dynamics of the Active Site Gorge of Acetylcholinesterase: Synergistic Use of Molecular Dynamics Simulation and X-Ray Crystallography." *Protein Sci* **3**(2): 188-97.

Baker, E. L., Jr., Warren, M., Zack, M., Dobbin, R. D., Miles, J. W., Miller, S., Alderman, L. and Teeters, W. R. (1978). "Epidemic Malathion Poisoning in Pakistan Malaria Workers." *Lancet* **1**(8054): 31-4.

Ballantyne, B., Marrs, T. C. and (eds) (1992). *Clinical and Experimental Toxicology of Organophosphates and Carbamates.* Oxford, Butterworth-Heinemann.

Barak, D., Kronman, C., Ordentlich, A., Ariel, N., Bromberg, A., Marcus, D., Lazar, A., Velan, B. and Shafferman, A. (1994). "Acetylcholinesterase Peripheral Anionic Site Degeneracy Conferred by Amino Acid Arrays Sharing a Common Core." *J Biol Chem* **269**(9): 6296-305.

Barak, D., Ordentlich, A., Bromberg, A., Kronman, C., Marcus, D., Lazar, A., Ariel, N., Velan, B. and Shafferman, A. (1995). "Allosteric Modulation of Acetylcholinesterase Activity by Peripheral Ligands Involves a Conformational Transition of the Anionic Subsite." *Biochemistry* **34**(47): 15444-52.

Barinaga, M. (1991). "A New Buzz in the Medfly Debate." *Science* **253**: 1351.

Barnes, J. M. (1976). Hazards to People. *Pesticides and Human Welfare.* D. L. Gunn and J. G. R. Stevens. Oxford, Oxford University Press.

Barnes, J. M. (1999). "Problems in Monitoring Overexposure among Spray Workers in Fruit Orchards Chronically Exposed to Diluted Organophosphate Pesticides." *Int Arch Occup Environ Health* **73**(3): M68-M74.

Barr, D. B. (1999). "Exposure to Contemporary-Use Pesticides." *J Med Assoc Ga* **88**(4): 34-7.

Bell, I. R., Bootzin, R. R., Ritenbaugh, C., Wyatt, J. K., DeGiovanni, G., Kulinovich, T., Anthony, J. L., Kuo, T. F., Rider, S. P., Peterson, J. M., Schwartz, G. E. and Johnson, K. A. (1996). "A Polysomnographic Study of Sleep Disturbance in Community Elderly with Self-Reported Environmental Chemical Odor Intolerance." *Biol Psychiatry* **40**(2): 123-33.

Benschop, H. P., Konings, C. A., Van Genderen, J. and De Jong, L. P. (1984a). "Isolation, Anticholinesterase Properties, and Acute Toxicity in Mice of the Four Stereoisomers of the Nerve Agent Soman." *Toxicol Appl Pharmacol* **72**(1): 61-74.

Benschop, H. P., Konings, C. A., van Genderen, J. and de Jong, L. P. (1984b). "Isolation, in Vitro Activity, and Acute Toxicity in Mice of the Four Stereoisomers of Soman." *Fundam Appl Toxicol* **4**(2 Pt 2): S84-95.

Berkman, C. E. (1994). *Synthesis of Malathion, Malaoxon, and Isomalathion Enantiomers and Examination of Their Interactions with Acetylcholinesterase.* Chemistry. Loyola University of Chicago. Chicago.

Berkman, C. E., Quinn, D. A. and Thompson, C. M. (1993a). "Interaction of Acetylcholinesterase with the Enantiomers of Malaoxon and Isomalathion." *Chem Res Toxicol* **6**(5): 724-30.

Berkman, C. E., Ryu, S., Quinn, D. A. and Thompson, C. M. (1993b). "Kinetics of the Postinhibitory Reactions of Acetylcholinesterase Poisoned by Chiral Isomalathion: A Surprising Nonreactivation Induced by the Rp Stereoisomers." *Chem Res Toxicol* **6**(1): 28-32.

Berman, H. A. and Decker, M. M. (1989a). "Chiral Nature of Covalent Methylphosphonyl Conjugates of Acetylcholinesterase." *J Biol Chem* **264**(7): 3951-6.

Berman, H. A. and Leonard, K. (1989b). "Chiral Reactions of Acetylcholinesterase Probed with Enantiomeric Methylphosphonothioates. Noncovalent Determinants of Enzyme Chirality." *J Biol Chem* **264**(7): 3942-50.

Berman, H. A., Yguerabide, J. and Taylor, P. (1980). "Fluorescence Energy Transfer on Acetylcholinesterase: Spatial Relationship between Peripheral Site and Active Center." *Biochemistry* **19**(10): 2226-35.

Bertoni-Freddari, C., Fattoretti, P., Casoli, T., Meier-Ruge, W. and Ulrich, J. (1990). "Morphological Adaptive Response of the Synaptic Junctional Zones in the Human Dentate Gyrus During Aging and Alzheimer's Disease." *Brain Res* **517**(1-2): 69-75.

Beyreuther, K. and Masters, C. L. (1994). "Neurobiology. Catching the Culprit Prion." *Nature* **370**(6489): 419-20.

Bhatt, M. H., Elias, M. A. and Mankodi, A. K. (1999). "Acute and Reversible Parkinsonism Due to Organophosphate Pesticide Intoxication: Five Cases." *Neurology* **52**(7): 1467-71.

Bigbee, J. W., Sharma, K. V., Chan, E. L. and Bogler, O. (2000). "Evidence for the Direct Role of Acetylcholinesterase in Neurite Outgrowth in Primary Dorsal Root Ganglion Neurons." *Brain Res* **861**(2): 354-62.

Bigbee, J. W., Sharma, K. V., Gupta, J. J. and Dupree, J. L. (1999). "Morphogenic Role for Acetylcholinesterase in Axonal Outgrowth During Neural Development." *Environ Health Perspect* **107 Suppl 1**: 81-7.

Black, R. M. and Pearson, G. S. (1993). "Unequivocal Evidence." *Chem Britain* **29**: 584-587.

Botti, S. A., Felder, C. E., Lifson, S., Sussman, J. L. and Silman, I. (1999). "A Modular Treatment of Molecular Traffic through the Active Site of Cholinesterase." *Biophys J* **77**(5): 2430-50.

Botti, S. A., Felder, C. E., Sussman, J. L. and Silman, I. (1998). "Electrotactins: A Class of Adhesion Proteins with Conserved Electrostatic and Structural Motifs." *Protein Eng* **11**(6): 415-20.

Bourne, Y., Grassi, J., Bougis, P. E. and Marchot, P. (1999a). "Conformational Flexibility of the Acetylcholinesterase Tetramer Suggested by X-Ray Crystallography." *J Biol Chem* **274**(43): 30370-6.

Bourne, Y., Taylor, P., Bougis, P. E. and Marchot, P. (1999b). "Crystal Structure of Mouse Acetylcholinesterase. A Peripheral Site- Occluding Loop in a Tetrameric Assembly." *J Biol Chem* **274**(5): 2963-70.

Bourne, Y., Taylor, P. and Marchot, P. (1995). "Acetylcholinesterase Inhibition by Fasciculin: Crystal Structure of the Complex." *Cell* **83**(3): 503-12.

Broomfield, C., Millard, C. B., Lockridge, O. and Caviston, T. L. (1995). *Enzymes of the Cholinesterase Family*. New York, Plenum Press.

Brugere-Picoux, J. and Rerat, A. (1996). "[Human and Animal Spongiform Encephalopathy. Update on December 17, 1996]." *Bull Acad Natl Med* **180**(9): 2127-35; discussion 2135-7.

Buccafusco, J. J. and Aronstam, R. S. (1987). "Adrenergic Agonists Protect against Soman, an Irreversible Acetylcholinesterase Inhibitor." *Toxicol Lett* **38**(1-2): 67-76.

Buccafusco, J. J. and Jackson, W. J. (1991). "Beneficial Effects of Nicotine Administered Prior to a Delayed Matching- to-Sample Task in Young and Aged Monkeys." *Neurobiol Aging* **12**(3): 233-8.

Burns, C. J., Cartmill, J. B., Powers, B. S. and Lee, M. K. (1998). "Update of the Morbidity Experience of Employees Potentially Exposed to Chlorpyrifos." *Occup Environ Med* **55**(1): 65-70.

Caglioti, L. (1983). *The Two Faces of Chemistry*. Cambridge, MIT Press.

Carlson, K., Jortner, B. S. and Ehrich, M. (2000). "Organophosphorus Compound-Induced Apoptosis in Sh-Sy5y Human Neuroblastoma Cells." *Toxicol Appl Pharmacol* **168**(2): 102-13.

Carson, K. A., Geula, C. and Mesulam, M. M. (1991). "Electron Microscopic Localization of Cholinesterase Activity in Alzheimer Brain Tissue." *Brain Res* **540**(1-2): 204-8.

Changeux, J. P. (1966). "Responses of Acetylcholinesterase from *Torpedo Marmorata* to Salts and Curarizing Drugs." *Mol Pharmacol* **2**: 369-392.

Chukwudebe, A., March, R. B., Othman, M. and Fukuto, T. R. (1989). "Formation of Trialkyl Phosphorothioate Esters from Organo-Phosphorus Insecticides after Exposure to Either Ultraviolet-Light or Sunlight." *J Agric Food Chem* **37**: 539-545.

Claudio, L., Kwa, W. C., Russell, A. L. and Wallinga, D. (2000). "Testing Methods for Developmental Neurotoxicity of Environmental Chemicals." *Toxicol Appl Pharmacol* **164**(1): 1-14.

Clothier, B., Johnson, M. K. and Reiner, E. (1981). "Interaction of Some Trialkyl Phosphorothiolates with Acetylcholinesterase. Characterization of Inhibition, Aging and Reactivation." *Biochim Biophys Acta* **660**(2): 306-16.

Cohen, J. A. and Oosterbaan, R. A. (1963). The Active Site of Acetylcholinesterase and Related Esterases and Its Reactivity toward Substrates and Inhibitors. *Handbuch Der Experimentellen Pharmakologie*. G. B. Koelle. Berlin, Springer-Verlag. **15:** 300-370.

Cohen, S. D. (1984). "Mechanisms of Toxicological Interactions Involving Organophosphate Insecticides." *Fundam Appl Toxicol* **4**: 315-324.

Cohen, S. G., Neuwirth, Z. and Weinstein, S. Y. (1966). "Association of Substrates with "-Chymotrypsin, Diethyl "-Acetoxysuccinate, and Diethyl Malate." *J Am Chem Soc* **88**: 5306-5315.

Corrigan, F. M., MacDonald, S., Brown, A., Armstrong, K. and Armstrong, E. M. (1994). "Neurasthenic Fatigue, Chemical Sensitivity and Gabaa Receptor Toxins." *Med Hypotheses* **43**(4): 195-200.

Cummings, J. L. (2000). "Cholinesterase Inhibitors: A New Class of Psychotropic Compounds." *Am J Psychiatry* **157**(1): 4-15.

Dale, H. H. (1914). "The Action of Certain Esters and Ethers of Choline, and Their Relation to Muscarine." *J Pharmacol Exp Ther* **6**: 147-190.

de Jong, L. P., Bijleveld, E. C., van Dijk, C. and Benschop, H. P. (1987). "Assay of the Chiral Organophosphate, Soman, in Biological Samples." *Int J Environ Anal Chem* **29**(3): 179-97.

de Jong, L. P., Verhagen, M. A., Langenberg, J. P., Hagedorn, I. and Loffler, M. (1989). "The Bispyridinium-Dioxime Hlo-7. A Potent Reactivator for Acetylcholinesterase Inhibited by the Stereoisomers of Tabun and Soman." *Biochem Pharmacol* **38**(4): 633-40.

de Jong, L. P. and Wolring, G. Z. (1984). "Stereospecific Reactivation by Some Hagedorn-Oximes of Acetylcholinesterases from Various Species Including Man, Inhibited by Soman." *Biochem Pharmacol* **33**(7): 1119-25.

de la Escalera, S., Bockamp, E. O., Moya, F., Piovant, M. and Jimenez, F. (1990). "Characterization and Gene Cloning of Neurotactin, a Drosophila Transmembrane Protein Related to Cholinesterases." *Embo J* **9**(11): 3593-601.

De Matteis, F. (1989). Phosphorothionates. *Sulphur Containing Drugs and Related Organic Compounds: Chemistry, Biochemistry, and Toxicology*. L. A. Damani. New York, Halsted Press.

Debord, J., Penicaut, B. and Labadie, M. (1986). "Kinetics of Cholinesterase Inhibition by Organophosphorus Compounds." *Phosphorus and Sulfur* **29**: 57-65.

Dembele, K., Haubruge, E. and Gaspar, C. (2000). "Concentration Effects of Selected Insecticides on Brain Acetylcholinesterase in the Common Carp." *Ecotoxicology and Environmental Safety* **45**: 49-54.

Dementi, B. (1994). "Ocular Effects of Organophosphates: A Historical Perspective of Saku Disease." *J Appl Toxicol* **14**(2): 119-29.

Doorn, J. A., Gage, D. A., Schall, M., Talley, T. T., Thompson, C. M. and Richardson, R. J. (2000). "Inhibition of Acetylcholinesterase by (1s,3s)-Isomalathion Proceeds with Loss of Thiomethyl: Kinetic and Mass Spectral Evidence for an Unexpected Primary Leaving Group." *Chem Res Toxicol* **13**(12): 1313-20.

Dupree, J. L. and Bigbee, J. W. (1994). "Retardation of Neuritic Outgrowth and Cytoskeletal Changes Accompany Acetylcholinesterase Inhibitor Treatment in Cultured Rat Dorsal Root Ganglion Neurons." *J Neurosci Res* **39**(5): 567-75.

Dupree, J. L., Maynor, E. N. and Bigbee, J. W. (1995). "Inverse Correlation of Acetylcholinesterase (Ache) Activity with the Presence of Neurofilament Inclusions in Dorsal Root Ganglion Neurons Cultured in the Presence of a Reversible Inhibitor of Ache." *Neurosci Lett* **197**(1): 37-40.

Duran, R., Cervenansky, C., Dajas, F. and Tipton, K. F. (1994). "Fasciculin Inhibition of Acetylcholinesterase Is Prevented by Chemical Modification of the Enzyme at a Peripheral Site." *Biochim Biophys Acta* **1201**(3): 381-8.

Ellman, G. L., Courtney, K. D., Andres, V. and Featherstone, R. M. (1961). "A New and Rapid Colorimetric Determination of Acetylcholinesterase Activity." *Biochem Pharmacol* **7**: 88-95.

Ember, L. (1996). "Probe of Troops' Exsousure to Chemical Arms Failed." *Chem Eng News*: 40-41.

EPA (2000). Organophosphate Pesticides in Food, a Primer on Reassessment of Residue Limits.

Eriksson, P. and Talts, U. (2000). "Neonatal Exposure to Neurotoxic Pesticides Increases Adult Susceptibility: A Review of Current Findings." *Neuro Toxicology* **21**: 3748.

Ernest, K., Thomas, M., Paulose, M., Rupa, V. and Gnanamuthu, C. (1995). "Delayed Effects of Exposure to Organophosphorus Compounds." *Indian J Med Res* **101**: 81-4.

Eto, M. (1974). *Organophosphorus Pesticides: Organic and Biological Chemistry*. Cleveland. OH, CRC Press.

Eya, B. K. and Fukuto, T. R. (1985). "The Effect of Chiral Debromoleptophos Oxon Isomers on Acute and Delayed Neurotoxicity and Their Inhibitory Activity against Acetylcholinesterases and Neurotoxic Esterase." *J Agric Food Chem* **33**: 884-887.

Fest, C. and Schmidt, K. J. (1973). *The Chemistry of Organophosphorus Pesticides*. New York, Springer-Verlag.

Fisher, T. C., Crane, M. and Callaghan, A. (2000). "An Optimized Microtiterplate Assay to Detect Acetylcholinesterase Activity in Individual *Chironomus Riparius* Meigen." *Environ Toxical and Chem* **19**(7): 1749-1752.

Fordham, C. L., Tessari, J. D., Ramsdell, H. S. and Keefe, T. J. (2001). "Effects of Malathion on Survival, Growth, Development, and Equilibrium Posture of Bullfrog Tadpoles." *Environ Toxical and Chem* **20**(1): 179-184.

Forget, G. (1991). "Pesticides in the Third World." *J Toxicol Environ Health* **32**: 11-31.

Froede, H. C. and Wilson, I. B. (1971). *The Enzymes*. New York, Academic Press.

Froede, H. C., Wilson, I. B. and Kaufman, H. (1986). "Acetylcholinesterase: Theory of Noncompetitive Inhibition." *Arch Biochem Biophys* **247**(2): 420-3.

Fukuto, T. R. (1990). "Mechanism of Action of Organophosphorus and Carbamate Insecticides." *Environ Health Perspect* **87**: 245-54.

Fukuto, T. R. and Metcalf, R. L. (1956). "Structure and Insecticidal Activity of Some Diethyl Substituted Phenyl Phosphates." *J Agric Food Chem* **4**: 930-935.

Fukuto, T. R. and Metcalf, R. L. (1958). "The Effect of Structure on the Reactivity of Alkylphosphonate Esters." *J Am Chem Soc* **81**: 372-377.

Gallo, M. A. and Lawryk, N. J. (1991). Organic Phosphorus Pesticides. *Handbook of Pesticide Toxicology*. W. J. Hayes, Jr. and E. R. Laws, Jr. San Diego, Academic Press. **2:** 917-1123.

George, K. and Sandevol, L. (2000). "Observation of Impurities in Commercial Preparations of Electric Eel Ache."

Geula, C., Greenberg, B. D. and Mesulam, M. M. (1994). "Cholinesterase Activity in the Plaques, Tangles and Angiopathy of Alzheimer's Disease Does Not Emanate from Amyloid." *Brain Res* **644**(2): 327-30.

Giacobini, E. (1998a). "Cholinergic Foundations of Alzheimer's Disease Therapy." *J Physiol Paris* **92**(3-4): 283-7.

Giacobini, E. (1998b). "Invited Review: Cholinesterase Inhibitors for Alzheimer's Disease Therapy: From Tacrine to Future Applications." *Neurochem Int* **32**(5-6): 413-9.

Giacobini, E. (2000). "Cholinesterase Inhibitors Stabilize Alzheimer Disease." *Neurochem Res* **25**(9-10): 1185-90.

Gibney, G., MacPhee-Quigley, K., Thompson, B., Vedvick, T., Low, M. G., Taylor, S. S. and Taylor, P. (1988). "Divergence in Primary Structure between the Molecular Forms of Acetylcholinesterase." *J Biol Chem* **263**(3): 1140-5.

Goldman, L. R. and Koduru, S. (2000). "Chemicals in the Environment and Developmental Toxicity to Children: A Public Health and Policy Perspective." *Environ Health Perspect* **108 Suppl 3**: 443-8.

Golicnik, M., Fournier, D. and Stojan, J. (2001). "Interaction of Drosophila Acetylcholinesterases with D-Tubocurarine: An Explanation of the Activation by an Inhibitor." *Biochemistry* **40**(5): 1214-1219.

Gordon, C. J. and Rowsey, P. J. (1998a). "Poisons and Fever." *Clin Exp Pharmacol Physiol* **25**(2): 145-9.

Gordon, I., Abdulla, E. M., Campbell, I. C. and Whatley, S. A. (1998b). "Phosmet Induces up-Regulation of Surface Levels of the Cellular Prion Protein." *Neuroreport* **9**(7): 1391-5.

Gray, M. G. and Hammitt, J. K. (2000). "Risk/Risk Trade-Offs in Pesticide Regulation: An Exploratory Analysis of the Public Health Effects of a Ban on Organophosphate and Carbamate Pesticides." *Risk Analysis* **20**(5): 665-680.

Greenblatt, H. M., Kryger, G., Lewis, T., Silman, I. and Sussman, J. L. (1999). "Structure of Acetylcholinesterase Complexed with (-)-Galanthamine at 2.3 a Resolution." *FEBS Lett* **463**(3): 321-6.

Greenfield, S. A., Chubb, I. W., Grunewald, R. A., Henderson, Z., May, J., Portnoy, S., Weston, J. and Wright, M. C. (1984). "A Non-Cholinergic Function for Acetylcholinesterase in the Substantia Nigra: Behavioural Evidence." *Exp Brain Res* **54**(3): 513-20.

Grubic, Z., Stalc, A., Sentjurc, M., Pecar, S., Gentry, M. K. and Doctor, B. P. (1995). "Different Effects of Two Peripheral Anionic Site-Binding Ligands on

Acetylcholinesterase Active-Site Gorge Topography Revealed by Electron Paramagnetic Resonance." *Biochim Biophys Acta* **1249**(2): 155-60.

Hajjar, N. P. and Hodgson, E. (1982). "Sulfoxidation of Thioether-Containing Pesticides by the Flavin-Adenine Dinucleotide- Dependent Monooxygenase of Pig Liver Microsomes." *Biochem Pharmacol* **31**(5): 745-52.

Han, J. H., Stratowa, C. and Rutter, W. J. (1987). "Isolation of Full-Length Putative Rat Lysophospholipase Cdna Using Improved Methods for Mrna Isolation and Cdna Cloning." *Biochemistry* **26**(6): 1617-25.

Harel, M., Kleywegt, G. J., Ravelli, R. B., Silman, I. and Sussman, J. L. (1995). "Crystal Structure of an Acetylcholinesterase-Fasciculin Complex: Interaction of a Three-Fingered Toxin from Snake Venom with Its Target." *Structure* **3**(12): 1355-66.

Harel, M., Quinn, D. M., Nair, H. K., Silman, I. and Sussman, J. (1996). "The X-Ray Structure of a Transition State Analog Complex Reveals the Molecular Origins of the Catalytic Power and Substrate Specificity of Acetylcholinesterase." *J Am Chem Soc* **118**: 2340-2346.

Harel, M., Schalk, I., Ehret-Sabatier, L., Bouet, F., Goeldner, M., Hirth, C., Axelsen, P. H., Silman, I. and Sussman, J. L. (1993). "Quaternary Ligand Binding to Aromatic Residues in the Active-Site Gorge of Acetylcholinesterase." *Proc Natl Acad Sci U S A* **90**(19): 9031-5.

Harel, M., Su, C. T., Frolow, F., Ashani, Y., Silman, I. and Sussman, J. L. (1991). "Refined Crystal Structures of "Aged" and "Non-Aged" Organophosphoryl Conjugates of Gamma-Chymotrypsin." *J Mol Biol* **221**(3): 909-18.

Hayes, W. J. (1991). Introduction. *Handbook of Pesticide Toxicology.* W. J. Hayes and E. R. Laws. San Diego, Academic Press: 1-37.

Heath, D. F. (1961). *Organophosphorus Poisons, Anticholinesterases and Related Compounds.* Oxford, Pergamon.

Hilgetag, G. (1969). " Optisch Aktive Dithiophosphorsaureester." *Z Chem* **9**: 310-311.

Hirashima, A., Kuwano, E. and Eto, M. (2000). "Docking Study of Enantiomeric Fonofos Oxon Bound to the Active Site of Torpedo Californica Acetylcholinesterase." *Bioorg Med Chem* **8**(3): 653-6.

Hodgson, E. (1982). "Production of Pesticide Metabolites by Oxidative Reactions." *J Toxicol Clin Toxicol* **19**(6-7): 609-21.

Hodgson, M. J. and Smith, A. D. (1992). Commercial and Residential Poisoning with Anticholinesterase. *Clinical and Experimental Toxicology of Organophosphates and Carbamates.* B. Ballantyne and T. C. Marrs. Oxford, Butterworth-Heinemann: 353-354.

Holmstedt, B. (1972). The Ordeal Bean of Old Calabar: The Pageant of Physostigma Venenosum in Medicine. *Plants in the Development of Modern Medicine.* T. Swain. Cambridge, Mass, Harvard University Press: 303-360.

Hosea, N. A., Berman, H. A. and Taylor, P. (1995). "Specificity and Orientation of Trigonal Carboxyl Esters and Tetrahedral Alkylphosphonyl Esters in Cholinesterases." *Biochemistry* **34**(36): 11528-36.

Hosea, N. A., Radic, Z., Tsigelny, I., Berman, H. A., Quinn, D. M. and Taylor, P. (1996). "Aspartate 74 as a Primary Determinant in Acetylcholinesterase Governing Specificity to Cationic Organophosphonates." *Biochemistry* **35**(33): 10995-1004.

Inestrosa, N. C. and Alarcon, R. (1998). "Molecular Interactions of Acetylcholinesterase with Senile Plaques." *J Physiol Paris* **92**(5-6): 341-4.

Iyer, V. and Parmar, B. S. (1984). "The Isomalathion Problem - a Review." *Intern J Trop Agri* **2**: 199-204.

Jamal, G. A. (1998). "Gulf War Syndrome--a Model for the Complexity of Biological and Environmental Interaction with Human Health." *Adverse Drug React Toxicol Rev* **17**(1): 1-17.

Jarv, J. (1984). "Stereochemical Aspects of Cholinesterase Catalysis." *Bioorg Chem* **12**: 259-278.

Jianmongkol, S., Berkman, C. E., Thompson, C. M. and Richardson, R. J. (1996). "Relative Potencies of the Four Stereoisomers of Isomalathion for Inhibition of Hen Brain Acetylcholinesterase and Neurotoxic Esterase in Vitro." *Toxicol Appl Pharmacol* **139**(2): 342-8.

Jianmongkol, S., Marable, B. R., Berkman, C. E., Talley, T. T., Thompson, C. M. and Richardson, R. J. (1999). "Kinetic Evidence for Different Mechanisms of Acetylcholinesterase Inhibition by (1r)- and (1s)-Stereoisomers of Isomalathion." *Toxicol Appl Pharmacol* **155**(1): 43-53.

Kaiser, E. T., Lee, T. W. and Boer, F. P. (1971). "Structure and Enzymatic Reactivity of an Aromatic Five-Membered Cyclic Phosphate Diester. Biological Implications." *J Am Chem Soc* **93**(9): 2351-3.

Kardos, S. A. and Sultatos, L. G. (2000). "Interactions of the Organophosphates Paraoxon and Methyl Paraoxon with Mouse Brain Acetylcholinesterase." *Toxicol Sci* **58**(1): 118-26.

Katz, B. and Miledi, R. (1965). "Release of Acetylcholine from a Nerve Terminal by Electric Pulses of Variable Strength and Duration." *Nature* **207**(1): 1097-8.

Kelly, J. S. (1999). "Alzheimer's Disease: The Tacrine Legacy." *Trends Pharmacol Sci* **20**(4): 127-9.

Kirby, A. J. and Lancaster, P. W. (1970). "Steric Assistance for Intramolecular Catalysis." *Biochem Soc Symp* **31**: 99-103.

Kocisko, D. A., Come, J. H., Priola, S. A., Chesebro, B., Raymond, G. J., Lansbury, P. T. and Caughey, B. (1994). "Cell-Free Formation of Protease-Resistant Prion Protein." *Nature* **370**(6489): 471-4.

Koellner, G., Kryger, G., Millard, C. B., Silman, I., Sussman, J. L. and Steiner, T. (2000). "Active-Site Gorge and Buried Water Molecules in Crystal Structures of Acetylcholinesterase from Torpedo Californica." *J Mol Biol* **296**(2): 713-35.

Korza, G. and Ozols, J. (1988). "Complete Covalent Structure of 60-Kda Esterase Isolated from 2,3,7,8- Tetrachlorodibenzo-P-Dioxin-Induced Rabbit Liver Microsomes." *J Biol Chem* **263**(7): 3486-95.

Kossiakoff, A. A. and Spencer, S. A. (1980). "Neutron Diffraction Identifies His 57 as the Catalytic Base in Trypsin." *Nature* **288**(5789): 414-6.

Kossiakoff, A. A. and Spencer, S. A. (1981). "Direct Determination of the Protonation States of Aspartic Acid-102 and Histidine-57 in the Tetrahedral Intermediate of the Serine Proteases: Neutron Structure of Trypsin." *Biochemistry* **20**(22): 6462-74.

Kraut, D., Goff, H., Pai, R. K., Hosea, N. A., Silman, I., Sussman, J. L., Taylor, P. and Voet, J. G. (2000). "Inactivation Studies of Acetylcholinesterase with Phenylmethylsulfonyl Fluoride." *Mol Pharmacol* **57**(6): 1243-8.

Krieger, R. I. and Dinoff, T. M. (2000). "Malathion Deposition, Metabolite Clearance, and Cholinesterase Status of Date Dusters and Harvesters in California." *Arch Environ Contam Toxicol* **38**(4): 546-53.

Kyger, E. M., Wiegand, R. C. and Lange, L. G. (1989). "Cloning of the Bovine Pancreatic Cholesterol Esterase/Lysophospholipase." *Biochem Biophys Res Commun* **164**(3): 1302-9.

Langenberg, J. P., DeJong, L. P. A., Otto, M. F. and Benschop, H. P. (1988). "Spontaneous and Oxime-Induced Reactivation of Acetylcholinesterase Inhibited by Phosphoramidates." *Arch Toxicol* **62**: 305-310.

Lanks, K. W. and Seleznick, M. J. (1981). "Spontaneous Reactivation of Acetylcholinesterase Inhibited by Diisopropylfluorophosphate." *Biochem Biophys Acta* **660**: 91-95.

Lauder, J. M. and Schambra, U. B. (1999). "Morphogenetic Roles of Acetylcholine." *Environ Health Perspect* **107 Suppl 1**: 65-9.

Layer, P. G. (1995a). "Nonclassical Roles of Cholinesterases in the Embryonic Brain and Possible Links to Alzheimer Disease." *Alzheimer Dis Assoc Disord* **9**(Suppl 2): 29-36.

Layer, P. G. and Willbold, E. (1995b). "Novel Functions of Cholinesterases in Development, Physiology and Disease." *Prog Histochem Cytochem* **29**(3): 1-94.

Lee, P. W., Allahyari, R. and Fukuto, T. R. (1978). "Studies on the Chiral Isomers of Fonofos and Fonofos Oxon." *Pestic Biochem Physiol* **8**: 146-157.

Lesser, J., Blodgett, D. and Ehrich, M. (2000). "Comparison of Oxime-Initiated Reactivation of Organophosphorous- Inhibited Acetylcholinesterase in Brains of Avian Embryos." *J Toxicol Environ Health A* **59**(1): 57-66.

Levi, P. E. and Hodgson, E. (1985). "Oxidation of Pesticides by Purified Cytochrome P-450 Isozymes from Mouse Liver." *Toxicol Lett* **24**(2-3): 221-8.

Levi, P. E. and Hodgson, E. (1988). "Stereospecificity in the Oxidation of Phorate and Phorate Sulphoxide by Purified Fad-Containing Mono-Oxygenase and Cytochrome P-450 Isozymes." *Xenobiotica* **18**(1): 29-39.

Lieske, C. N., Clark, J. H., Meyer, H. G. and Lowe, J. R. (1980). "Spontaneous and Induced Reactivation of Eel Acetylcholinesterase Inhibited by Three Organophosphinates." *Pestic Biochem Physiol* **13**: 205-212.

Lieske, C. N., Gepp, R. T., Maxwell, D. M., Clark, J. H., Broomfield, C. A., Blumbergs, P. and Tseng, C. C. (1992). "Cholinesterase Studies with (R) (+)- and (S)(-)-5-(1,3,3-Trimethylindolinyl)-N-(1-Phenylethyl)Carbamate." *J Enzyme Inhib* **6**(4): 283-91.

Lieske, C. N., Gessner, C. E., Gepp, R. T., Clark, J. H., Meyer, H. G. and Broomfield, C. A. (1990). "Ph Effects in the Spontaneous Reactivity of Phosphinylated Acetylcholinesterase." *Life Sci* **46**: 1189-1196.

Lim, S. L., Sim, M. K. and Loke, W. K. (2000). "Acetylcholinesterase-Independent Action of Diisopropyl-Flurophosphate in the Rat Aorta." *Eur J Pharmacol* **404**(3): 353-9.

Lin, A. R., Main, A. R., Tucker, W. P., Motoyama, N. and Dauterman, W. C. (1984). "Studies on Organophosphorus Impurities in Technical Malathion: Inhibition of Carboxylesterase and the Stability of Isomalathion." *Pestic Biochem Physiol* **21**: 223-231.

Lin, G., Tsai, Y. C., Liu, H. C., Liao, W. C. and Chang, C. H. (1998). "Enantiomeric Inhibitors of Cholesterol Esterase and Acetylcholinesterase." *Biochim Biophys Acta* **1388**(1): 161-74.

Lockridge, O., Bartels, C. F., Vaughan, T. A., Wong, C. K., Norton, S. E. and Johnson, L. L. (1987). "Complete Amino Acid Sequence of Human Serum Cholinesterase." *J Biol Chem* **262**(2): 549-57.

Lockridge, O. and Masson, P. (2000). "Pesticides and Susceptible Populations: People with Butyrylcholinesterase Genetic Variants May Be at Risk." *Neurotoxicology* **21**(1-2): 113-26.

Long, R. M., Satoh, H., Martin, B. M., Kimura, S., Gonzalez, F. J. and Pohl, L. R. (1988). "Rat Liver Carboxylesterase: Cdna Cloning, Sequencing, and Evidence for a Multigene Family." *Biochem Biophys Res Commun* **156**(2): 866-73.

Lotti, M. (1991). "Treatment of Acute Organophosphate Poisoning." *Med J Aust* **154**(1): 51-5.

Lotti, M. and Moretto, A. (1999). "Promotion of Organophosphate Induced Delayed Polyneuropathy by Certain Esterase Inhibitors." *Chem Biol Interact* **119-120**: 519-24.

Luo, C., Saxena, A., Smith, M., Garcia, G., Radic, Z., Taylor, P. and Doctor, B. P. (1999). "Phosphoryl Oxime Inhibition of Acetylcholinesterase During Oxime Reactivation Is Prevented by Edrophonium." *Biochemistry* **38**(31): 9937-47.

Main, A. R. (1964). "Affinity and Phosphorylation Constants for the Inhibition of Esterases by Organophosphates." *Science* **144**: 992-993.17.

Mallender, W. D., Szegletes, T. and Rosenberry, T. L. (1999). "Organophosphorylation of Acetylcholinesterase in the Presence of Peripheral Site Ligands. Distinct Effects of Propidium and Fasciculin." *J Biol Chem* **274**(13): 8491-9.

Mallender, W. D., Szegletes, T. and Rosenberry, T. L. (2000). "Acetylthiocholine Binds to Asp74 at the Peripheral Site of Human Acetylcholinesterase as the First Step in the Catalytic Pathway." *Biochemistry* **39**(26): 7753-63.

Mallipudi, N. M., Talcott, R. E., Ketterman, A. and Fukuto, T. R. (1980). " Properties and Inhibition of Rat Malathion Carboxylesterase." *J Toxicol Environ Health* **6**: 585-596.

Mani, A., Thomas, M. S. and Abraham, A. P. (1992). "Type Ii Paralysis or Intermediate Syndrome Following Organophosphorous Poisoning." *J Assoc Physicians India* **40**(8): 542-4.

Marchot, P. (1999). "[the Fasciculin-Acetylcholinesterase Interaction]." *J Soc Biol* **193**(6): 505-8.

Marchot, P., Bourne, Y., Prowse, C. N., Bougis, P. E. and Taylor, P. (1998). "Inhibition of Mouse Acetylcholinesterase by Fasciculin: Crystal Structure of the Complex and Mutagenesis of Fasciculin." *Toxicon* **36**(11): 1613-22.

Marchot, P., Ravelli, R. B., Raves, M. L., Bourne, Y., Vellom, D. C., Kanter, J., Camp, S., Sussman, J. L. and Taylor, P. (1996). "Soluble Monomeric Acetylcholinesterase from Mouse: Expression, Purification, and Crystallization in Complex with Fasciculin." *Protein Sci* **5**(4): 672-9.

Marrs, T. C. (1995). *Organophosphate Sheep Dips and Human Health. An Overview of the Delayed Effects of Organophosphates.* Seminar for Farmers, Medical Practitioners and Policy Makers.

Massoulie, J., Pezzementi, L., Bon, S., Krejci, E. and Vallette, F. M. (1993). "Molecular and Cellular Biology of Cholinesterases." *Prog Neurobiol* **41**: 31-91.

Matolczy, G., Nadasy, M. and Andriska, V. (1988). *Pesticide Chemistry*. Amsterdam, Elsevier.

McConnell, R., Keifer, M. and Rosenstock, L. (1994). "Elevated Quantitative Vibrotactile Threshold among Workers Previously Poisoned with Methamidophos and Other Organophosphate Pesticides." *Am J Ind Med* **25**(3): 325-34.

Meinert, R., Schuz, J., Kaletsch, U., Kaatsch, P. and Michaelis, J. (2000). "Leukemia and Non-Hodgkin's Lymphoma in Childhood and Exposure to Pesticides: Results of a Register-Based Case-Control Study in Germany." *Am J Epidemiol* **151**(7): 639-46; discussion 647-50.

Metcalf, R. L. and March, R. B. (1953). " The Isomerization of Organic Thionophosphate Insecticides." *J Econ Entomol* **46**: 288-294.

Millard, C. B., Koellner, G., Ordentlich, A., Shafferman, A., Silman, I. and Sussman, J. (1999a). "Reaction Products of Acetylcholinesterase and Vx Reveal a Mobile Histidine in the Catalytic Triad." *J Am Chem Soc* **121**: 9883-9884.

Millard, C. B., Kryger, G., Ordentlich, A., Greenblatt, H. M., Harel, M., Raves, M. L., Segall, Y., Barak, D., Shafferman, A., Silman, I. and Sussman, J. L. (1999b). "Crystal Structures of Aged Phosphonylated Acetylcholinesterase: Nerve Agent Reaction Products at the Atomic Level." *Biochemistry* **38**(22): 7032-9.

Millard, C. B., Lockridge, O. and Broomfield, C. A. (1995). "Design and Expression of Organophosphorus Acid Anhydride Hydrolase Activity in Human Butyrylcholinesterase." *Biochemistry* **34**(49): 15925-33.

Monje Argiles, A., Lison, D., Lauwerys, R., Mahieu, P., Brucher, J. M. and Van den Bergh, P. (1990). "Acute Polyneuropathy after Malathion Poisoning." *Acta Neurol Belg* **90**(4): 190-9.

Moran, M. A., Mufson, E. J. and Gomez-Ramos, P. (1993). "Colocalization of Cholinesterases with Beta Amyloid Protein in Aged and Alzheimer's Brains." *Acta Neuropathol* **85**(4): 362-9.

Morel, N., Bon, S., Greenblatt, H. M., Van Belle, D., Wodak, S. J., Sussman, J. L., Massoulie, J. and Silman, I. (1999). "Effect of Mutations within the Peripheral Anionic Site on the Stability of Acetylcholinesterase." *Mol Pharmacol* **55**(6): 982-92.

Moretto, A., Jokanovic, M. and Lotti, M. (2000). "The Relevance of Inhibitor-Substrate Interactions When Measuring Neuropathy Target Esterase Inhibition." *Arch Toxicol* **73**(12): 655-60.

Moretto, A. and Lotti, M. (1998). "Poisoning by Organophosphorus Insecticides and Sensory Neuropathy." *J Neurol Neurosurg Psychiatry* **64**(4): 463-8.

Mortensen, S. R., Brimijoin, S., Hooper, M. J. and Padilla, S. (1998). "Comparison of the *in Vitro* Sensitivity of Rats Acetylcholinesterase to Chlorpyrifos: What Do Tissue Ic50 Values Represent." *Toxicol Appl Pharmacol* **148**: 46-49.

Muller-Vahl, K. R., Kolbe, H. and Dengler, R. (1999). "Transient Severe Parkinsonism after Acute Organophosphate Poisoning." *J Neurol Neurosurg Psychiatry* **66**(2): 253-4.

Mullner, H. and Sund, H. (1980). "Essential Arginine Residue in Acetylcholinesterase from *Torpedo Californica*." *FEBS Lett* **119**: 283-286.

Nguyen, J., Baldwin, M. A., Cohen, F. E. and Prusiner, S. B. (1995). "Prion Protein Peptides Induce Alpha-Helix to Beta-Sheet Conformational Transitions." *Biochemistry* **34**(13): 4186-92.

Noort, D., Hulst, A. G., Platenburg, D. H., Polhuijs, M. and Benschop, H. P. (1998). "Quantitative Analysis of O-Isopropyl Methylphosphonic Acid in Serum Samples of Japanese Citizens Allegedly Exposed to Sarin: Estimation of Internal Dosage." *Arch Toxicol* **72**(10): 671-5.

O'Brien, R. D. (1967). *Insecticides: Action and Metabolism.* New York, Academic Press.

Ohayo-Mitoko, G. J., Kromhout, H., Simwa, J. M., Boleij, J. S. and Heederik, D. (2000). "Self Reported Symptoms and Inhibition of Acetylcholinesterase Activity among Kenyan Agricultural Workers." *Occup Environ Med* **57**(3): 195-200.

Ollis, D. L., Cheah, E., Cygler, M., Dijkstra, B., Frolow, F., Franken, S. M., Harel, M., Remington, S. J., Silman, I., Schrag, J. and et al. (1992). "The Alpha/Beta Hydrolase Fold." *Protein Eng* **5**(3): 197-211.

Olson, P. F., Fessler, L. I., Nelson, R. E., Sterne, R. E., Campbell, A. G. and Fessler, J. H. (1990). "Glutactin, a Novel Drosophila Basement Membrane-Related Glycoprotein with Sequence Similarity to Serine Esterases." *Embo J* **9**(4): 1219-27.

Ooms, A. J. J. and Boter, H. L. (1965). "Stereospecificity of Hydrolytic Enzymes in Their Reaction with Optically Active Organophosphorus Compounds." *Biochem Pharmacol* **14**: 1839-1846.

Ordentlich, A., Barak, D., Kronman, C., Ariel, N., Segall, Y., Velan, B. and Shafferman, A. (1995). "Contribution of Aromatic Moieties of Tyrosine 133 and of the Anionic Subsite

Tryptophan 86 to Catalytic Efficiency and Allosteric Modulation of Acetylcholinesterase." *J Biol Chem* **270**(5): 2082-91.

Ordentlich, A., Barak, D., Kronman, C., Ariel, N., Segall, Y., Velan, B. and Shafferman, A. (1998). "Functional Characteristics of the Oxyanion Hole in Human Acetylcholinesterase." *J Biol Chem* **273**(31): 19509-17.

Ordentlich, A., Barak, D., Kronman, C., Benschop, H. P., De Jong, L. P., Ariel, N., Barak, R., Segall, Y., Velan, B. and Shafferman, A. (1999). "Exploring the Active Center of Human Acetylcholinesterase with Stereomers of an Organophosphorus Inhibitor with Two Chiral Centers." *Biochemistry* **38**(10): 3055-66.

Osweiler, G. D., Carson, T. L., Buck, W. B. and Van Gelder, G. A. (1984). *Clinical and Diagnostic Veterinary Toxicology*. Dubuque, Kendall/Hunt Publishing Company.

Panemangalore, M. and Bebe, F. N. (2000). "Dermal Exposure to Pesticides Modifies Antioxidant Enzymes in Tissues of Rats." *J Environ Sci Health B* **35**(4): 399-416.

Parsons, S. M., Prior, C. and Marshall, I. G. (1993). "Acetylcholine Transport, Storage, and Release." *Int Rev Neurobiol* **35**: 279-390.

Perry, E. K. (1986). "The Cholinergic Hypothesis--Ten Years On." *Br Med Bull* **42**(1): 63-9.

Perutz, M. (1991). *Is Science Necessary?* Oxford, Oxford University Press.

Porschke, D., Creminon, C., Cousin, X., Bon, C., Sussman, J. and Silman, I. (1996). "Electrooptical Measurements Demonstrate a Large Permanent Dipole Moment Associated with Acetylcholinesterase." *Biophys J* **70**(4): 1603-8.

Prendergast, M. A., Terry, A. V. and Buccafusco, J. J. (1997). "Chronic, Low-Level Exposure to Diisopropylfluorophosphate Causes Protracted Impairment of Spatial Navigation Learning." *Psychopharmacology (Berl)* **129**(2): 183-91.

Prendergast, M. A., Terry, A. V. and Buccafusco, J. J. (1998). "Effects of Chronic, Low-Level Organophosphate Exposure on Delayed Recall, Discrimination, and Spatial Learning in Monkeys and Rats." *Neurotoxicol Teratol* **20**(2): 115-22.

Purdey, M. (1996a). "The Uk Epidemic of Bse: Slow Virus or Chronic Pesticide-Initiated Modification of the Prion Protein? Part 1: Mechanisms for a Chemically Induced Pathogenesis/Transmissibility." *Med Hypotheses* **46**(5): 429-43.

Purdey, M. (1996b). "The Uk Epidemic of Bse: Slow Virus or Chronic Pesticide-Initiated Modification of the Prion Protein? Part 2: An Epidemiological Perspective." *Med Hypotheses* **46**(5): 445-54.

Purdey, M. (1998). "High-Dose Exposure to Systemic Phosmet Insecticide Modifies the Phosphatidylinositol Anchor on the Prion Protein: The Origins of New Variant Transmissible Spongiform Encephalopathies?" *Med Hypotheses* **50**(2): 91-111.

Quinn, D. M. (1987). "Acetylcholinesterases: Enzyme Structure, Reaction Dynamics, and Virtual Transition States." *Chem Rev* **87**: 955-979.

Radic, Z., Duran, R., Vellom, D. C., Li, Y., Cervenansky, C. and Taylor, P. (1994). "Site of Fasciculin Interaction with Acetylcholinesterase." *J Biol Chem* **269**(15): 11233-9.

Radic, Z., Quinn, D. M., Vellom, D. C., Camp, S. and Taylor, P. (1995). "Allosteric Control of Acetylcholinesterase Catalysis by Fasciculin." *J Biol Chem* **270**(35): 20391-9.

Radic, Z., Reiner, E. and Simeon, V. (1984). "Binding Sites on Acetylcholinesterase for Reversible Ligands and Phosphorylating Agents. A Theoretical Model Tested on Haloxon and Phosphostigmine." *Biochem Pharmacol* **33**(4): 671-7.

Radic, Z., Reiner, E. and Taylor, P. (1991). "Role of the Peripheral Anionic Site on Acetylcholinesterase: Inhibition by Substrates and Coumarin Derivatives." *Mol Pharmacol* **39**(1): 98-104.

Radic, Z. and Taylor, P. (1999). "The Influence of Peripheral Site Ligands on the Reaction of Symmetric and Chiral Organophosphates with Wildtype and Mutant Acetylcholinesterases." *Chem Biol Interact* **119-120**: 111-7.

Radic, Z. and Taylor, P. (2000). "Interaction Kinetics of Reversible Inhibitors and Substrates with Actylcholinesterase and Its Fasciculin2 Complex." *J Biol Chem* **17**: 17.

Ragnarsdottir, K. V. (2000). "Environmental Fate and Toxicology of Organophosphate Pesticides." *Journal of the Geological Society, London* **157**: 859-876.

Randall, J. C., Yano, B. L. and Richardson, R. J. (1997). "Potentiation of Organophosphorus Compound-Induced Delayed Neurotoxicity (Opidn) in the Central and Peripheral Nervous System of the Adult Hen: Distribution of Axonal Lesions." *J Toxicol Environ Health* **51**(6): 571-90.

Reyes, A. E., Perez, D. R., Alvarez, A., Garrido, J., Gentry, M. K., Doctor, B. P. and Inestrosa, N. C. (1997). "A Monoclonal Antibody against Acetylcholinesterase Inhibits the Formation of Amyloid Fibrils Induced by the Enzyme." *Biochem Biophys Res Commun* **232**(3): 652-5.

Robertson, R. T. and Yu, J. (1993). "Acetylcholinesterase and Neural Development: New Tricks for an Old Dog?" *News Physiol Sci* **8**: 266-272.

Rosenberg, A. M. (1999). "Antinuclear Antibodies in Mice Exposed to Pesticides." *J Agric Safety and Health* **5**(2): 173-177.

Rosenberry, T. L. (1975). "Catalysis by Acetylcholinesterase: Evidence That the Rate-Limiting Step for Acylation with Certain Substrates Precedes General Acid-Base Catalysis." *Proc Natl Acad Sci U S A* **72**(10): 3834-8.

Rosenberry, T. L., Mallender, W. D., Thomas, P. J. and Szegletes, T. (1999). "A Steric Blockade Model for Inhibition of Acetylcholinesterase by Peripheral Site Ligands and Substrate." *Chem Biol Interact* **119-120**: 85-97.

Rosenberry, T. L., Rabl, C. R. and Neumann, E. (1996). "Binding of the Neurotoxin Fasciculin 2 to the Acetylcholinesterase Peripheral Site Drastically Reduces the Association and Dissociation Rate Constants for N-Methylacridinium Binding to the Active Site." *Biochemistry* **35**(3): 685-90.

Ryan, D. L. and Fukuto, T. R. (1985). "The Effect of Impurities on the Toxicokinetics of Malathion in Rats." *Pestic Biochem Physiol* **23**: 413-424.

Ryu, S., Lin, J. and Thompson, C. M. (1991). "Comparative Anticholinesterase Potency of Chiral Isoparathion Methyl." *Chem Res Toxicol* **4**: 517-520.

Satoh, T. and Hosokawa, M. (2000). "Organophosphates and Their Impact on the Global Environment." *Neurotoxicology* **21**(1-2): 223-7.

Schuhmann, G. (1976). The Economic Impact of Pesticides on Advanced Countries. *Pesticides and Human Welfare*. D. L. Gunn and J. G. R. Stevens. Oxford, Oxford University Press: 55-71.

Schumacher, M., Camp, S., Maulet, Y., Newton, M., MacPhee-Quigley, K., Taylor, S. S., Friedmann, T. and Taylor, P. (1986). "Primary Structure of Acetylcholinesterase: Implications for Regulation and Function." *Fed Proc* **45**(13): 2976-81.

Schuz, J., Kaletsch, U., Meinert, R., Kaatsch, P. and Michaelis, J. (2000). "Risk of Childhood Leukemia and Parental Self-Reported Occupational Exposure to Chemicals, Dusts, and Fumes: Results from Pooled Analyses of German Population-Based Case-Control Studies." *Cancer Epidemiol Biomarkers Prev* **9**(8): 835-8.

Schwartz, R. D. and Kellar, K. J. (1983). "Nicotinic Cholinergic Receptor Binding Sites in the Brain: Regulation in Vivo." *Science* **220**(4593): 214-6.

Segall, Y., Waysbort, D., Barak, D., Ariel, N., Doctor, B. P., Grunwald, J. and Ashani, Y. (1993). "Direct Observation and Elucidation of the Structures of Aged and Nonaged Phosphorylated Cholinesterases by 31p Nmr Spectroscopy." *Biochemistry* **32**(49): 13441-50.

Sentjurc, M., Pecar, S., Stojan, J., Marchot, P., Radic, Z. and Grubic, Z. (1999). "Electron Paramagnetic Resonance Reveals Altered Topography of the Active Center Gorge of Acetylcholinesterase after Binding of Fasciculin to the Peripheral Site." *Biochim Biophys Acta* **1430**(2): 349-58.

Shafferman, A., Ordentlich, A., Barak, D., Stein, D., Ariel, N. and Velan, B. (1996). "Aging of Phosphylated Human Acetylcholinesterase: Catalytic Processes Mediated by Aromatic and Polar Residues of the Active Centre." *Biochem J* **318**(Pt 3): 833-40.

Shafferman, A., Velan, B., Ordentlich, A., Kronman, C., Grosfeld, H., Leitner, M., Flashner, Y., Cohen, S., Barak, D. and Ariel, N. (1992). "Substrate Inhibition of

Acetylcholinesterase: Residues Affecting Signal Transduction from the Surface to the Catalytic Center." *Embo J* **11**(10): 3561-8.

Sharma, K. V., Koenigsberger, C., Brimijoin, S. and Bigbee, J. W. (2001). "Direct Evidence for an Adhesive Function in the Noncholinergic Role of Acetylcholinesterase in Neurite Outgrowth." *J Neurosci Res* **63**(2): 165-175.

Sherman, J. D. (1996). "Chlorpyrifos (Dursban)-Associated Birth Defects: Report of Four Cases." *Arch Environ Health* **51**(1): 5-8.

Small, D. H., Michaelson, S. and Sberna, G. (1996). "Non-Classical Actions of Cholinesterases: Role in Cellular Differentiation, Tumorigenesis and Alzheimer's Disease." *Neurochem Int* **28**(5-6): 453-83.

Soto, C., Castano, E. M., Frangione, B. and Inestrosa, N. C. (1995). "The Alpha-Helical to Beta-Strand Transition in the Amino-Terminal Fragment of the Amyloid Beta-Peptide Modulates Amyloid Formation." *J Biol Chem* **270**(7): 3063-7.

Spruit, H. E., Langenberg, J. P., Trap, H. C., van der Wiel, H. J., Helmich, R. B., van Helden, H. P. and Benschop, H. P. (2000). "Intravenous and Inhalation Toxicokinetics of Sarin Stereoisomers in Atropinized Guinea Pigs." *Toxicol Appl Pharmacol* **169**(3): 249-54.

Steenland, K., Jenkins, B., Ames, R. G., O'Malley, M., Chrislip, D. and Russo, J. (1994). "Chronic Neurological Sequelae to Organophosphate Pesticide Poisoning." *Am J Public Health* **84**(5): 731-6.

Stephens, R., Spurgeon, A., Calvert, I. A., Beach, J., Levy, L. S., Berry, H. and Harrington, J. M. (1995). "Neuropsychological Effects of Long-Term Exposure to Organophosphates in Sheep Dip." *Lancet* **345**(8958): 1135-9.

Sternfeld, M., Ming, G., Song, H., Sela, K., Timberg, R., Poo, M. and Soreq, H. (1998). "Acetylcholinesterase Enhances Neurite Growth and Synapse Development through Alternative Contributions of Its Hydrolytic Capacity, Core Protein, and Variable C Termini." *J Neurosci* **18**(4): 1240-9.

Sticht, H., Bayer, P., Willbold, D., Dames, S., Hilbich, C., Beyreuther, K., Frank, R. W. and Rosch, P. (1995). "Structure of Amyloid A4-(1-40)-Peptide of Alzheimer's Disease." *Eur J Biochem* **233**(1): 293-8.

Stine, K. E. and Brown, T. M. (1996). *Principles of Toxicology*. New York, Lewis.

Stone, J. F., Eichner, M. L., Kim, C. and Koehler, K. (1988). "Relationships between Clothing and Pesticide Poisoning." *J Environ Health* **50**: 210-215.

Sudakin, D. L., Mullins, M. E., Horowitz, B. Z., Abshier, V. and Letzig, L. (2000). "Intermediate Syndrome after Malathion Ingestion Despite Continuous Infusion of Pralidoxime." *Clin Tox* **31**(1): 47-50.

Sultatos, L. G. (1994). "Mammalin Toxicology of Organophosphorus Pesticides." *J Toxicol Environ Health* **43**: 271-289.

Sung, S. C. and Ruff, B. A. (1987). "Intracellular Distribution of Molecular Forms of Acetylcholinesterase in Rat Brain and Changes after Diisopropylfluorophosphate Treatment." *Neurochem Res* **12**: 15-19.

Sussman, J. L., Harel, M., Frolow, F., Oefner, C., Goldman, A., Toker, L. and Silman, I. (1991). "Atomic Structure of Acetylcholinesterase from Torpedo Californica: A Prototypic Acetylcholine-Binding Protein." *Science* **253**(5022): 872-9.

Swillens, S. (1986a). "Inactivation of Macromolecules by Ionizing Radiation. Deterministic Single-Hit or Stochastic Multievent Process?" *Biochem J* **233**(3): 655-9.

Swillens, S., Ludgate, M., Mercken, L., Dumont, J. E. and Vassart, G. (1986b). "Analysis of Sequence and Structure Homologies between Thyroglobulin and Acetylcholinesterase: Possible Functional and Clinical Significance." *Biochem Biophys Res Commun* **137**(1): 142-8.

Szegletes, T., Mallender, W. D. and Rosenberry, T. L. (1998). "Nonequilibrium Analysis Alters the Mechanistic Interpretation of Inhibition of Acetylcholinesterase by Peripheral Site Ligands." *Biochemistry* **37**(12): 4206-16.

Szegletes, T., Mallender, W. D., Thomas, P. J. and Rosenberry, T. L. (1999). "Substrate Binding to the Peripheral Site of Acetylcholinesterase Initiates Enzymatic Catalysis. Substrate Inhibition Arises as a Secondary Effect." *Biochemistry* **38**(1): 122-33.

Talcott, R. E., Denk, H. and Mallipudi, N. M. (1979). "Inactivation of Esterases by Impurities Isolated from Technical Malathion." *Toxicol Appl Pharmacol* **49**: 373-376.

Taylor, P. (1996). Anticholinesterase Agents. *Goodman & Gilman's the Pharmacological Basis of Therapeutics*. J. G. Hardman, L. E. Limbird, P. B. Molinoff, A. N. Richards and R. W. Ruddon. New York, McGraw-Hill: 161-176.

Taylor, P. and Lappi, S. (1975). "Interaction of Fluorescence Probes with Acetylcholinesterase. The Site and Specificity of Propidium Binding." *Biochemistry* **14**(9): 1989-97.

Taylor, P. and Radic, Z. (1994). "The Cholinesterases: From Genes to Proteins." *Annu Rev Pharmacol Toxicol* **34**: 281-320.

Taylor, P., Wong, L., Radic, Z., Tsigelny, I., Bruggemann, R., Hosea, N. A. and Berman, H. A. (1999). "Analysis of Cholinesterase Inactivation and Reactivation by Systematic

Structural Modification and Enantiomeric Selectivity." *Chem Biol Interact* **119-120**: 3-15.

Terry, A. V., Jackson, W. J. and Buccafusco, J. J. (1993). "Effects of Concomitant Cholinergic and Adrenergic Stimulation on Learning and Memory Performance by Young and Aged Monkeys." *Cereb Cortex* **3**(4): 304-12.

Thomas, P. T. (1995). "Pesticide-Induced Immunotoxicity: Are Great Lakes Residents at Risk?" *Environ Health Perspect* **103 Suppl 9**: 55-61.

Thompson, C. M. (1992). Preparation, Analysis, and Toxicity of Phosphorothiolates. *Organophosphates: Chemistry, Fate and Effects*. J. E. Chambers and P. E. Levi. San Diego, Academic Press.

Thompson, C. M., Frick, J. A., Natke, B. C. and Hansen, L. K. (1989). "Preparation, Analysis, and Anticholinesterase Properties of O,O-Dimethylphosphorothioate Isomerides." *Chem Res Toxicol* **2**: 386-391.

Thompson, C. M. and Fukuto, T. R. (1982). "Mechanism of Cholinesterase Inhibition by Methamidophos." *J Agric Food Chem* **30**: 282-284.

Toia, R. F., March, R. B., Umetsu, N., Mallipudi, N. M., Allahyari, R. and Fukuto, T. R. (1980). "Identification and Toxicological Evaluation of Impurities in Technical Malathion and Fenthion." *J Agric Food Chem* **28**: 599-604.

Trabace, L., Cassano, T., Steardo, L., Pietra, C., Villetti, G., Kendrick, K. M. and Cuomo, V. (2000a). "Biochemical and Neurobehavioral Profile of Chf2819, a Novel, Orally Active Acetylcholinesterase Inhibitor for Alzheimer's Disease." *J Pharmacol Exp Ther* **294**(1): 187-94.

Trabace, L., Coluccia, A., Gaetani, S., Tattoli, M., Cagiano, R., Pietra, C., Kendrick, K. M. and Cuomo, V. (2000b). "In Vivo Neurochemical Effects of the Acetylcholinesterase Inhibitor Ena713 in Rat Hippocampus." *Brain Res* **865**(2): 268-71.

Ulrich, J. (1990a). "Recent Progress in the Characterization of the Pathological Hallmarks for Alzheimer's Disease." *Acta Neurol Scand Suppl* **129**: 5-7.

Ulrich, J., Meier-Ruge, W., Probst, A., Meier, E. and Ipsen, S. (1990b). "Senile Plaques: Staining for Acetylcholinesterase and A4 Protein: A Comparative Study in the Hippocampus and Entorhinal Cortex." *Acta Neuropathol* **80**(6): 624-8.

Umetsu, N., Grose, F. H., Allahyari, R., Abu-El-Haj, S. and Fukuto, T. R. (1977). "Effect of Impurities on the Mammalian Toxicity of Technical Malathion and Acephate." *J Agric Food Chem* **4**: 946-953.

Van Wazer, J. R. (1958). *Phosphorus and Its Compounds, Volume I: Chemistry*. New York, Interscience Publishers Inc.

Velan, B., Barak, D., Ariel, N., Leitner, M., Bino, T., Ordentlich, A. and Shafferman, A. (1996). "Structural Modifications of the Omega Loop in Human Acetylcholinesterase." *FEBS Lett* **395**(1): 22-8.

Velan, B., Kronman, C., Ordentlich, A., Flashner, Y., Leitner, M., Cohen, S. and Shafferman, A. (1993). "N-Glycosylation of Human Acetylcholinesterase: Effects on Activity, Stability and Biosynthesis." *Biochem J* **296**(Pt 3): 649-56.

Vollhardt, K. P. C. and Schore, N. E. (1999). *Organic Chemistry: Structure and Function*. New York, W.H. Freeman and Company: 79.

Wallace, K. B. and Herzberg, U. (1988). "Reactivation and Aging of Phosphorylated Brain Acetylcholinesterase from Fish and Rodents." *Toxicol Appl Pharmacol* **92**(2): 307-14.

Wallace, K. B. and Kemp, J. R. (1991). "Species Specificity in the Chemical Mechanism of Organophosphorus, Anticholinesterase Activity." *Chem Res Toxicol* **4**: 41-49.

Ward, T. R., Ferris, D. J., Tilson, H. A. and Mundy, W. R. (1993). "Correlation of the Anticholinesterase Activity of a Series of Organophosphates with Their Ability to Compete with Agonist Binding to Muscarinic Receptors." *Toxicol Appl Pharmacol* **122**(2): 300-7.

Ward, T. R. and Mundy, W. R. (1996). "Organophosphorus Compounds Preferentially Affect Second Messenger Systems Coupled to M2/M4 Receptors in Rat Frontal Cortex." *Brain Res Bull* **39**(1): 49-55.

Wei, Y., Schottel, J. L., Derewenda, U., Swenson, L., Patkar, S. and Derewenda, Z. S. (1995). "A Novel Variant of the Catalytic Triad in the Streptomyces Scabies Esterase." *Nat Struct Biol* **2**(3): 218-23.

Weinbaum, Z., Schenker, M. B., Gold, E. B., Samuels, S. J. and O'Malley, M. A. (1997). "Risk Factors for Systemic Illnesses Following Agricultural Exposures to Restricted Organophosphates in California, 1984-1988." *Am J Ind Med* **31**(5): 572-9.

Weinbaum, Z., Schenker, M. B., O'Malley, M. A., Gold, E. B. and Samuels, S. J. (1995). "Determinants of Disability in Illnesses Related to Agricultural Use of Organophosphates (Ops) in California." *Am J Ind Med* **28**(2): 257-74.

Weiss, B. and Landrigan, P. J. (2000). "The Developing Brain and the Environment: An Introduction." *Environ Health Perspect* **108 Suppl 3**: 373-4.

Welling, W. (1988). Pesticides in Agriculture. *Stereoselectivity of Pesticides*. E. J. Ariens, J. J. S. Van Rensen and W. Welling. Amsterdam, Elsevier.

Wester, R. M., Tanojo, H., Maibach, H. I. and Wester, R. C. (2000). "Predicted Chemical Warfare Agent Vx Toxicity to Uniformed Soldier Using Parathion in Vitro Human Skin Exposure and Absorption." *Toxicol Appl Pharmacol* **168**: 149-152.

Westheimer, F. H. (1987). "Why Nature Chose Phosphates." *Science* **235**(4793): 1173-8.

Wilson, B. W., Hooper, M. J., Hansen, M. E. and Nieberg, P. S. (1992). Reactivation of Organophosphorus Inhibited Ache with Oximes. *Organophosphates: Chemistry, Fate, and Effects*. San Diego, Academic Press: 107-137.

Wilson, I. B. and Ginsburg, S. (1955). "A Powerful Reactivator of Alkylphosphate Inhibited Acetylcholinesterase." *Biochem Biophys Acta* **18**: 168-170.

Wilson, I. B., Ginsburg, S. and Quan, C. (1958). "Molecular Complementariness as Basis for Reactivation of Alkyl Phosphate-Inhibited Enzyme." *Arch Biochem Biophys* **77**: 286-296.

Wilson, I. B., Hatch, M. A. and Ginsburg, S. (1960). "Carbamylation of Acetylcholinesterase." *J Biol Chem* **235**: 2312-2315.

Wlodek, S. T., Clark, T. W., Scott, L. R. and McCammon, J. A. (1997). "Molecular Dynamics of Acetylcholinesterase Dimer Complexed with Tacrine." *J Am Chem Soc* **119**: 9513-9522.

Wlodek, S. T., Shen, T. and McCammon, J. A. (2000). "Electrostatic Steering of Substrate to Acetylcholinesterase: Analysis of Field Fluctuations." *Biopolymers* **53**(3): 265-71.

Wong, L., Radic, Z., Bruggemann, R. J., Hosea, N., Berman, H. A. and Taylor, P. (2000). "Mechanism of Oxime Reactivation of Acetylcholinesterase Analyzed by Chirality and Mutagenesis." *Biochemistry* **39**(19): 5750-7.

Wustner, D. A. and Fukuto, T. R. (1973). "Stereoselectivity in Cholinesterase Inhibition, Toxicity, and Plant Systemic Activity by the Optical Isomers of O-2-Butyl S-2-(Ethylthio)Ethyl Ethylphosphonothioate." *J Agric Food Chem* **21**(5): 756-61.

Xie, W., Stribley, J. A., Chatonnet, A., Wilder, P. J., Rizzino, A., McComb, R. D., Taylor, P., Hinrichs, S. H. and Lockridge, O. (2000). "Postnatal Developmental Delay and Supersensitivity to Organophosphate in Gene-Targeted Mice Lacking Acetylcholinesterase." *J Pharmacol Exp Ther* **293**(3): 896-902.

Xie, W., Wilder, P. J., Stribley, J., Chatonnet, A., Rizzino, A., Taylor, P., Hinrichs, S. H. and Lockridge, O. (1999). "Knockout of One Acetylcholinesterase Allele in the Mouse." *Chem Biol Interact* **119-120**: 289-99.

Yu, Q., Greig, N. H., Holloway, H. W. and Brossi, A. (1998). "Syntheses and Anticholinesterase Activities of (3as)-N1, N8- Bisnorphenserine, (3as)-N1,N8-Bisnorphysostigmine, Their Antipodal Isomers, and Other Potential Metabolites of Phenserine." *J Med Chem* **41**(13): 2371-9.

Zhang, Y., Carlen, P. L. and Zhang, L. (1997). "Kinetics of Muscarinic Reduction of Isahp in Hippocampal Neurons: Effects of Acetylcholinesterase Inhibitors." *J Neurophysiol* **78**(6): 2999-3007.

Zhou, H. X., Wlodek, S. T. and McCammon, J. A. (1998). "Conformation Gating as a Mechanism for Enzyme Specificity." *Proc Natl Acad Sci U S A* **95**(16): 9280-3.